

https://dspace.org/

Unveiling the biochemical pathway between Type 2 Diabetes Mellitus and early Alzheimer’s disease

Tooray, Shweta

2024-08

University of the Witwatersrand, Johannesburg

https://hdl.handle.net/10539/45164

Tooray, Shweta. (2024). Unveiling the biochemical pathway between Type 2 Diabetes Mellitus and early Alzheimer’s disease. [Master's dissertation, University of the Witwatersrand, Johannesburg]. WIReDSpace. https://hdl.handle.net/10539/45164

Downloaded from a DSpace repository. https://dspace.org/



Unveiling the biochemical pathway between Type 2 Diabetes Mellitus and early Alzheimer's disease

by

Shweta Tooray

(1363409)

Dissertation

Submitted in fulfilment of the requirements for the degree

Master of Science

in

Molecular and Cell Biology

in the Faculty of Science, University of the Witwatersrand, Johannesburg, South Africa

Supervisor: Dr. Eloise van der Merwe

August 2024

Declaration

I, Shweta Tooray (1363409), am a student registered for the degree of Master of Science by dissertation (MSc) in the academic year 2024.

I declare that this dissertation is my own, unaided work. It is being submitted for the Degree of Master of Science at the University of the Witwatersrand, Johannesburg. It has not been submitted before for any degree or examination at any other University.



(Signature of candidate)

08th day of August 2024 at Johannesburg

Table of Contents

List of Figures: 6

List of Tables: 7

List of Abbreviations: 8

Abstract 11

Acknowledgments 13

1. Introduction 14

1.1 Alzheimer's disease 14

1.2 Pathology of Alzheimer's disease 15

1.2.1 Hallmarks of Alzheimer's disease: extracellular senile plaques 16

1.2.2 Hallmarks of Alzheimer's disease: intraneuronal neurofibrillary tangles 17

1.3 Pathological pathways implicated in Alzheimer's disease 19

1.3.1 Oxidative stress 19

1.3.2 Mitochondrial dysfunction 20

1.3.3 Neuroinflammation 21

1.4 Type 2 Diabetes Mellitus and its link to Alzheimer's disease 22

1.4.1 The pathology of Type 2 Diabetes Mellitus and its link to Alzheimer's disease 23

1.5 Mitochondrial function and the link between Alzheimer's disease and Type 2 Diabetes Mellitus 25

1.6 The significance of telomere biology in Alzheimer's disease and Type 2 Diabetes Mellitus 26

1.6.1 Telomere biology 26

1.6.2 Telomere biology in Alzheimer's disease 27

1.6.3 Telomere biology in Type 2 Diabetes Mellitus 28

1.7 Glucose Lowering Drug (GLD) and its relevance to Alzheimer's disease 29

1.8 Rationale of the study 30

1.9 Scope of the study 30

2. Aims and objectives 31

2.1 Main aim 31

2.2 Specific objectives 31
3. Methods 32
3.1 Cell culture 32
3.2 Treatments 32
3.2.1 Glucose 33
3.2.2 Amyloid Beta 42 33
3.2.3 Glucose Lowering Drug (GLD) 34
3.3 Alamar Blue Assay 35
3.4 Glucose measurements 36
3.6 Aβ42 Enzyme-linked immunosorbent assay (ELISA) 37
3.7 DNA extraction 39
3.8 Agarose Gel Electrophoresis 40
3.9 Mitochondrial DNA content analysis by qPCR 41
3.10 Determination of telomerase activity by the qPCR TRAP assay 42
3.10.1 Non-denaturing protein Extraction 43
3.10.2 Modified telomere repeat amplification protocol (TRAP) based telomerase activity assay 44
3.11 Telomere length determination by qPCR 45
3.12 Statistical Analysis 46
4. Results 47
4.1 Hyperglycaemic-AD conditions caused cellular stress 47
4.2 Hyperglycaemic-AD conditions may lead to mitochondrial dysfunction over time 49
4.2.1 Hyperglycaemic-AD conditions increased mitochondrial activity over 10 days 49
4.2.2 Hyperglycaemic-AD conditions decreases mitochondrial DNA content after ten days 51
4.3 Constant hyperglycaemia resulted in decreased glucose uptake 54
4.4 Individual hyperglycaemic and Alzheimer's disease induced conditions increased ROS production over 24 hours whilst GLD prevented ROS spikes in the T2DM-AD cell model 55

4.5 GLD increases internalised Aβ42 and Aβ42 shedding under hyperglycaemic conditions compared to the T2DM cell model 58

4.6 Hyperglycaemic-AD conditions affect telomerase activity and telomere length: Hyperglycaemic-AD conditions increases telomerase activity and telomere length 60

5. Discussion 63

5.1 Hyperglycaemic-AD conditions caused cellular stress 64

5.2 Hyperglycaemic-AD conditions may lead to mitochondrial dysfunction over time 65

5.2.1 Hyperglycaemic-AD conditions increased mitochondrial activity over 10 days 65

5.2.2 Hyperglycaemic-AD conditions decreased mitochondrial DNA content 67

5.3 Constant hyperglycaemia resulted in decreased glucose uptake 70

5.4 Individual hyperglycaemic and Alzheimer's induced conditions increased ROS production over 24 hours whilst GLD prevented ROS spikes in the T2DM-AD cell model 72

5.5 GLD increases internalised Aβ42 and Aβ42 shedding under hyperglycaemic conditions compared to the T2DM cell model 76

5.6 Hyperglycaemic-AD conditions affect telomerase activity and telomere length 79

5.6.1 Hyperglycaemic-AD conditions increased telomerase activity 79

5.6.2 Hyperglycaemia-AD conditions increase telomere length 83

6. Conclusion 86

7. Future studies and limitation 88

8. References 89

9. Appendix 111

List of Figures:

Figure 1: The differences between a healthy and Alzheimer's disease brain. 14
Figure 3: Diagram illustrating the pathological pathways connecting Type 2 Diabetes Mellitus and Alzheimer's Disease. 24
Figure 4: Figure illustrating the connection between Type 2 Diabetes Mellitus and Alzheimer's Disease pathology through mitochondrial dysfunction. 26
Figure 5: The effects of hyperglycaemic Alzheimer's disease conditions on HEK293 cell morphology after two, five and ten days. 49
Figure 6: The effects of hyperglycaemic Alzheimer's disease conditions on HEK293 mitochondrial activity after two, five and ten days. 51
Figure 7. Hyperglycaemic and Alzheimer's induced conditions decreases total mitochondrial DNA content in HEK293 cells over ten days. 52
Figure 8. The effects of hyperglycaemic Alzheimer's disease conditions on glucose uptake in HEK293 cells after two, five and ten days. 54
Figure 9: Hyperglycaemic and Alzheimer's induced conditions increases ROS whilst GLD decreases spikes in ROS in a T2DM-AD HEK293 cell model. 57
Figure 11: The effects of hyperglycaemic Alzheimer's disease conditions on telomerase activity and telomere length in HEK293 cells using qPCR. 61
Figure 12: Agarose gel electrophoresis displaying DNA extracted samples from HEK293 cells post treatment. 112
Figure 13: Agarose gel electrophoresis showing temperature gradient PCR products after treatment in HEK293 cells. 113
Figure 14: Amplification curve and Melt peak analysis of the mtDNA and nuclear specific DNA sequence. 114
Figure 15: Amplification curves for telomerase activity in HEK293 cells post treatment. ...114
Figure 16: Amplification curve and Melt peak analysis for telomere length as well as the reference gene 36B4. 115

List of Tables:

Table 1: 1 % Agarose gel recipe 40
Table 2: 10 X TBE buffer pH 8.3 41
Table 3: PCR master mix 42
Table 4: qPCR master mix 42
Table 5: qPCR TRAP master mix 45
Table 6: List of Primer Sequences 111

List of Abbreviations:

Abbreviation	Meaning
µL	Microlitre
36B4	Acidic ribosomal phosphoprotein P0
8-OHdG	8-hydroxy-2'-deoxyguanosine
Aβ	Amyloid-β
A, C, G, T	Adenine, Cytosine, Guanine, Thymine
AD	Alzheimer's disease
AGE	Advanced glycation end products
AICD50	AβPP IntraCellular Domain
Akt	Protein kinase B
APP	Amyloid precursor protein
AQP1	Aquaporin-1
BAECs	Bovine aortic endothelial cells
BCA	Bicinchoninic acid
Bim	BCL2 homology domain 3-only protein
BSA	Bovine serum albumin
CDK-5	Cyclin-dependent kinase-5
CHAPS	3-[(3-Cholamidopropyl)dimethylammonio]-1-propanesulfonate
CNS	Central nervous system
DAG	Diacylglycerol
DMEM	Dulbecco's Modified Eagle's Medium
DMSO	Dimethyl sulfoxide
DNA	Deoxyribonucleic acid
DS	Double stranded
EDTA	Ethylene diaminetetraacetic acid
ELISA	Enzyme-linked Immunosorbent Assay
ETC	Electron transport chain
FBS	Foetal Bovine Serum
gDNA	genomic DNA
GLD	Glucose lowering drug

GSK-3β	Glycogen synthase kinase-3β
HEK293	Human Embryonic Kidney 293
HIF	Hypoxia-Inducible Factor
HLE	Human lens epithelial
HMEC-1	Human dermal microvascular endothelial
hTERC	Human Telomerase RNA Component
hTERT	Human Telomerase Reverse Transcriptase
HUVEC	Human umbilical vein endothelial cells
IDE	Insulin-degrading enzyme
IgG-HRP	Immunoglobulin G - Horseradish peroxidase
JNK	c-Jun NH2-terminal kinase
MAPK	Mitogen-activated protein kinase
MFN1/2	Mitofusin 1/2
MMP	Mitochondrial membrane potential
mRNA	Messenger Ribonucleic Acid
mtDNA	Mitochondrial DNA
MTT	3-(4,5-dimethylthiazol-2-yl)-2,5-diphenyltetrazolium bromide
NADPH	Nicotinamide adenine dinucleotide phosphate
NFT	Neurofibrillary Tangle
NP	Nanoparticle
NTC	No template control
PBS	Phosphate buffered saline
PCA	Protocatechuic acid
PCR	Polymerase Chain Reaction
PDLFs	Periodontal ligament fibroblast cells
Pen/Strep	Penicillin/streptomycin
PIP2	Phosphatidylinositol bisphosphate
PHD	HIF-prolyl hydroxylase
PI3K	Phosphatidylinositol 3-kinase
PKC	Protein kinase C
PP2A	Protein phosphatase 2A
PSEN1/2	Presenilin-1/2
PTP	Permeability transition pore

PVDF	Polyvinylidene fluoride
pVHL	von-Hippel Lindau tumor suppressor
qPCR	Quantitative Polymerase Chain Reaction
RAGE	Receptor for advanced glycation end products
RIPA	Radioimmunoprecipitation assay
RNA	Ribonucleic acid
ROS	Reactive Oxygen Species
SDS-PAGE	Sodium dodecyl sulphate - polyacrylamide gel electrophoresis
SH-SY5Y	Human neuroblastoma cells
T2DM	Type 2 Diabetes Mellitus
TNFα	Tumour necrosis factor-α
TNFR1/2	Tumour necrosis factor receptor 1/2
UV	Ultraviolet
WB	Western blot

Abstract

Research related to Alzheimer's Disease (AD) remains a focal point in neurodegeneration studies. This is due to the severity of AD and the clear necessity for non-palliative treatment approaches, as underscored by the high prevalence of the disease. The combined formation of extracellular senile plaques and neurofibrillary tangles (NFTs) plays a crucial role in the development of the cognitive and behavioural symptoms observed in individuals with AD. Despite extensive research efforts, discovering a definitive cure for the disease remains a challenge. Therefore, it is imperative to explore new perspectives and identify the upstream molecular mechanisms that contribute to the onset of the disease. Metabolic disorders are widely recognized as a significant risk factor for AD. Specifically, the metabolic syndrome, Type 2 Diabetes Mellitus (T2DM), is connected to neurodegeneration by promoting the accumulation of neurotoxins, inducing neuronal stress, affecting synaptic communication, and leading to brain atrophy. Individuals with T2DM have an increased risk of developing dementia, with hyperglycaemia exacerbating the impact of AD by causing mitochondrial dysfunction and oxidative stress through reactive oxygen species (ROS) formation, which are also present in AD. Additionally, patients with T2DM exhibit shorter telomeres linked to cell death, which is an associated risk factor for developing AD. These key pathways involved in connecting T2DM and AD were explored in the current study to enhance the understanding of the early events that precede AD. Glucose uptake was measured and observed to decrease over time as a potentially protective response of the cell. Subsequently, mitochondrial activity, assessed using the Alamar blue assay, was found to be heightened as an initial protective mechanism of Aβ42. This was later overwhelmed by the elevated ROS detected through a Total ROS assay kit, induced by the hyperglycaemic state of T2DM. In turn causing the amount of Aβ42 to become toxic and leading to a decline in mitochondrial DNA (mtDNA) over time as measured through qPCR. Additionally, the increases in ROS induced by hyperglycaemia resulted in oxidative damage to telomeres. Simultaneously, Aβ42 physically hinders telomere-telomerase binding, leading to reduced telomerase activity and consequently, shorter telomeres. Furthermore, this study reveals, for the first time, that the novel glucose-lowering drug (GLD) caused an increase in Aβ42 production in the T2DM cell model, whilst effectively decreasing ROS production over a 24-hour period compared to the untreated cell model. The rise in Aβ42 levels caused by GLD could potentially be working to prevent the increase in hyperglycaemia-induced ROS through its metal chelating antioxidant properties by scavenging ROS, in the

presence of oxidative stress associated with T2DM. These findings are indicative of an appealing function of GLD by reducing ROS and thereby impeding the progression towards AD. Hence making GLD an attractive therapeutic option for the treatment and/or prevention of AD.

Acknowledgments

I would like to express my sincerest gratitude to my supervisor Dr. Eloise van der Merwe, for offering me the chance to work in her lab as well as for the continuous guidance and patience she has provided during my Master's programme.

I would like to give a special thank you to my mentors Dr. Tyrone Otgaar, Dr. Monique Bignoux and Dr. Martin Bernert for the enormous amount of advice, guidance and support they have provided since Honours.

Thank you to all my colleagues at the Cell Biology and Signalling Research Laboratory for their support and friendship.

I would like to convey my deepest appreciation to my family for their unwavering love, support, and constant presence in offering advice and words of encouragement.

Financial aid:
National Research Foundation (NRF) – MND210621613790 (2022-2023)

1. Introduction

1.1 Alzheimer's disease

Alzheimer's disease (AD) is a detrimental neurological and neurodegenerative disease that is a prevalent cause of dementia amongst the elderly. While there are a few palliative therapeutic treatments available for AD, there is currently no known cure for the condition (Madhusudhanan *et al.,* 2020). The World Alzheimer Report, 2019, confirmed that over 55 million individuals were diagnosed with some form of dementia, with approximately 10 million new cases reported annually (WHO, 2021). Dementia is additionally ranked as the seventh leading cause of death and the economic burden has amounted to 1.3 trillion US dollars globally as of 2019 (WHO, 2021). It was reported that approximately 187 000 people older than 60 years of age were living with AD in South Africa. However, it was further established that due to limited published prevalence data, this statistic was an underestimation (de Jager *et al.,* 2017). Nonetheless, these stats are alarming since AD can encompass irreversible neurodegeneration, brain damage as well as reduced brain size (FIg. 1) which ultimately results is death (Madhusudhanan *et al.,* 2020).

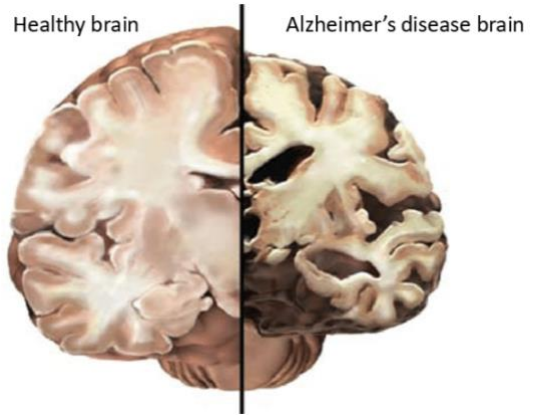

Figure 1: The differences between a healthy and Alzheimer's disease brain.
The image shows a comparison between a healthy human brain (left) and an Alzheimer's disease brain (right). Herein, the AD brain appears smaller in size as a result of brain atrophy. (Adapted from Kidd, 2008)

The symptoms of the neurodegenerative disease vary depending on the stage of the disease. AD can be categorized into presymptomatic, mild, and dementia based on the level of cognitive impairment. The primary and frequently observed symptom at the initial preclinical stage is episodic short-term memory loss (Kumar *et al.,* 2018). Following this memory impairment, individuals may experience difficulties in problem-solving and executive functioning. These challenges can lead to difficulties with multitasking and abstract thinking (Kumar *et al.,* 2018). Thereafter, language disorders and visuospatial skill impairment may occur. Whilst neuropsychiatric symptoms are common in the mid to late stages. Late in the disease, individuals may experience difficulty performing learned motor tasks as well as extrapyramidal motor signs, followed by primitive reflexes and complete dependence on caregivers (Kumar *et al*., 2018). Understanding the mechanisms behind AD is of utmost importance. Despite extensive efforts, finding a cure for the disease has proven to be unsuccessful thus far. Therefore, it is necessary to approach the problem from new perspectives (Korczyn, 2012). It is unlikely that targeting downstream clinical manifestations and pathology alone can cure or prevent the progression of AD. Epidemiological studies have identified both genetic and environmental factors that can be targeted as a concerted effort to combat AD upstream of the disease (Korczyn, 2012).

1.2 Pathology of Alzheimer's disease

AD can be classified into two forms, namely, late-onset AD occurring in individuals aged 65 years or older and early-onset AD affecting individuals younger than 65. Moreover, AD can be categorized as either familial or sporadic. Familial cases involve the inheritance of mutations, are primarily early-onset AD and affect less than 5% of the AD population (Piaceri *et al*., 2013). These cases are characterized by autosomal mutations inherited in genes expressing proteins associated with beta-amyloid (Aβ) aggregates, namely, amyloid precursor protein (APP), presenilin-1 (PSEN1), or presenilin-2 (PSEN2) (Piaceri *et al*., 2013). Mutations in the APP gene can lead to an increase or alteration in the production of Aβ, as these mutations often occur near the cleavage site of α-secretase or γ-secretase (Fig. 2). Whereas most mutations in the genes encoding PSEN1 or PSEN2, which encode the major component of γ-secretase responsible for the sequential proteolytic cleavage of APP, lead to an increased production of toxic Aβ fragments (Piaceri *et al*., 2013).

The majority (over 95%) of AD cases are classified as sporadic. This form of the disease is considered to be multi-factorial, with both genetic predisposition and environmental factors contributing to its development and progression. Researchers suggest that environmental risk factors may play a role during the pre-clinical phase of the disease, occurring decades before the onset of clinical dementia (Chakrabarti *et al*., 2015). One such environmental risk factor is metabolic risk factors, which are being studied to understand their biological implications in the pathogenesis of the disease and potential therapeutic strategies. This area of research holds great promise for the future development of treatment strategies for AD, as identifying clear metabolic risk factors for AD would provide an opportunity to intervene and slow down the progression of the disease (Chakrabarti *et al*., 2015).

1.2.1 Hallmarks of Alzheimer's disease: extracellular senile plaques

There are two fundamental hallmarks of AD, the first neuropathological marker being the extracellular senile plaques formed by the hydrophobic peptide, Aβ (Madhusudhanan *et al.,* 2020). These plaques are more abundantly composed of the Aβ42 isoform, due to its characteristics of being both insoluble and having a higher fibrillization rate. Additionally, in line with being neurotoxic, these Aβ oligomers can elicit synaptic and neuron loss (Serrano-Pozo *et al.,* 2011). Under physiological conditions, the transmembrane glycoprotein APP follows the non-amyloidogenic pathway (Fig. 2). Herein APP initially targeted by α-secretase, resulting in the generation of soluble α-APP fragment (also known as sAPPα) and the C-terminal fragment α, CTFα (also known as CTF 83). Subsequently, CTF 83 is cleaved by γ-secretase, leading to the production of non-toxic P3 and AICD50 fragments (Madhusudhanan *et al.,* 2020). Normally, APP forms an essential part of brain synapses, whilst Aβ is involved in neuronal survival and growth (Madhusudhanan *et al.,* 2020). Conversely, under pathological conditions, genetic, epigenetic, environmental and age-related factors promote a metabolic shift favouring proteolytic amyloidogenic cleavage of APP (Fig. 2). Wherein APP cleaved sequentially, initially by β-secretase, which removes the N-terminus sAPPβ fragment (Caetano *et al.,* 2013). Thereafter, cleavage at the C-terminus by γ-secretase produces the 4.2 kDa and 40 or 42 amino acid Aβ peptide, which is then exported into the extracellular space (Caetano *et al.,* 2013 and Madhusudhanan *et al.,* 2020). In AD imbalanced manufacturing or breakdown of the protein can lead Aβ to build up and polymerise into synaptotoxic soluble intermediate

oligomers, or the more predominant plaque constituent, β-sheet pleated amyloid fibrils (mostly Aβ42) (Madhusudhanan *et al.,* 2020 and Serrano-Pozo *et al.,* 2011).

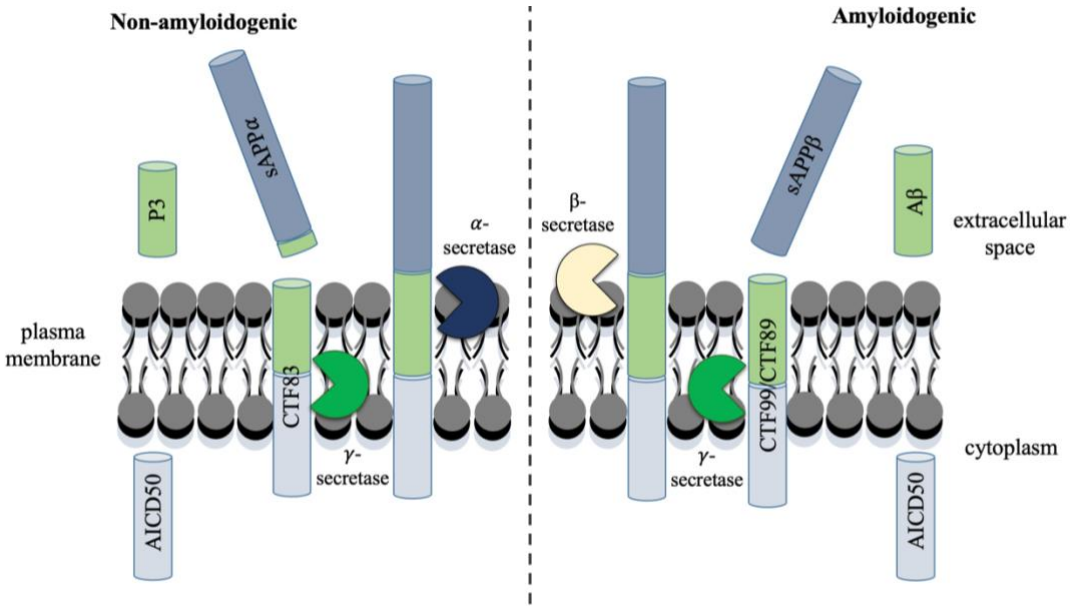

Figure 2: Schematic diagram displaying the non-amyloidogenic and amyloidogenic processing of APP.

During the non-amyloidogenic pathway (left) APP is cleaved sequentially, initially by alpha-secretase, which removes the N-terminus sAPPα ectodomain fragment, producing CTF 83. Thereafter, cleavage at the C-terminus by gamma-secretase, removes the intracellular C-terminal fragment (AICD50) producing the P3 peptide, which is then exported into the extracellular space. Alternatively, during the amyloidogenic pathway (right) APP is cleaved sequentially, initially by beta-secretase, which removes the N-terminus sAPPβ ectodomain fragment. Thereafter, cleavage at the C-terminus by gamma-secretase, removes the AICD50 fragment producing the Aβ peptide, which is then exported into the extracellular space.

1.2.2 Hallmarks of Alzheimer's disease: intraneuronal neurofibrillary tangles

The other hallmark of Alzheimer's disease is the intraneuronal neurofibrillary tangle (NFT) formation (Serrano-Pozo *et al.,* 2011). This is owed to misfolding and subsequent aggregating, of the microtubule binding protein, Tau, after hyperphosphorylation (Avila, 2006 and Madhusudhanan *et al.,* 2020). The binding of Tau to microtubules is regulated by its phosphorylation at various sites. In pathological situations the kinases, cyclin-dependent kinase-5 (CDK-5), glycogen synthase kinase-3β (GSK-3β), and mitogen-activated protein kinases (MAPKs) play a role in the excessive phosphorylation of Tau. This causes Tau protein to detach from microtubules and leads to the formation of NFTs (Zhang *et al*., 2021). These

NFTs result in elevated cytoskeletal proteins, disturbances in axonal transport, neuronal death, decreased connections between neurons and neuronal degeneration. Progressively, these plaques and NFTs lead to the cognitive and behavioural impairments of AD. Contrastingly, under regulated physiological conditions, Tau protein functions to support the neuronal cytoskeleton. Whereas, in the case of AD Tau protein aggregates and bypasses autophagy resulting in progressive protein accumulation (Madhusudhanan *et al.,* 2020). In turn, allowing for Tau deposits which have been reported to bring about cellular oxidative stress and mitochondrial reactive oxygen species (ROS) production, which further activates programmed cell death signals ultimately killing neuronal cells (Madhusudhanan *et al.,* 2020). Furthermore, without the regeneration of these cells, as in the case of mature neurons, these events decrease connections between neurons affecting memory retention and lead to dementia (Madhusudhanan *et al.,* 2020).

Additionally, the severity of NFT-AD pathology is measured by the six Braak stages of disease propagation, which can be differentiated based on the location of tangle-bearing neurons and the extent of changes (Braak and Braak, 1991). Stages I and II, which are clinically silent, exhibit limited NFTs in the transentorhinal and entorhinal cortex and are typically linked to normal cognitive profiles. Limbic stages III and IV mark the onset of AD, with involvement of limbic regions like the hippocampus (Braak and Braak, 1991). Stages V and VI in the Braak classification represent fully developed AD, characterized by the highest number and spread of NFTs and often associated with severe cognitive and functional decline (Braak and Braak, 1991; Malek-Ahmadi *et al*., 2020). Aβ furthermore enhances Tau hyperphosphorylation by facilitating the activation of CDK-5 and GSK-3β. Tau is phosphorylated by CDK-5 resulting in conformational changes that makes other sites more easily recognized and accessible to GSK-3β for subsequent phosphorylation (Singh *et al*., 1995; Zheng *et al*., 2002). GSK-3β is closely associated with Aβ, plays a significant role in the phosphorylation of Tau, and exacerbates Tau-associated neurotoxicity (Zhang *et al*., 2021). Aβ aggregation enhances GSK-3β and CDK-5 activity, leading to the hyperphosphorylation of Tau. This, in turn, causes Tau to dissociate from microtubules, elevating the binding affinity among Tau monomers. Consequently, neurotoxic Tau oligomers are formed, increasing the propensity to form NFTs and contributing to neurofibrillary degeneration (Shafiei *et al*., 2017; Zhang *et al*., 2021).

Aβ also triggers the cleavage of Tau by caspase-3, resulting in a truncated Tau lacking its C-terminal which assembles more rapidly into filaments than full-length Tau (Gamblin *et al*.,

2003). Additionally, Aβ activates calpain-1 in hippocampal neurons, leading to the generation of Tau fragments. Cleaved Tau self-aggregates and misfolds, forming soluble oligomers which act as seeds to induce the misfolding of Tau. These neurotoxic Tau oligomers can be disseminated between neurons leading to neuroinflammation (Zhang *et al*., 2021). Although Aβ accumulation and Tau hyperphosphorylation have been described in AD, the upstream events leading to these markers are not fully understood. Therefore, by uncovering the upstream molecular mechanisms involving these hallmark proteins eventually leading to AD new drug targets can be brought to light, which can pave the way for novel and effective therapeutic tools to prevent, manage or treat the disease.

1.3 Pathological pathways implicated in Alzheimer's disease

1.3.1 Oxidative stress

Mitochondrial damage and oxidative stress have been implicated in the early pathogenesis of neurodegenerative diseases (Guo *et al*., 2013). Oxidative stress is marked by the excessive production of ROS such as superoxide anion, hydrogen peroxide, and the hydroxyl radical (Nita and Grzybowski, 2016). The mitochondrial electron transport chain (ETC) utilizes a hydrogen atom from the oxidation of organic acids with atomic oxygen to produce water. Normally, approximately 1-5 % of oxygen is converted to ROS, indicating that the majority of intracellular ROS production is attributed to mitochondria (Wei *et al*., 2001). Mitochondrial ROS production are primarily generated at two locations within the ETC, specifically at complex I and complex III. Consequently, free radical attacks occur directly within the mitochondrial respiratory chain (Selivanov *et al*., 2011). Excessive production of ROS can lead to mitochondrial damage, such as mitochondrial DNA (mtDNA) mutations and damage, impairment of the mitochondrial respiratory chain, disruption of mitochondrial membrane permeability, and disturbances in Ca^{2+} balance (Guo *et al*., 2013).

Herein, ROS can damage proteins involved in the respiratory chain by inducing oxidative modifications, such as protein carbonylation through the addition of carbonyl groups to amino acid side chains (Andrés Jua *et al*., 2021; Guo *et al*., 2013). This oxidative damage disrupts the structural integrity of the respiratory chain proteins cytochrome c oxidase, NADH dehydrogenase, and Adenosine triphosphate (ATP) synthase. Ultimately, this process

contributes to the loss of their biological activity leading to the impairment of mitochondrial energy production (Andrés Jua *et al*., 2021; Guo *et al*., 2013). These, hydroxyl radicals have the ability to directly damage DNA bases, hence making mtDNA especially vulnerable to oxidative stress-related ROS attacks (Guo *et al*., 2013). The continued damage to mtDNA eventually results in mutations in the mitochondrial genome, leading to additional mitochondrial dysfunction that initiates and exacerbates diseases. Normally, calcium ion fluxes are effectively regulated across the plasma membrane and within intracellular compartments (Guo *et al*., 2013). Excessive generation of ROS can directly damage Ca^{2+}-regulating proteins, leading to increased levels of Ca^{2+}, that disrupt the Ca^{2+} balance. The resulting increase in calcium cation levels can disrupt mitochondrial potential, leading to the generation of superoxide ion radicals, creating a harmful cycle. When mitochondria are exposed to an excess of these ions, they undergo mitochondrial permeability transition, leading to swelling and rupture of the outer mitochondrial membrane (Ross, 2012). Furthermore, ROS generated in the mitochondria enhance Ca^{2+} uptake and increase membrane permeability, triggering the release of cytochrome c and initiating apoptosis (Ross, 2012). Therefore, prolonged high levels of intracellular Ca^{2+} can lead to cell death and contribute to neuronal degeneration.

Furthermore, ROS produced by mitochondria are transported to the cytoplasm, where they trigger β-secretase activation and aid in the cleavage of APP. This process results in increased levels of Aβ protein and protein deposition, which may lead to neuronal dysfunction, initiating neurodegeneration and ultimately culminating in AD. Aβ can interact with mitochondria, resulting in additional mitochondrial dysfunction by binding to alcohol dehydrogenase and hindering cytochrome c oxidase function. This leads to a decrease in ATP production, ultimately resulting in cell death due to insufficient ATP levels. Hence, it is evident that dysfunction in mitochondria together with oxidative stress plays a role in neuronal damage and neurodegeneration in AD.

1.3.2 Mitochondrial dysfunction

Mitochondria play a crucial role in energy metabolism and significantly influence neuronal function and survival (Jiang *et al*., 2018). It is hypothesized that mitochondrial dysfunction in AD, characterized by mitochondrial fragmentation resulting from an imbalance in fission and fusion processes, contributing to neurodegenerative alterations in hippocampal and cortical

neurons (Jiang *et al*., 2018). Briefly, mitochondrial fusion is coordinated by the mitofusin proteins MFN1 and MFN2 joining two mitochondria together. While mitochondrial fission separates a single organelle two or more independent structures (Scott and Youle, 2010). Excessive fission results in a decrease in mtDNA copy number, leading to decreased expression of crucial oxidative phosphorylation proteins that play a role in fuelling cell signalling and neuronal activity processes such as postsynaptic currents, synaptic action potentials and neurotransmitter release, ultimately causing mitochondrial dysfunction (Bergman and Ben-Shachar, 2016; Jiang *et al*., 2018).

Control of microglial activation has been linked to neuronal mitochondria, where neuroinflammation is correlated with mitochondrial dysfunction via the outer mitochondrial membrane GTP-binding neuronal protein MFN2, which plays a role in mitochondrial fusion and function (Harland *et al*., 2020). Normally, neuronal MFN2 suppresses microglial activation, prevents mitochondrial fragmentation in neurons and upregulates the neuronal expression of the microglial inhibitor CX3CL1. Interestingly, MFN2 is reduced in patients with AD leading to potent pro-inflammatory cytokine release and neuroinflammation (Harland *et al*., 2020). Hence it is evident that mitochondrial dysfunction through decreased mtDNA copy number and neuroinflammation results in substantial neurodegeneration in the hippocampus and cortex. Furthermore, mitochondrial dysfunction inevitably leads to elevated oxidative stress which may further damage mitochondrial ultrastructure worsen mitochondrial dysfunction (Jiang *et al*., 2018).

1.3.3 Neuroinflammation

Microglia are the main immune effector cells in the central nervous system (CNS) and play a critical role in neuroinflammatory responses in AD, thereby making neuroinflammation another attractive research area. In their inactive state, microglial cells continuously monitor their surroundings without affecting neurons (Xie *et al*., 2022). However, in the presence of inflammatory stimuli microglia are activated, their morphology and functions change, leading them to migrate to injury sites where they trigger an innate immune response (Schwabenland *et al*., 2021). Prolonged microglia activation can inhibit adult neurogenesis and lead to the release of neurotoxic agents like ROS and the pro-inflammatory cytokine Tumour necrosis factor (TNF) through the p38/MAPK signalling pathway, causing neuronal cell damage and

death (Bachstetter *et al*., 2011; Heppner *et al*., 2015; Xie *et al*., 2022). These neuronal immune cells express pattern recognition cell surface receptors (PRRs), which recognize misfolded proteins like Aβ and initiate an immune response.

Aβ accumulation is influenced by the balance between its production and clearance, involving several pathways. These include phagocytosis and macropinocytosis by microglia, which is the regulated form of endocytosis that mediates the uptake of soluble Aβ, as well as Aβ degradation by Aβ-degrading enzymes like, insulin-degrading enzyme (IDE) (Hardy and Selkoe, 2002; Rabinovici, 2021; Xie *et al*., 2022). Furthermore, aging studies in mice show that microglial cells exhibit reduced expression of Aβ-degrading enzymes, while their capacity to produce pro-inflammatory cytokines remains intact. The systemic inflammatory cytokine TNF indirectly affects Aβ pathology by regulating immune cell trafficking and glial responses in the brain (Xie *et al*., 2022). Herein, prolonged exposure to immune-stimulating lipopolysaccharide (LPS) impairs microglial phagocytosis of Aβ, leading to increased Aβ deposition in AD mice models (Holmes, 2013; Xie *et al*., 2021). Therefore, it is clear that neuronal inflammation contributes to the nondegenerative pathology of AD through persistent microglial activation, leading to the accumulation of Aβ in the brain.

1.4 Type 2 Diabetes Mellitus and its link to Alzheimer's disease

The previously described Aβ and Tau pathologies are downstream symptoms of AD. To prevent or slow down the progression of the disease, it is necessary to address the upstream aetiology (Korczyn, 2012). In this regard, researchers have identified metabolic disorders as one of the risk factors associated with AD (Nguyen., 2020). Wherein the metabolic syndrome, Diabetes Mellitus is linked to neurodegeneration through the accumulation of neurotoxins, neuronal stress, synaptic communication, and brain atrophy (Correia *et al*., 2012). Type 2 Diabetes Mellitus (T2DM) can be characterized by chronic hyperglycaemia, which is a state of dysregulated glucose metabolism, causing increased blood glucose levels (Barbagallo and Dominguez, 2014). By itself hyperglycaemia poses as a risk factor for both cognitive decline as well as dementia (Barbagallo and Dominguez, 2014). This is owed to persistent hyperglycaemia often leading to damage or disabling of biological systems by various mechanisms, in turn promoting neurodegeneration (Goyal and Jialal, 2020). Moreover, it is thought that insulin resistance, characterized by the diminished biologic response of hepatic

tissues with insulin receptors to insulin stimulation, impairs glucose disposal resulting in hyperglycaemia. It is believed that the insulin resistance precedes and contributes to the development T2DM by up to 15 years (Freeman *et al*., 2023).

Similar to AD, the incidence of T2DM has also been described to increase with age, with over 536 million people diagnosed with diabetes globally in 2021 (CDC, 2014; Kukull *et al.,* 2002; Sun *et al.,* 2021). This global burden is expected to rise to 783.2 million by the year 2045 (Sun *et al.,* 2021). Whilst the estimated global health expenditures amounted to 966 billion USD in 2021 and are expected to reach to 1.054 trillion USD by the year 2045 (Sun *et al.,* 2021). This is significant with respect to identifying upstream AD molecular pathways, as clinical studies correlate T2DM with the neurodegenerative disease, suggesting a physiopathological link (Barbagallo and Dominguez, 2014). Wherein, individuals suffering with diabetes possess a 65% greater risk of developing AD and T2DM patients displayed a greater risk of developing dementia, in addition to having an increased incidence rate for cognitive dysfunction (Arvanitakis *et al.,* 2004; Barbagallo and Dominguez, 2014).

1.4.1 The pathology of Type 2 Diabetes Mellitus and its link to Alzheimer's disease

However, how the metabolic disorder leads to the neurodegenerative disease is not fully understood. Although, some of the links that have been shown include oxidative stress, inflammation, advanced glycation end products (AGE), as well as autophagic dysfunction (Fig. 3) (Chatterjee and Mudher, 2018). In this regard, a common mechanism of glucose toxicity in T2DM involves oxidative stress caused by ROS formation and reduced ROS removal systems. In turn, leading to mitochondrial damage and dysfunction, which triggers apoptotic signals and initiates neuronal cell death (Butterfield *et al.,* 2014; Chatterjee and Mudher, 2018). Similarly, glucose toxicity can lead to inflammation and activation of the immune system, resulting in the brain immune cells, microglia, upregulating the proinflammatory cytokine, TNFα (Chang *et al.,* 2017; Chatterjee and Mudher, 2018). TNFα promotes the amyloidogenic cleaving of APP into Aβ, by enhancing the expression of β- and γ-secretases, as well as hindering the removal of Aβ by microglia dysfunction, wherein microglia Aβ-binding receptors and Aβ-degradation enzymes are downregulated (Hickman *et al.,* 2008; Liao *et al.,* 2004; Ren *et* al., 2021; Yamamoto *et al.,* 2007).

Additionally, the oxidative stress caused by the dysregulated metabolism of glucose in T2DM activates glycation reactions. This promotes glycation through the production and accumulation of AGE products which are linked with the cognitive decline in AD (Li *et al*., 2013). Wherein elevations in AGE products within the T2DM brain have been associated with impaired Aβ42 removal and promote its aggregation (Moreira *et al*., 2003). These AGE products additionally increase the expression of their receptors or RAGE in AD brains causing subsequent pro-inflammatory cytokine activation, further escalating cognitive decline and memory impairment through vascular complications (Choi *et al*., 2014; Liu *et al*., 2009; Solito and Sastre, 2012; Srikanth *et al*., 2011). Post-translational O-GlcNAcylation in the brain acts as a neuroprotective mechanism by counteracting Aβ neuronal toxicity. This is achieved by reducing the formation of Aβ through the inhibition of γ-secretase activity (Hanover and Wang, 2013). The hyperglycaemic conditions of T2DM elevate O-GlcNAcylation, however, the reduction of γ-secretase activity is offset by the accumulation of neurotoxic AGE products promoting neurodegeneration (Hanover and Wang, 2013). Hence, considering that T2DM can initiate and coincide with AD pathogenesis through multiple mechanisms, it becomes apparent that investigating the pathways connecting T2DM to upstream AD could be advantageous in discovering new biomarkers.

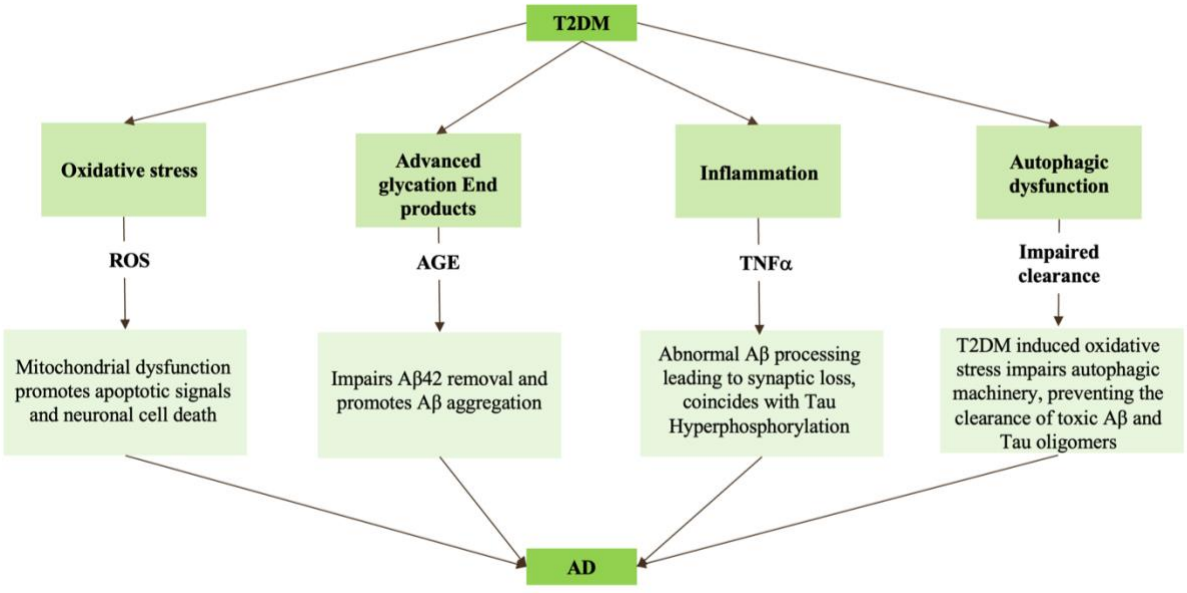

Figure 3: Diagram illustrating the pathological pathways connecting Type 2 Diabetes Mellitus and Alzheimer's Disease.

Pathways linking T2DM and AD include oxidative stress, inflammation, advanced glycation end products (AGE), as well as autophagic dysfunction. Glucose toxicity in T2DM leads to oxidative stress through ROS formation and reduced ROS removal systems, causing mitochondrial damage and

dysfunction, ultimately triggering apoptotic signals and neuronal cell death. Additionally, glucose toxicity can induce inflammation and activate the immune system, leading to microglia upregulating the proinflammatory cytokine TNFα. TNFα promotes the amyloidogenic cleaving of APP into Aβ by enhancing the expression of β- and γ-secretases, while hindering Aβ removal by microglia dysfunction. This results in downregulation of microglia Aβ-binding receptors and Aβ-degradation enzymes. Together these pathways contribute to neurodegeneration and AD pathology.

1.5 Mitochondrial function and the link between Alzheimer's disease and Type 2 Diabetes Mellitus

One pathway linking the diseases in early pathogenesis is through increased ROS promoting oxidative damage (Fig. 4) (Sharma *et al*., 2021). Mitochondria generate ATP through oxidative phosphorylation, which is subsequently used for cellular functions including, neurotransmitter production and synaptic plasticity (Pagani and Eckert, 2011). Hence, mitochondrial number is high in neurons and synapses. Neurons are additionally dependent on mitochondrial function for energy production, as neurons have a limited capacity to perform glycolysis. However, mitochondria are the major producers of ROS leading them to being a potential centre of ROS toxicity. Accordingly, with age, mitochondria accumulate oxidative damage and subsequently cause the formation of free radicals such as ROS, as a result of electrons leaking during ATP production (Pagani and Eckert, 2011). Moreover, the hyperglycaemic environment characteristic of T2DM triggers the activation of the ETC and glycation within the mitochondria, leading to the generation of ROS as a by-product, initiating a cascade effect. Here ROS promotes the expression of both β- and γ-secretases as well as their activity, in turn exacerbating Aβ production (Pagani and Eckert, 2011; Payne and Chinnery, 2015; Macdonald *et al*., 2018). These Aβ oligomers then translocate into mitochondria and impair mitochondrial function further promoting ROS, which can activate kinases such as GSK-3β that hyperphosphorylate Tau, leading to NFT formation, synaptic dysfunction, apoptosis and ultimately Alzheimer’s disease (Agrawal and Jha, 2020).

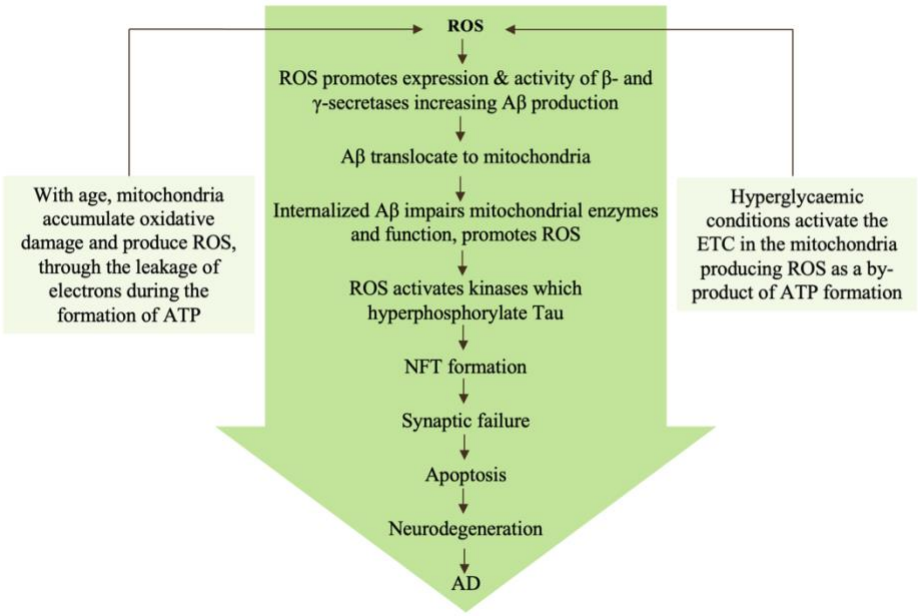

Figure 4: Figure illustrating the connection between Type 2 Diabetes Mellitus and Alzheimer's Disease pathology through mitochondrial dysfunction.

The T2DM-hyperglycaemic environment activates the ETC and glycation in mitochondria, resulting in ROS production. ROS triggers the expression and activity of β- and γ-secretases, increasing Aβ production. Aβ oligomers move to mitochondria, impairing function and generating more ROS. This cycle can activate kinases like GSK-3β, leading to Tau hyperphosphorylation, NFT formation, synaptic dysfunction, apoptosis, and ultimately Alzheimer's disease.

1.6 The significance of telomere biology in Alzheimer's disease and Type 2 Diabetes Mellitus

1.6.1 Telomere biology

As previously mentioned, there are numerous factors that contribute to neurotoxicity and subsequently, AD, these include oxidative stress, mitochondrial dysfunction and hyperglycaemia (Gendron and Petrucelli, 2009; Fani *et al*., 2020). In addition to this, previous studies have found that telomere length, could also be a contributing risk factor towards AD (Fani *et al*., 2020). Telomeres are found at the ends of chromosomes and are made up of double stranded DNA (dsDNA) repeats and proteins. In humans these dsDNA sequences are ~10-15kbp TTAGGG repeats (Allshire *et al*., 1989). Telomeres serve a protective function by working to stabilize chromosomes, prevent chromosome end shortening and subsequent loss of genomic DNA (gDNA). The progressive shortening of chromosome ends occurs with each successive round of cellular division, resulting in the erosion of gDNA as a natural process of

ageing, as a result shorter telomeres are more frequent in the elderly (Shammas, 2011). Normal somatic cells may divide until they reach the “Hayflick limit”. This limit describes the capacity of a cell to divide, which is predisposed by telomere length, and is a consequence of shortened telomeres (Shay and Wright, 2011). Wherein, a substantial number of cells with shortened telomeres enter replicative senescence, a state in which metabolically active cells are unable to replicate further, resulting in the permanent loss of the cell's proliferative capacity and inducing growth arrest (Campisi and Di Fagagna, 2007; Hayflick and Moorhead, 1961; Lu *et al*., 2013; Shay and Wright, 2011). Telomeres are elongated by the enzyme, telomerase, which is comprised of two essential subunits, namely, the human telomerase RNA component (hTERC) which acts as an RNA template for the human telomerase reverse transcriptase component (hTERT). Wherein, hTERT acts as the catalytic subunit and adds telomeric repeats to the telomere ends, through a controlled process of telomeric synthesis (Glasspool *et al*., 2005).

1.6.2 Telomere biology in Alzheimer’s disease

Telomerase, through its reverse transcription activity, elongates telomeres to counteract the attrition of chromosome ends. This process helps safeguard chromosome ends from DNA damage and degradation, thereby preventing the accumulation of shortened telomeres that can result in telomere dysfunction (Harley *et al*., 1990; Lee and Pellegrini, 2022). Most neurons do not exhibit telomerase activity. In the brain telomerase activity is primarily observed in neural stem cells located in specific regions like the hippocampal dentate gyrus (Lee *et al*., 2012). The hippocampus plays a crucial role in spatial cognition and is implicated in neurodegenerative disorders like AD (Miwa *et al*., 2016). The regulation of telomere length involves a combination of telomerase-dependent elongation and telomere trimming events (Fani *et al*., 2020). Imbalanced telomere length has been associated with an increased risk of amnestic mild cognitive impairment (Fani *et al*., 2020). Specifically, increased risk of AD has been associated with both overly elongated telomeres, which accumulate DNA damage, and significantly shortened telomeres which have been linked to cell death (Fani *et al*., 2020). When telomeres become shortened, they trigger molecular mechanisms associated with DNA damage responses, which can contribute to cellular senescence or apoptosis. As a result, shortened telomeres are recognized as one of the key indicators of aging, as they are associated with various aging-related characteristics including a decline in regenerative capacity (López-Otín *et al*., 2023). Notably, telomere shortening has been strongly associated with risk of AD. A

study done on leukocytes proposed that with a single kilobase pair reduction in telomere length, the probability of developing AD was exacerbated by 21% (Honig *et al*., 2012).

There is evidence suggesting that Aβ can inhibit telomerase activity, by the physical binding of Aβ oligomers to the telomeric TERT-TERC complex. This obstruction by Aβ could explain the shortened telomeres associated with AD (Wang *et al*., 2015). While there is more understanding about the potential connection between shorter telomeres and an increased risk of AD, less is known about the biological relationship between longer telomere length and the disease (Fani *et al*., 2020). The hypothesis suggests that longer telomeres could be associated with the presence of extracellular plaques. This association may occur from the resulting decrease in intracellular Aβ levels, due to the increase in extracellular Aβ transport for plaque formation. Thereby reducing intracellular Aβ-mediated telomerase inhibition, consequently leading to longer telomeres (LaFerla *et al*., 2007; Mahoney *et al*., 2019; Wang *et al*., 2015). Additionally, telomeres that are excessively elongated can become fragile and prone to accumulating DNA damage (Fani *et al*., 2020). Further investigation is needed to establish the exact biological connection between excessively elongated telomeres and the heightened risk of developing AD.

1.6.3 Telomere biology in Type 2 Diabetes Mellitus

These findings link back to T2DM, where studies have found that individuals suffering from diabetes, display shorter telomeres. Thereby, suggesting that the disease could potentially cause telomere shortening, possibly by altering telomerase activity (Garcia-Martin *et al*., 2018). In conjunction with this and as previously stated, individuals suffering with T2DM display increased levels of cellular glucose (hyperglycaemia), which mediates the dysfunction and destruction of pancreatic beta cells through cellular injury, and reduces sensitivity to insulin (Zhao *et al*., 2013). In turn, the hyperglycaemic conditions induce ROS through glucose toxicity, further promoting oxidative stress (Kaneto *et al*., 2010). This can be detrimental, since telomeres are Guanine (G) rich, making them prone to oxidative stress, leading to DNA damage, decreased telomerase activity and subsequent telomere shorting (Lu *et al*., 2013; Singh *et al*., 2019; Zhao *et al*., 2013). Consequently, this telomere shortening as a result of hyperglycaemia could be increasing the potential risk for AD development (Honig *et al*., 2012;

Kaneto *et al*., 2010). Therefore, validating the further investigation of upstream AD using T2DM as a causative starting point.

1.7 Glucose Lowering Drug (GLD) and its relevance to Alzheimer's disease

On account of the previously proposed links between the neurological and metabolic disorder, the effects of a novel glucose lowering drug (hereafter referred to as GLD due to IP protection) were investigated. GLD is undergoing trials in T2DM pathophysiology and is said to reduce oxidative stress through the reduction of hepatic glucose production, as well as by causing increased glucose uptake in muscles (Fouqueray *et al*., 2014). Results from an animal study demonstrated that GLD protects mitochondrial function from oxidative stress, which normalized both insulin sensitivity and glucose tolerance (Vial *et al*., 2015). Moreover, the drug was found to protect against high glucose induced apoptosis of β-cells (Fouqueray *et al*., 2014). GLD was investigated in the human dermal microvascular endothelial (HMEC-1) cell line with respect to hyperglycaemia-induced cell death. During the study it was found that the drug prevents cell death using the mitochondrial inner membrane Ca^{2+} sensitive channel, permeability transition pore (PTP) (Detaille *et al*., 2016). GLD prevents PTP from opening by increasing the required amount Ca^{2+} needed to allow the opening of PTP. This in turn prevents the release of proapoptotic mitochondrial proteins such as cytochrome c. Which would otherwise promote cell death once entering the cytosol. By the drug keeping the channel closed, ATP synthesis and mitochondrial respiration is not halted, thus not causing increased ROS production (Detaille *et al*., 2016). The proposed mechanism reported is that GLD decreases the production of ROS caused by the generation of superoxide at the respiratory chain's reversible proton pump, complex I, which gets converted into hydrogen peroxide by the enzyme superoxide dismutase. GLD promotes reverse electron flux through the proton pump and thus reduces ROS production (Detaille *et al*., 2016). Therefore, GLD could potentially be used to address the increase in ROS associated with the hyperglycaemic conditions of T2DM leading to decreased precursor-AD pathologies and in turn potentially be used as a therapeutic for AD.

1.8 Rationale of the study

Given the severity of AD and the clear necessity for non-palliative treatment approaches, as underscored by the high prevalence and economic burden of the diseases, research related to AD remains a focal point in neurodegeneration studies. It has been established that the accumulation of Aβ leads to the formation of extracellular senile plaques, causing synaptic and neuron loss. It is also understood that hyperphosphorylation of Tau leads to the creation of NFTs, which can reduce connections between neurons and initiate neuronal degeneration. Collectively, these hallmarks contribute to the severe cognitive and behavioural symptoms observed in individuals with AD. Despite extensive efforts, finding a cure for the disease remains elusive. Therefore, it is necessary to approach the problem from new perspectives and identify the upstream molecular mechanisms leading up to the disease. It is well known that metabolic disorders are one of the risk factors associated with AD. Wherein the metabolic syndrome, T2DM is linked to neurodegeneration through the accumulation of neurotoxins, neuronal stress, synaptic communication, and brain atrophy. It has additionally been established that patients suffering from T2DM, possess a greater risk of obtaining dementia, whilst hyperglycaemia can exacerbate the effects of AD. Herein, some of key the pathways implicated in linking the diseases include cellular and oxidative stress, mitochondrial dysfunction as well as alterations in telomere biology. Despite significant research in these areas, many aspects remain unclear. By further exploring the link between T2DM and AD, we are able to better understand the upstream events that lead up to AD. This will aid in uncovering novel biomarkers and drug targets, in order to design efficacious therapeutic tools to diagnose, prevent, manage or treat the disease.

1.9 Scope of the study

To investigate the pathways involved in a hyperglycaemic AD state, an *in vitro* cell culture model was developed. The Human Embryonic Kidney (HEK) 293 cell line was grown and used to establish disease models via treatments with Aβ42 and glucose. To gain a comprehensive understanding of the mechanisms linking T2DM to AD, various aspects along this pathway were explored. The HEK293 cells were treated with various concentrations of Aβ42 and glucose during a time study, while the effects of the hyperglycaemic-Aβ42 environment on cell proliferation and morphology were investigated using light microscopy. Mitochondrial

function was assessed by measuring mitochondrial activity with the Alamar blue assay and mtDNA content with qPCR, while glucose uptake was determined through glucose assays. ROS levels were measured to investigate oxidative stress induced by the treatments, and ELISAs were used to assess the impacts of high glucose on the AD-related protein, Aβ42. Finally, considering that T2DM can contribute to telomere shortening, which is a risk factor for AD, telomerase activity and telomere length was measured using qPCR.

2. Aims and objectives

2.1 Main aim

Identifying how Type 2 Diabetes Mellitus leads to early Alzheimer's Disease and investigating the effects of a novel glucose lowering drug.

2.2 Specific objectives

1. Create a hyperglycaemic AD cell model, by treating with glucose and Aβ42.

2. Assess the morphology and mitochondrial activity of the treated cells to determine the ideal hyperglycaemic AD cell model.

3. Assess Aβ42 protein concentrations of the treated cells using Aβ42 ELISAs.

4. Investigate the mitochondrial function and oxidative stress, through measuring mitochondrial DNA content and ROS.

5. Assess telomere biology of the hyperglycaemic AD model using the qPCR TRAP Assay to measure telomerase activity and qPCR to measure telomere length.

3. Methods

3.1 Cell culture

Several culture systems have been developed to study the underlying mechanisms of neurodegenerative diseases. The immortalized Human Embryonic Kidney (HEK) 293 (ATCC® CRL-1573™) cell line is well-established cellular model for Alzheimer's disease and was therefore used in the present study (Mo *et al*., 2020). The cells were grown in 5 mM glucose DMEM media, supplemented with 10 % Foetal Bovine Serum (FBS) and 1 % Penicillin/Streptomycin (Pen/Strep) as the antibiotic (Liste-Calleja *et al.,* 2015). The FBS supplement provided the cells with essential nutrients, whilst the antibiotics prevented bacterial contamination. During culturing, to maintain an optimal and constant pH, as well as mimic *in vivo* conditions, the cells were grown in an environment that sustains the CO_2/HCO_3^- buffering system and were therefore cultured in a humidified incubator at 5 % CO_2, 37 °C (Liste-Calleja *et al.,* 2015). The aforementioned steps provided the optimal conditions to ensure maximum cell growth, which was monitored using an inverted light microscope, until the cells reached the required confluency, upon which the cells were either sub-cultured or harvested (Ruparel *et al.,* 2012). The cells were washed with 1x phosphate buffered saline (PBS) to rinse off the excess media and cell debris, followed by incubation with 1x trypsin-EDTA for 5 minutes to detach the cells (Ruparel *et al.,* 2012). Thereafter, culture medium was added to inactivate the trypsin-EDTA, when the cells had detached. For sub-culturing, new media was added to the flasks, after the excess cells had been detached and removed. Alternatively, after the cells were harvested, counted, and seeded, flasks or plates containing the seeded cells were either treated or used as controls in subsequent experiments. Additionally, any surplus cells were cryopreserved at -80 °C in cryogenic tubes. These cells were collected by centrifugation at 519 x g for 2 minutes, followed by resuspension in 1 ml of a solution consisting of 10 % dimethyl sulfoxide (DMSO) and 90 % culture media.

3.2 Treatments

Due to the previously reported link between T2DM and AD, a hyperglycaemic AD cell model was created by culturing HEK293 cells in low glucose media and followed by treatments with various combinations of glucose, Aβ42 and a glucose lowering drug (GLD). For the 2-, 5- and

10-day studies, cells were seeded at a density of $1x10^4$ cells per well in 96-well and 48-well and 6-well plates, respectively to provide ample space for cell growth and prevent contact inhibition. Notably, for assays that required DNA or protein extractions the cells were seeded at a density of $1x10^6$ cells per well in 6-well plates to ensure sufficient sample collection. Post seeding the cells were allowed to attach overnight, after which the cells were then washed with 1 x PBS and subjected to various singular and co- treatments with glucose, Aβ42, GLD for a duration of up to 10 days. Additionally, on days 2, 5, and 7, the cells were washed with 1 x PBS and re-treated with their respective treatments.

3.2.1 Glucose

Hyperglycaemia was found to coincide with elevated levels of Aβ and leads to modifications of Tau (Kim *et al.,* 2013; Yang *et al.,* 2013). In this regard, a cell model mimicking a hyperglycaemic state was created using a 25 mM high glucose treatment (Chen *et al.,* 2018), a 35 mM higher glucose treatment (Mayfield, 1998; Meng *et al.,* 2014; Russell *et al.,* 2002) and a 5 mM low glucose control group (Chen *et al.,* 2018). To create these treatments culture media was supplemented with a sterile D-(+)-Glucose solution (BioXtra, Sigma-Aldrich, United Kingdom). Notably, increasing the glucose concentration above 35 mM was previously found to induce hyperglycaemic stress, ROS, and cell injury, which could lead to cell death (Russell *et al*., 2002). Hence, to avoid killing the cells before subsequent experiments, the highest glucose concentration treatment did not surpass 35 mM. Additionally, a time study was included to investigate the effects of the glucose over a prolonged period of time. Herein, the time periods; 2, 5 and 10 days were used.

3.2.2 Amyloid Beta 42

Aβ peptides are known to reduce mitochondrial functions, increase ROS production, and induce both cytotoxicity and apoptosis (Chen and Petranovic, 2015). Aβ oligomers can bind directly to the telomere-TERC structure, inhibiting telomerase from elongating telomeric DNA. Consequently, treatment with Aβ42 was anticipated to reduce telomerase activity (Wang *et al.,* 2015). In order to investigate the early events that take place during AD progression, cells were treated with non-lethal concentrations of Aβ42, namely, 200 nM and 400 nM Aβ42 (Danysz and Parsons, 2012; Gilson *et al.,* 2015; Teich and Arancio, 2012). Herein, the lyophilized Aβ42 peptide (abcam, USA) was reconstituted in sterilized DMSO following the

manufacturer's guidelines to achieve a concentration of 1 mg/mL. Prior to cell treatment, the 1 mg/mL Aβ42 stock was diluted to 400 nM and 200 nM in culture media. To address potential effects of the organic low toxicity solvent, a vehicle control was included with 1.8 % and 0.09 % DMSO for the 400 nM Aβ42 and 200 nM treatments, respectively. Given the cytotoxic potential of DMSO at higher concentrations or prolonged exposure, efforts were made to minimize the DMSO concentration for longer incubation periods (Lynch et al., 2021). Herein, the lyophilized Aβ42 peptide (abcam, USA) was reconstituted in sterilized DMSO to achieve a concentration of 2 mg/mL, which was further diluted to 1 mg/mL with the addition of sterile PBS. Prior to cell treatment, the 1 mg/mL Aβ42 stock was diluted to 400 nM Aβ42 in culture media, with a 0.09 % DMSO / 0.09 % PBS vehicle control being included. In a final attempt to mitigate the effects of DMSO and to ensure that the solvent does not influence the effects of the drug GLD being tested, the lyophilized Aβ42 peptide (Sigma-Aldrich, USA) was reconstituted in a 50 mM Tris-HCL buffer at pH 9 to achieve a concentration of 1 mg/mL. The solution was then incubated at 37 °C for 24 hours and subsequently diluted in culture media to the required concentration prior to treating the cells. Any remaining solution was stored at -20 °C. Additionally, a time study was conducted for the following time periods; 2, 5 and 10 days.

3.2.3 Glucose Lowering Drug (GLD)

There are numerous factors that contribute to neurotoxicity and subsequently, AD which are additionally associated with T2DM, these include hyperglycaemia, oxidative stress, mitochondrial dysfunction, and telomere shortening. Due to these suggested connections between the neurological and metabolic disorder, the effects of the novel drug GLD were explored. The Glucose Lowering Drug (GLD) (Sigma-Aldrich, Missouri, USA) is a drug undergoing trials in T2DM pathophysiology. GLD is said to reduce oxidative stress through the reduction of hepatic glucose production, as well as by causing increased glucose uptake in muscles (Fouqueray *et al*., 2014). Results from an animal study demonstrated that GLD protects mitochondrial function from oxidative stress, which in turn normalized glucose tolerance (Vial *et al*., 2015). Additionally, it was proposed that GLD prevents the production of ROS through reverse electron flux without inhibiting either complex I or forward electron flux (Detaille *et al*., 2016). Therefore, the drug was included to investigate the effects of GLD in hyperglycaemia in addition to the effects on the progression of AD. In this study a 48 hour, 100 μM GLD treatment was included, wherein, dehydrated GLD (Sigma-Aldrich, Missouri,

USA) was reconstituted in a dH_2O under sterile conditions to reach a concentration of 2 mg/mL. The resulting solution was then further diluted to 100 µM GLD in culture media for cell treatment, with any remaining solution being stored at 2-8 °C.

3.3 Alamar Blue Assay

The Alamar Blue Assay was used to investigate the effects of the hyperglycaemic AD conditions on mitochondrial activity. The assay is based on the principle that viable cells with functional mitochondrial can reduce blue resazurin into red fluorescent resorufin which can be quantified as an indicator of cell viability. The assay was performed using alamarBlue® reagent (Invitrogen, Thermo Fisher, USA) as per the manufactures protocol. Herein, the cells were seeded at a density of $1x10^4$ cells per well in either a 96, 48 and 24 -well plates for the respective 2, 5 and 10 day incubation periods. Each plate included three biological repeats per group. These consisted of experimental treatment groups, positive (dead cell) controls using 8 mM of the apoptotic inducer, Protocatechuic acid (PCA), and no cell controls. After cells were seeded into each of the wells, they were left to attach for 24 hours. This was followed by treatments with either 5 mM (untreated group), 25 mM or 35 mM glucose, and/ or 200 nM or 400 nM Aβ42 and left to incubate for 2, 5 or 10 days. Additionally, re-treatments and washes were completed as per method 3.2. Notably, for the 2 day experiment each plate included three biological repeats per treatment group along with 4 technical repeats per biological repeat. Post incubation, the media was gently removed as to not disturb the cells, thereafter 90 µL of media and 10 µL of alamarBlue® reagent (Invitrogen, Thermo Fisher, USA) were added per well and left to incubate at 37 ºC for 4 hours.

However, following the longer 5 and 10 day incubation periods, the media was aspirated, and the cells were detached using a 5-minute incubation with 1x trypsin-EDTA. Subsequently, once the cells had detached culture medium was added to neutralize the trypsin-EDTA. The cells were then pelleted at 519 x g for 10 minutes, and the excess media was decanted. The cell pellet was resuspended in culture medium first and then mixed with alamarBlue® reagent (Invitrogen, Thermo Fisher, USA) in a 9:1 ratio. Thereafter, 100 µL of the cell mixture was gently pipetted up and down to achieve a homogeneous consistency of the cell solution before transferring to a 96-well plate, ensuring an even distribution of cells for division into 4 technical repeats per biological repeat. The variation in plate sizes was intended to accommodate the

extended incubation periods, providing ample space for cell growth and reducing contact inhibition. This adjustment also aimed to standardize volumes and minimize large differences in error bars among individual treatment groups within each biological replicate. Additionally, the decision to split each biological repeat into technical repeats after harvesting, rather than before treatments, was made to optimize treatment usage and lower costs associated with treatments and the alamarBlue® reagent. However, since cell counts were not conducted to standardize the cell amounts harvested across the different time periods, the data was displayed on separate graphs for trend comparisons.

Lastly, after the 4 hour incubation period with the alamarBlue® reagent (Invitrogen, Thermo Fisher, USA) the resulting fluorescence was measured at an excitation/ emission wavelength of 560/ 590 nm using the VICTOR® Nivo™ Multimode Plate Reader (Avantor®, PerkinElmer, USA). Absorbance values of the controls, untreated and treated samples were recorded and compared where, the average absorbance value of the biological repeats for each sample were calculated. The average absorbance of the no cell control was then subtracted from all other samples. A higher absorbance value was directly related with increased mitochondrial activity.

3.4 Glucose measurements

To measure and compare the glucose uptake of the various T2DM-AD cell models, a glucose concentration and time study was completed, where glucose uptake of the cells was investigated using the CONTOUR®PLUS ONE blood glucose monitoring system. The study involved measuring the amount of glucose present in the media at different time intervals over a 10-day period. Glucose uptake measurements were taken on days 0, 1, 2, 5, 7, and 10. During each measurement, the sample media was gently mixed by pipetting and 2 µL of media was loaded onto a test strip for measurement using the device. These measurements were performed in triplicates to ensure accuracy. To normalize the data, a standard curve was created. This involved preparing a series of dilutions using the cell culture media supplemented with glucose, with concentrations ranging from 0 mM to 30 mM. The glucose monitoring device was used to measure absorbance values of these dilutions, and a standard curve was plotted based on these measurements which allowed for the quantification of glucose concentrations in the samples. By normalizing the data using the standard curve, the glucose uptake over time was

represented in a line graph to provide insights into the glucose uptake patterns of the various conditions.

3.5 Total Reactive Oxygen Species (ROS) Assay

A mechanism of glucose toxicity in T2DM involves oxidative stress caused by ROS formation and reduced ROS removal systems. Hence, the Total Reactive Oxygen Species (ROS) Assay Kit 520 nm (Invitrogen, Thermo Fisher, USA) was used to assess how ROS levels were affected by the hyperglycaemic conditions of T2DM, the upstream conditions of AD as well as the glucose modulating drug GLD. Cells were seeded in triplicates at a density of $1x10^5$ cells per well in a 96-well plate and allowed to attach overnight, after which the cells were then washed with PBS and subjected to various singular and co- treatments with 25 mM glucose, 400 nM Aβ42 and 100 µM GLD, with 5 mM glucose and 250 mM H_2O_2 respectively used as the untreated low glucose and positive control groups. The assay was conducted following the manufacturer's guidelines. In summary, the protocol involved incubating the cells with the 1X ROS Assay stain (Invitrogen, Thermo Fisher, USA), notably, this was done concurrently with the various treatments. This was achieved by adding 2 µL of the 500X ROS Assay Stain stock solution (Invitrogen, Thermo Fisher, USA) for every 1 mL of cells. Thereafter the cells were left to incubate for 30 minutes, 2, 3 and 24 hours at 30 °C with 5 % CO_2. The stain functions as a sensor for free radicals by reacting with the ROS produced, resulting in the generation of fluorescence. This fluorescence occurs when molecules emit light at a specific wavelength upon being exposed to light of a shorter wavelength (Hibbs, 2004). Using the VICTOR® Nivo™ Multimode Plate Reader (Avantor®, PerkinElmer, USA), the ROS levels were measured by measuring Fluorescence at an excitation/ emission wavelength of 495/ 520 nm. The signal measured is directly proportional to the ROS present in the solution.

3.6 Aβ42 Enzyme-linked immunosorbent assay (ELISA)

To assess the AD related Aβ42 protein concentrations of the treated cells the Human Aβ1-42 (Amyloid Beta 1-42) enzyme-linked immunosorbent assay (ELISA) kit (Elabscience, Wuhan, China) was used. The assay operates on the principle of specific antibody-antigen interactions, allowing for the detection and quantification of antigens. Whilst the sensitivity of the assay is enhanced by utilizing enzyme-labelled antibodies. Herein, $1x10^6$ cells were seeded per well in

6-well plates, left to attach over overnight. Thereafter the cells were washed with 1 x PBS and treated for 48 hours with individual treatments of 5 mM glucose (untreated control group), 25 mM glucose, 100 µM GLD (Sigma-Aldrich, Missouri, USA), and a combination treatment of 25 mM glucose and 100 µM GLD.

3.6.1 Protein Extraction for ELISA

Prior to conducting the ELISA, the cells were prepared through a series of steps. Firstly, the media containing the cells was collected and centrifuged at 1000 xg for 20 minutes at 2-8 °C. The resulting supernatant was then utilized for measuring Aβ42 shedding. The remaining cells were washed with cooled 1 x PBS and detached from the plate using 500 µL of 1 x trypsin-EDTA for 5 minutes, followed by 500 µL culture media to inactivate the trypsin. The cell suspension was collected and centrifuged at 1000 xg for 5 minutes. The resulting medium was discarded, and the cells were washed three times with cooled PBS. The cells were made into $1x10^6$ cells/ 150 µL PBS aliquots and sonicated on ice 3 times at 35 Hz for 10 seconds. Following sonication, the samples were centrifuged at 1500 xg for 10 minutes at 2-8 °C. The resulting supernatant was used for measuring internalized Aβ42.

3.6.2 ELISA

To perform the assay, 100 µL of standard or sample was added to the wells. The assay was conducted with 3 biological sample repeats and 2 technical repeats. The plate was then incubated for 90 minutes at 37°C. After discarding the liquid, 100 µL of Biotinylated Detection Ab working solution was added to each well, followed by a 60-minute incubation at 37 °C. The plate was washed three times, and then 100 µL of Avidin-Horseradish Peroxidase (HRP) conjugate working solution was added. The plate was incubated for 30 minutes at 37 °C until a blue colour change was observed. After 5 wash steps to remove any unbound antibody, 90 µL of Substrate Reagent (Elabscience, Wuhan, China) was added and incubated for 15 minutes at 37 °C. The enzyme-substrate reaction was stopped by adding 50 µL of Stop Solution (Elabscience, Wuhan, China), resulting in a yellow colour change. Then using the VICTOR® Nivo™ Multimode Plate Reader (Avantor®, PerkinElmer, USA), the optical density or intensity of the colour change of the solution was measured at a wavelength of 450 nm (Alhajj and Farhana, 2021). To analyse the absorbance data, a standard curve was plotted for the protein. From the plotted values, the equation of the graph and subsequent coefficient of determination

was calculated to determine the level of variation. Finally, the concentration of Aβ42 in the optimized cell model was calculated using the standard curve equation (Alhajj and Farhana, 2021).

3.7 DNA extraction

Cellular DNA was extracted prior to the quantification of mitochondrial DNA and measurements of telomere length using qPCR. Herein, $1x10^6$ cells were seeded per well in 6-well plates, left to attach over overnight. Thereafter the cells were washed with PBS and treated for up to 10 days with individual treatments of 5 mM glucose (untreated group), 25 mM glucose, 400 nM Aβ42 and combination treatments of 5 mM glucose - 400 nM Aβ42 and 25 mM glucose - 400 nM Aβ42. These cells were washed with 1 x PBS and retreated with their respective treatments on days 2, 5 and 7. Additionally, the cells were either harvested on day 2 or 10. The DNA extraction was completed using the Genomic DNA Isolation Reagent Kit (PureDireX, BIO-HELIX, Taiwan), whilst working in sterile conditions and on ice. As per the manufactures guidelines, the cells were centrifuged at 6000 xg for 1 minute. The resulting supernatant was discarded and 50 µl of the 0.1-5 % Edetic Acid buffer (PureDireX, BIO-HELIX, Taiwan) was added. For cellular lysis, 300 µl of the 0.5-2% Sodium Dodecyl Sulphate buffer (PureDireX, BIO-HELIX, Taiwan) was added, followed by a vortex step. The resuspended cells were incubated for 10 minutes at 60 °C where the centrifuge tubes were inverted every 3 minutes to facilitate cell lysis. To ensure the isolation of high-quality gDNA without RNA and protein contamination, an additional step of RNA and protein degradation was incorporated. Herein, 5 µl of 10 mg/ml RNase A and 10 µl of 5 mg/ml Proteinase K were sequentially added and incubated for 5 minutes each at room temperature.

For protein removal 400 µl of the 5-10 % Guanidine Hydrochloride Buffer (PureDireX, BIO-HELIX, Taiwan) was added to break apart the hydrogen bonds between amino acid residues. To avoid searing the DNA and ensure thorough mixing, the lysate was carefully pipetted in a slow and controlled manner before being transferred to a new centrifuge tube. This was followed by centrifugation for 1 minute at 12000 xg to pellet out the protein. The resulting supernatant was transferred to a column placed in a collection tube for DNA binding. The samples were centrifuged for 1 minute at 14000 xg, the flow-through was discarded, 400 µl of wash buffer (PureDireX, BIO-HELIX, Taiwan) was added and the sample was centrifuged for

1 minute at 14000 xg. Once again, the flow-through was discarded and 600 µl of an ethanol based wash buffer (PureDireX, BIO-HELIX, Taiwan) was added. The sample was centrifuged for 1 minute at 14000 xg, the flow-through was discarded and the sample was centrifuged again for 2 minutes at 14000 xg for excess buffer removal before DNA elution. The columns were transferred to new centrifuge tubes and 75 µl of slightly cooled 65 °C elution buffer was added (PureDireX, BIO-HELIX, Taiwan) directly on to the matrix, avoiding the sides of the column to minimize contamination. The samples were incubated for 3 minutes at 60 °C, followed by a final centrifugation step of 14000 xg for 2 minutes to elute the purified DNA. Afterwards, the NanoDrop® ND-1000 (Thermo Scientific) was utilized to quantify the DNA in each sample. Each sample was then made up into 50 ng/ µL 50 µL aliquots and the DNA was resolved on a 1 % agarose gel (Supplementary Fig. 12) to confirm the integrity of the extracted DNA. Finally, the samples were stored at -20 °C for the subsequent experimentation.

3.8 Agarose Gel Electrophoresis

To evaluate genomic integrity, the DNA samples were resolved on a 1 % agarose gel (Table 1) which was run in 1 X TBE buffer (Table 2). Herein, samples were prepared on ice under sterile conditions. Subsequently, 10 µL of DNA sample was combined with 2 µL of Orange DNA Loading Dye (6 X) (Fermentas, Thermo Fisher Scientific). After which, 3 µL of a O'GeneRuler 1 kb DNA Ladder (Fermentas, Thermo Fisher Scientific) (MWM) of known fragment lengths was loaded into the first well of the agarose gel, followed by 5 µL of the prepared sample in each subsequent well. The gel was then run at 70 V for 1.5 hours to separate the DNA fragments based on size. Lastly, the resolved gel (Supplementary Fig. 10) was visualized under UV light using the ChemiDoc™ Imaging System (Bio-Rad, California, USA).

Table 1: 1 % Agarose gel recipe

Reagent	**Amount**
Electron agarose (DNA grade)	0.5 g
1 X TBE buffer	50 mL
EZ-Vision blue light DNA dye	3 µL

Table 2: 10 X TBE buffer pH 8.3

Reagent	**Amount**
Tris	108 g
Boric Acid	55 g
0.5 M EDTA	40 mL
dH_2O	Up to 1 L

3.9 Mitochondrial DNA content analysis by qPCR

Mitochondrial dysfunction has been previously described as a one of the facets linking T2DM and AD (Agrawal and Jha, 2020). To investigate the mitochondrial function of the hyperglycaemic AD cell models, mtDNA content was measured post treatment. DNA was extracted as per method 3.7. Following this, the optimal annealing temperature for the mtDNA and genomic DNA primers targeting mitochondrial DNA and a reference gDNA region (Table 6), respectively, were investigated using PCR. For this, various annealing temperatures were tested using a temperature gradient. Herein, PCR was performed using a BioRad T100™ Thermal Cycler (Bio- Rad, California, USA). The PCR reaction mix consisted of (Table 3) 6.25 µL OneTaq® Quick-Load (New England Biolabs), 0.5 µL of each primer, 1.25 µL PCR water and 4 µL of sample/ control for a final volume of 12.5 µL. The PCR temperature cycling used consisted of an initial denaturing step at 95 °C for 3 minutes, followed by 34 cycles of denaturing at 95 °C for 30 seconds, annealing using a temperature gradient from 62 °C to 55 °C for 30 seconds and extension at 72 °C for 30 seconds.

The resulting PCR products were resolved on a 1 % agarose gel (Supplementary Fig. 13). The optimal temperature was indicated by the presence of a thick distinct band in the lane corresponding to an annealing temperature of 60 °C (Supplementary Fig. 9.2) Thereafter qPCR was performed, for accuracy purposes, qPCR of both the mtDNA and the reference gene was conducted on the same plate. The qPCR reaction was prepared as per Table 4 and consisted of 5 µL SYBR green master mix (Bioline, London, UK), 0.5 µM of each primer, 3 µL PCR water and 1 µL of sample/ control for a final volume of 10 µL. The samples were pipetted into separate wells of a MicroAmp™ Optical 96-Well Reaction Plate (Thermo Fisher Scientific). Additionally, for each primer set a no template control (NTC) was included. Thereafter, the

QuantStudio™ 5 Real-Time PCR System (Thermo Fisher Scientific) was used. Herein, the thermal cycling parameters included an initial denaturation step at 95 °C for 3 minutes, followed by another 40 cycles of denaturation at 95 °C for 10 second, after which an annealing and extension step was completed at 60 °C for 30 seconds. Additionally, to ensure that a single product was amplified a melt curve (supplementary Fig. 12) was included with the qPCR run. Lastly, the Ct value for each sample was obtained using the HID Real-Time PCR Analysis Software v1.3. The data was then analysed using the $2^{-\Delta\Delta CT}$ method for relative quantification and to find the difference in fold change between samples.

Table 3: PCR master mix

Reagent	Volume per well (µL)
OneTaq® Quick-Load (New England Biolabs)	6.25
Forward Primer (10 µM)	0.5
Reverse Primer (10 µM)	0.5
PCR dH_2O	1.25
Sample/ control	4
Total	12.5

Table 4: qPCR master mix

Reagent	Volume per well (µL)
Sensi-FastTM SYBR green master mix (Bioline, London, UK)	5
Forward Primer (10 µM)	0.5
Reverse Primer (10 µM)	0.5
PCR dH_2O	3
Sample/ control	1
Total	10

3.10 Determination of telomerase activity by the qPCR TRAP assay

The Telomeric Repeat Amplification Protocol (TRAP) using the QuantStudio™ 5 Real-Time PCR System (Thermo Fisher Scientific) was used to measure telomerase activity. Additionally, any subsequent changes in activity in the optimized hyperglycaemic AD model, was confirmed

by measuring relative changes in telomere length using qPCR. Herein, $1x10^6$ cells were seeded per well in 6-well plates and allowed to attach overnight. The cells were then washed with 1 X PBS and subjected to different treatments for a duration of up to 10 days. The treatments included: 5 mM glucose (untreated group), 25 mM glucose (T2DM group), 400 nM Aβ42 (AD group), and combinations of 25 mM glucose with 400 nM Aβ42 (T2DM-AD group). On days 2, 5, and 7, the cells were washed with 1 X PBS and re-treated with their respective treatments.

3.10.1 Non-denaturing protein Extraction

Prior to conducting the TRAP assay, a non-denaturing protein extraction technique was employed to extract cellular telomerase while ensuring the preservation of its enzymatic functionality. The procedure involved harvesting and pelleting the treated cells through centrifugation at 519 x g for 10 minutes. The resulting supernatant was discarded, and the cells were washed once with 200 µL of 1 X PBS. The cells were then pelleted through centrifugation at 519 x g for 10 minutes, and the supernatant was removed. The cell pellets were then resuspended in non-denaturing 3-[(3-Cholamidopropyl)dimethylammonio]-1-propanesulfonate (CHAPS) lysis buffer (200µL) (Merck Millipore, Massachusetts, USA), and left to incubate for 30 minutes on ice. The lysis buffer was used to facilitate the extraction of proteins from the cells, while the low temperature during the incubation prevented protein degradation and the loss of enzymatic activity (Letsolo *et al.,* 2020).

To separate and pellet the cell debris, all samples were centrifuged at 4 °C for 20 minutes at 12000 xg. After which, 10 µL of the supernatant containing cellular protein was transferred to sterile centrifuge tubes, whilst the remaining portion was aliquoted and snap frozen, to prevent the loss of telomerase activity. Subsequently, the 10 µL aliquots were used to quantify the protein in each sample with the NanoDrop® ND-1000 (Thermo Scientific). The readings obtained were averaged and the protein concentration of each sample was adjusted to 500 ng/µL using nuclease-free water, to prepare two 50 µL aliquots. One of the aliquots was snap frozen, while the other underwent heat treatment to deactivate telomerase (95°C for 20 minutes on a heating block), serving as a negative control. Lastly, all samples were snap frozen again and stored at -80°C until further use.

3.10.2 Modified telomere repeat amplification protocol (TRAP) based telomerase activity assay

Quantitative PCR (qPCR) can be used to measure telomerase activity, by employing a double enzyme system, namely, a HotStart Taq DNA polymerase and extracted non-denatured telomerase. During the extension step of the assay, telomerase extends a non-telomeric oligonucleotide, namely the telomerase substrate. Subsequently, amplification of the extension products is carried out through a PCR reaction, using sequence specific primers, these include a downstream (reverse) ACX primer which Taq DNA polymerase extends, and an upstream (forward) TS primer (Mender and Shay, 2015). The resulting fluorescent signal produced, is directly proportional to the quantity of telomeric repeats added (telomerase activity).

The qPCR Master mix (SYBR green master mix, 10 μM Forward Primer, 10 μM Reverse Primer, 25 mM EGTA and Nuclease Free Water) was prepared as per the Table 5 and the protein samples were added into a 96-well plate. In addition to samples, various controls were included; 1 heat treated control per sample, nuclease free water, NTC and CHAPS buffer. Thereafter, using the QuantStudio™ 5 Real-Time PCR System (Thermo Fisher Scientific), telomerase activity was detected. The first thermal cycle was a pre-incubation process and comprised of a single cycle, at 37 ˚C for 30 minutes (to mimic *in vivo* conditions) to allow telomerase to extend the telomerase substrate and 95 ˚C for 2 minutes to inactivate telomerase (Mender and Shay, 2015). This was followed by an amplification process, consisting of 45 cycles at 95 ˚C, 59 ˚C and 45 ˚C for 30 seconds, 1 minute and 10 seconds, respectively (Mender and Shay, 2015; Butler, 2011). The data was then analysed by subtracting the Cq value of each sample from its respective heat-treated control and converting it to a percentage with respect to the untreated sample which was set to 100%.

Table 5: qPCR TRAP master mix

Reagent	Volume per well (µL)
Sensi-FastTM SYBR green master mix (Bioline, London, UK)	6.5
10 µM Forward Primer	0.5
10 µM Reverse Primer	0.5
25 mM EGTA	0.5
Nuclease free water	2.5
Sample/ control	2
Total	12.5

3.11 Telomere length determination by qPCR

To confirm subsequent changes in telomerase activity and to investigate the impact of the various treatments on telomere length, the relative mean telomere length was measured using qPCR. The qPCR reaction was prepared as per Table 2 and consisted of 5 µL SYBR green master mix (Bioline, London, UK), 0.5 µM of each primer, 3 µL PCR water and 1 µL of 500 ng/µL sample/ control for a final volume of 10 µL. The samples were pipetted into separate wells a 96-well plate. Additionally, 3 biological repeats were included per treatment group, along with a positive DNA control from a cell line previously confirmed to amplify producing multiple copies of the targeted telomeric DNA sequence, as well as a negative control containing no template. Additionally, the reference gene included in this reaction and used for normalising the results was the acidic ribosomal phosphoprotein human gene (36B4) due to its stable single copy number (Ashby *et al*., 2023). Thereafter, the QuantStudio™ 5 Real-Time PCR System (Thermo Fisher Scientific) was used with the following parameters: a denaturation step and subsequent amplification cycles: 95 °C for 10 min followed by 95 °C, 58 °C and 72 °C for 10 seconds, 10 seconds and 60 seconds, respectively. The data was analysed using the following equation, $\frac{2\triangle \text{CT (Telomere length)}}{2\triangle \text{CT(Reference gene length)}}$ to calculate the average telomere length.

3.12 Statistical Analysis

All collected data was analysed using Microsoft Excel version 16.70 (Microsoft Corporation). Additionally, for statistically reliable and trustworthy data, a minimum of 3 biological repeats were used in each experiment. Additionally, the two-tailed Student's t-test was conducted, using a confidence interval of 95%. Here, values in the range of, $p<0.05$, were considered significant, values in the ranges of; $p<0,01$ and $p<0,00$, was concluded as highly significant, and values outside these ranges were considered non-significant.

4. Results

Due to the previously reported links between T2DM and AD, a hyperglycaemic AD cell model was created by culturing HEK293 cells in low glucose media, followed by treatments with various combinations of glucose, Aβ42 and a glucose lowering drug (GLD). Thereafter, a series of experiments were performed investigating the various facets linking the diseases to highlight potential risk factors connecting T2DM to AD. These included; investigating the influence of hyperglycaemia on cellular stress, mitochondrial activity and subsequently mtDNA content, glucose uptake, ROS production, as well as the production of the AD hallmark protein Aβ42 and telomerase activity along with the resulting effect on telomere length.

4.1 Hyperglycaemic-AD conditions caused cellular stress

Previous studies show that high glucose concentrations can induce hyperglycaemic stress, ROS and cell injury, which could lead to cell death (Russell *et al*., 2002; Yu *et al*., 2008). Hence, post treatment an inverted light microscope was used to monitor the morphology of the treated cells as shown in Figure 5. Cells were treated with 25 mM or 35 mM glucose media alone or with either 200 nM or 400 nM Aβ42 for two, five and ten days to mimic hyperglycaemic AD conditions.

1.

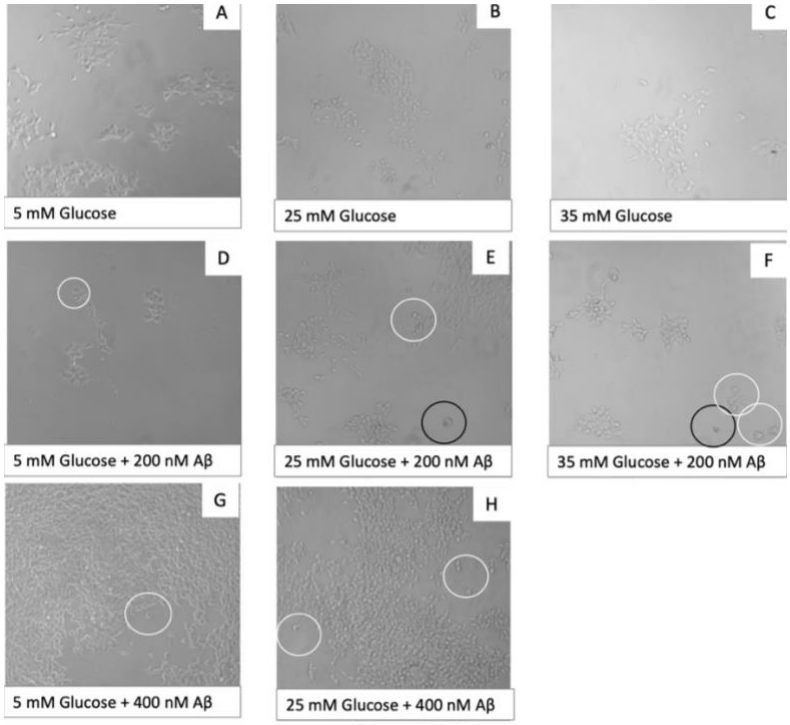
A
5 mM Glucose
B
25 mM Glucose
C
35 mM Glucose
D
5 mM Glucose + 200 nM Aβ
E
25 mM Glucose + 200 nM Aβ
F
35 mM Glucose + 200 nM Aβ
G
5 mM Glucose + 400 nM Aβ
H
25 mM Glucose + 400 nM Aβ

2

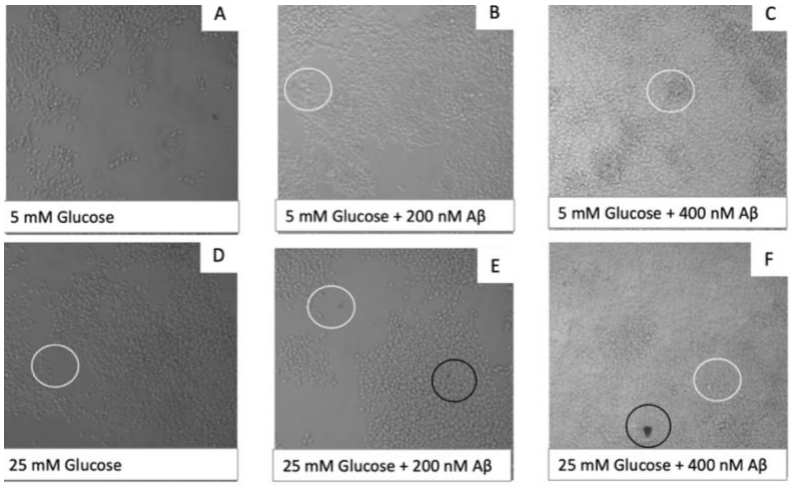
A
5 mM Glucose
B
5 mM Glucose + 200 nM Aβ
C
5 mM Glucose + 400 nM Aβ
D
25 mM Glucose
E
25 mM Glucose + 200 nM Aβ
F
25 mM Glucose + 400 nM Aβ

3.

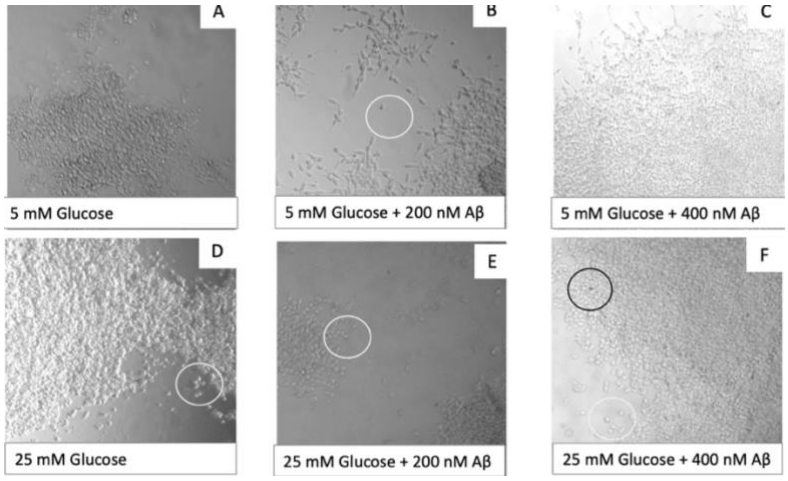
A
5 mM Glucose
B
5 mM Glucose + 200 nM Aβ
C
5 mM Glucose + 400 nM Aβ
D
25 mM Glucose
E
25 mM Glucose + 200 nM Aβ
F
25 mM Glucose + 400 nM Aβ

Figure 5: The effects of hyperglycaemic Alzheimer's disease conditions on HEK293 cell morphology after two, five and ten days.

Images displaying the effects hyperglycaemic Alzheimer's disease conditions on HEK293 cell morphology after two (1A-H), five (2A-F) and ten (3A-F) days. As the concentration of glucose increased the confluency of the cells decreased. Post treatment with Aβ42 cells appeared rounded as indicated by the white circles. The higher glucose-Aβ co-treated cells displayed some cell debris, indicated by the black circles. Additionally, as the incubation periods increased, an increase in both cell confluency and cell shrinking was observed.

Upon microscopy analysis (Fig. 5) it was determined that as the concentration of glucose increased from 5 mM up to 35 mM, the cells exhibited heightened indications of cellular stress and a significant decrease in cell confluency. As a result, the 35 mM treatment was omitted from the 10-day incubation period. Furthermore, exposure to Aβ triggered cellular stress, with this effect being magnified in the glucose-Aβ co-treatment groups as the cells presented with rounded shape, cell shrinking and increased cellular debris. Following this observation, the impact of high glucose and Aβ on mitochondrial function was examined to assess the role of these treatments in AD.

4.2 Hyperglycaemic-AD conditions may lead to mitochondrial dysfunction over time

Mitochondrial dysfunction is key facet linking T2DM and AD. In literature it has been shown that the hyperglycaemic conditions resulting from the metabolic disorder leads to ROS production, thus exacerbating Aβ production, after which Aβ translocates into mitochondria and impairs mitochondrial function further promoting ROS (Macdonald *et al*., 2018; Pagani and Eckert, 2011; Payne and Chinnery, 2015). This cascade activates kinases causing Tau hyperphosphorylation ultimately leading to Alzheimer's disease (Agrawal and Jha, 2020). To investigate the implications of these diseases on the mitochondria, mitochondrial activity was measured using the Alamar Blue Assay and mtDNA content was measured using qPCR.

4.2.1 Hyperglycaemic-AD conditions increased mitochondrial activity over 10 days

The Alamar Blue Assay was used to investigate the effects of the hyperglycaemic AD conditions on mitochondrial activity. Cells were treated with 25 mM or 35 mM glucose media alone or with 200 nM or 400 nM Aβ for two, five and ten days. A microplate reader was used

to measure fluorescence using an excitation wavelength of 560 nm and emission wavelength 590 nm. The results of the Alamar blue assay were recorded in Figure 6.

A

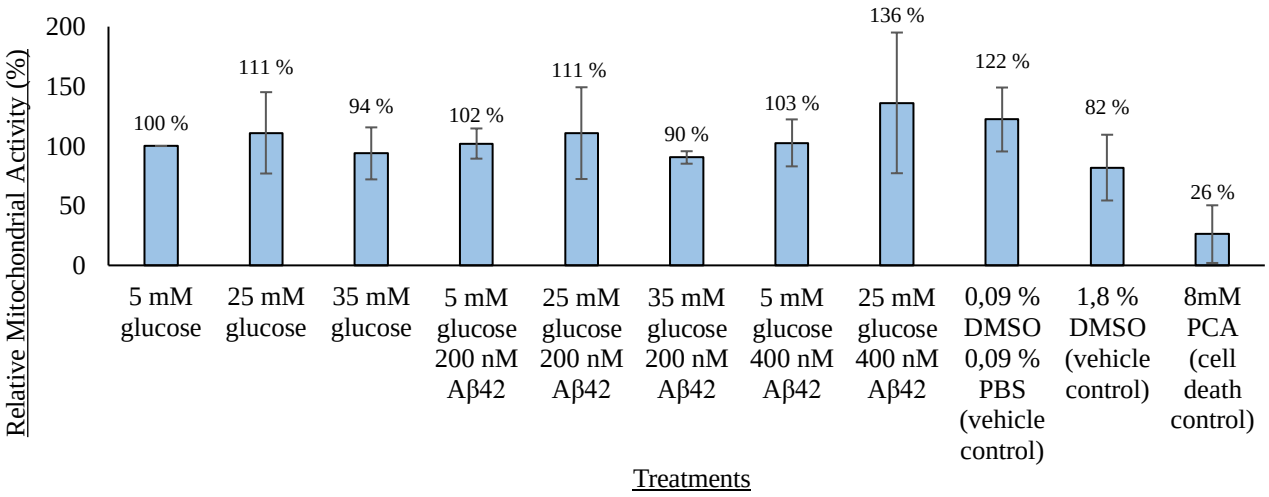

B.

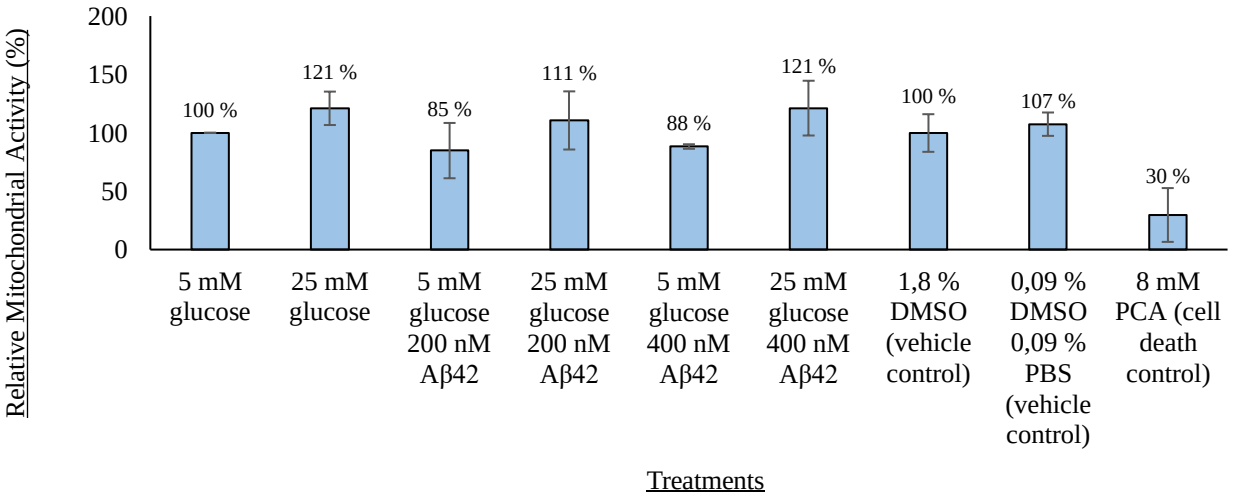

C.

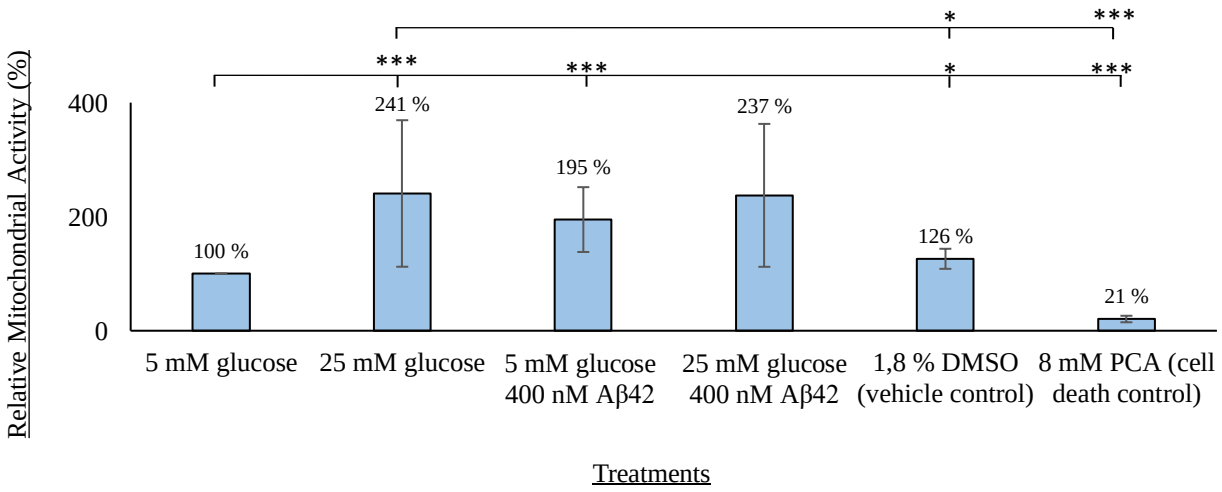

Figure 6: The effects of hyperglycaemic Alzheimer's disease conditions on HEK293 mitochondrial activity after two, five and ten days.

An Alamar Blue assay was conducted on the HEK293 cell line. Here, 8 mM PCA, 0.09 % DMSO, 1.8 % DMSO, 0.09 % PBS/ 0.09 % DMSO and 5 mM glucose were respectively used as the positive cell death control, vehicle control and as the untreated low glucose control group. The cells were treated with 25 mM or 35 mM glucose and 200 nM or 400 nM Aβ42 for two (A), five (B) or ten (C) days. Increased mitochondrial activity is observed post treatment in the hyperglycaemic (11 %, 21 %, 141 %) and hyperglycaemic -AD (36 %, 21 %, 137 %) groups after two, five and ten days respectively. All treated samples where then compared to the untreated 5 mM control group, using student's *t* test at a confidence interval of 95 % (where *p<0.05, **p<0.01, ***p<0.001 and p>0.05 was considered non-significant (NS)). Additionally, standard deviation (SD) is represented by the error bars.

4.2.2 Hyperglycaemic-AD conditions decreases mitochondrial DNA content after ten days

To investigate the link between the diseases with respect to mtDNA content, total cellular DNA was extracted. The integrity of the DNA was assessed using agarose gel electrophoresis. The DNA was then quantified, followed by qPCR, using primers (Table 6) specific for mtDNA and genomic DNA to measure the mtDNA content of the cell post treatment. Statistical analysis was completed as per method 3.12 and resulting data is presented as a bar graph below in Figure 7.

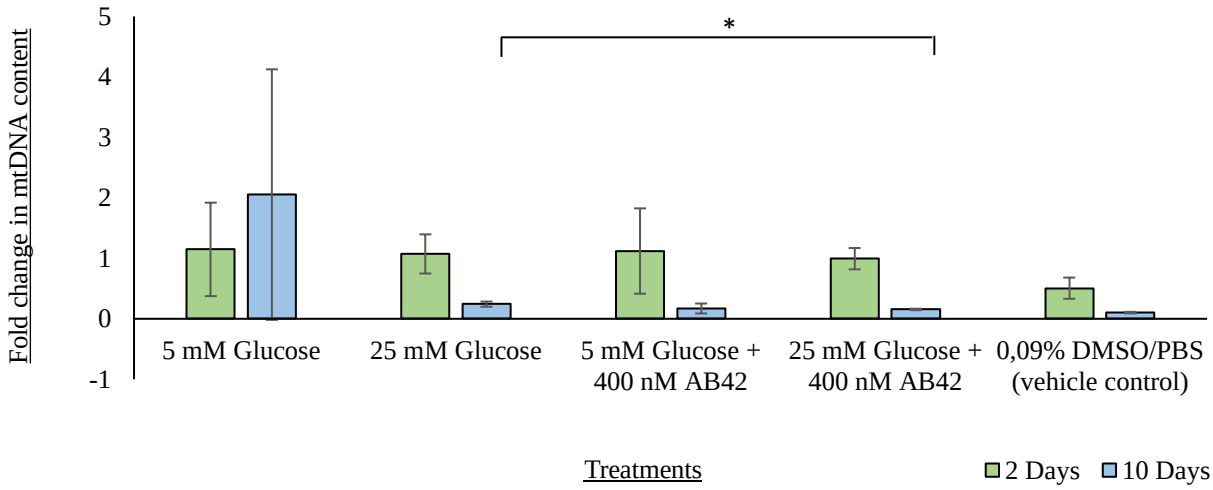

Figure 7. Hyperglycaemic and Alzheimer's induced conditions decreases total mitochondrial DNA content in HEK293 cells over ten days.

Using qPCR, the mtDNA content in HEK293 cells after two days was found have a subsequent non-significant ± 0.07, ± 0.03, ± 0.12 and ± 0.64-fold decrease when treated with 25 mM glucose, 400 nM Aβ42, 25 mM glucose and 400 nM Aβ42 co-currently and 0.09 % DMSO/ PBS (vehicle control) respectively. The mtDNA content in HEK293 cells after ten days was found have a subsequent non-significant ± 1.81, ± 1.88, ± 1.90 and ± 1.95-fold decrease when treated with 25 mM glucose, 400 nM Aβ42, 25 mM glucose and 400 nM Aβ42 co-currently and 0.09 % DMSO/ PBS respectively. For sample normalization the ch11: 2170993 – 2171170 nuclear DNA region was amplified. The data presented is a representative of the mean taken across three biological replicates with two technical repeats each. All treated samples were compared to their untreated control groups, using the student's *t* test at a confidence interval of 95 % (where *p<0.05, **p<0.01, ***p<0.0001 and p>0.05 was non-significant (NS)). Additionally, standard deviation (SD) is represented by the error bars.

Following 2, 5, and 10 days of treatment with 25 mM glucose (T2DM group) and 25 mM glucose with 400 nM Aβ42 (T2DM-AD group), there was a respective 11 and 36 %, 21 and 21 %, and 141 and 137 % increase in mitochondrial activity observed (Fig. 6). Concurrently, the T2DM, AD and T2DM-AD groups displayed a respective 6, 2, 13 % and 88, 92, 92 % decrease in mtDNA after 2 and 10 days of treatment in comparison to the untreated 5 mM glucose control group (Fig. 7). The T2DM-AD groups displayed a respective 7 and 36 % decrease in mtDNA after 2 and 10 days of treatment in comparison to the 25 mM glucose – T2DM group (Fig. 7). These results indicate that both high glucose and Aβ, whether administered together or separately, enhance mitochondrial activity, and diminish mtDNA levels in HEK293 cells over time. Furthermore, these effects were more pronounced in the 10-day treatment groups

compared to the 2-day treatment groups (Fig. 6 – 7). The treatment groups receiving 35 mM glucose and 35 mM glucose with 200 nM Aβ42 exhibited a 6 and 10 % decrease in mitochondrial activity (Fig. 6). After comparing the various treatment groups, the 35 mM glucose groups presented with a reduction in mitochondrial activity (Fig. 6) together with the substantial cellular stress and decreased cell confluency (Fig. 5: 1C and 1F) over a 48-hour period. Consequently, this treatment group was excluded from all subsequent experiments, and 25 mM glucose was selected as the high glucose concentration for all future experiments.

Upon treatment with 5 mM glucose with 200 nM Aβ42, as well as 25 mM glucose with 200 nM Aβ42 for 2 and 5 days, an increase of 2 and 11 %, and a decrease of 15 % and an increase of 11 % in mitochondrial activity (Fig. 6) were found in these lower Aβ42 treatment groups. Following 2 and 10 days of treatment with 5 mM glucose with 400 nM Aβ42 (AD group), a respective increase of 3 and 95 % in mitochondrial activity was observed, with a 12 % decrease in activity seen after 5 days. Additionally, the 25 mM glucose with 200 nM Aβ42 treatment group resulted in a 6 % increase and 8 % decrease in mitochondrial activity (Fig. 6) after 2 and 5 days of treatment in comparison to the T2DM group. Whilst the 25 mM glucose with 400 nM Aβ42 (T2DM-AD) treatment group resulted in a 12 % increase, 0 and 1 % decrease in mitochondrial activity (Fig. 6) after 2, 5 and 10 days of treatment in comparison to the T2DM group. Following the comparison of different treatment groups, it was observed that the 200 nM Aβ42 groups showed minor variances in mitochondrial activity (Fig. 6) and cell morphology (Fig. 5: 1D – F and 2E – F). In contrast, the 400 nM Aβ42 group exhibited more substantial differences in mitochondrial activity (Fig. 6) and cell morphology (Fig. 5: 1D – F and 2E – F) when compared to the untreated 5 mM glucose group. Consequently, the 200 nM Aβ42 treatment was excluded due to its closer resemblance to the 5 mM group, while the 400 nM Aβ42 treatment was selected to represent the AD model for all subsequent experiments. Given that mitochondria play a crucial role in supplying cellular energy through oxidative phosphorylation, a key aspect of cellular respiration involved in converting glucose into ATP, the uptake of cellular glucose was subsequently assessed to delve deeper into the effects of high glucose and Aβ over time.

4.3 Constant hyperglycaemia resulted in decreased glucose uptake

The dysregulated metabolism of glucose in T2DM has previously been linked to AD. Whereby dysregulated glucose metabolism was found to hinder Aβ42 removal in the brain and promote Aβ aggregation (Moreira *et al*., 2003). Hence the glucose uptake of the various hyperglycaemic AD cell models were investigated using the CONTOUR®PLUS ONE blood glucose monitoring system. All data was normalized using a standard curve and the results are displayed in Figure 8.

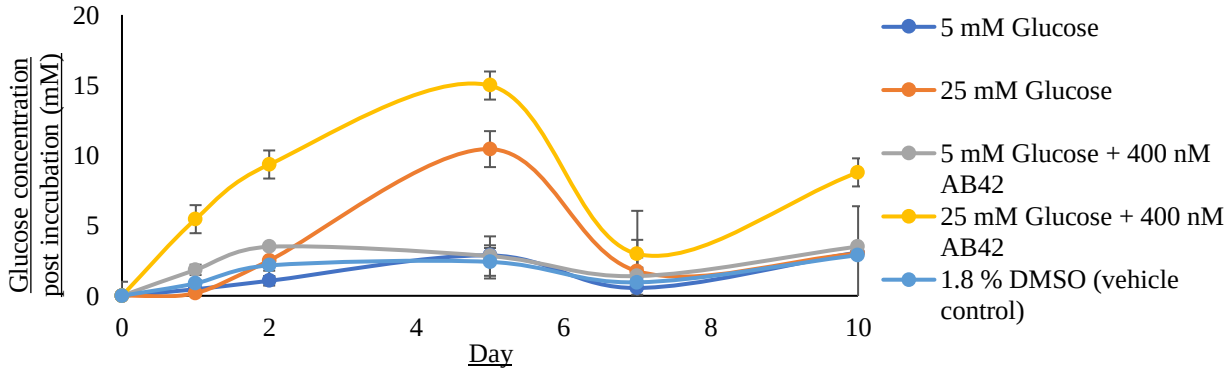

Figure 8. The effects of hyperglycaemic Alzheimer's disease conditions on glucose uptake in HEK293 cells after two, five and ten days.

The CONTOUR®PLUS ONE blood glucose monitoring system was used to measure the amount of glucose uptake after ten days. Here, 1.8 % DMSO and 5 mM glucose were respectively used as the vehicle control and as the untreated low glucose control groups. The hyperglycaemic group (orange graph) and hyperglycaemic-AD group (yellow graph) showed a gradual rise in glucose uptake until day five, followed by a decrease until day seven, and then an increase in glucose uptake until day 10. The AD group without hyperglycaemia (grey graph) exhibited a slight increase in glucose uptake until day two, followed by a subtle decrease until day seven, and then an increase in glucose uptake until day 10. The other treatment groups maintained a consistent level of glucose uptake throughout the 10-day period. The data presented is a representative of the mean taken across three biological replicates with two technical repeats each. All treated samples were compared to their untreated control groups, using the student's *t* test at a confidence. Standard deviation (SD) is represented by the error bars.

Upon analysis of the glucose uptake measurements (Fig. 8), the hyperglycaemic and AD treatments were found to influence and potentially reduce glucose uptake over time. This is evident from the graphs showing that the disease groups exhibit trends in glucose uptake that

deviate from that of the untreated control group. Herein, the hyperglycaemic and hyperglycaemic-AD groups displayed a progressive increase in glucose uptake up to day five, followed by a decline until day seven, and then a subsequent rise in glucose uptake until day ten. In contrast, the other treatment groups showed minimal fluctuations in glucose uptake over the 10-day duration. However, the AD group exhibited a minor increase in glucose uptake until day two, followed by a modest decrease until day seven, and then a slight increase in glucose uptake until day 10. Notably, these variations were subtle, as evidenced by the flattened slopes.

4.4 Individual hyperglycaemic and Alzheimer's disease induced conditions increased ROS production over 24 hours whilst GLD prevented ROS spikes in the T2DM-AD cell model

As previously mentioned T2DM leads to the neurodegenerative disease through oxidative stress (Chatterjee and Mudher, 2018). A common mechanism of glucose toxicity in T2DM involves, oxidative stress caused by ROS formation and reduced ROS removal systems (Butterfield *et al*., 2014; Chatterjee and Mudher, 2018). Hence, the Total ROS Assay Kit 520 nm (Invitrogen, Thermo Fisher, USA) was used to assess how ROS levels are affected by the hyperglycaemic conditions of T2DM and GLD upstream of AD. Differences in ROS levels are presented below in Figure 9.

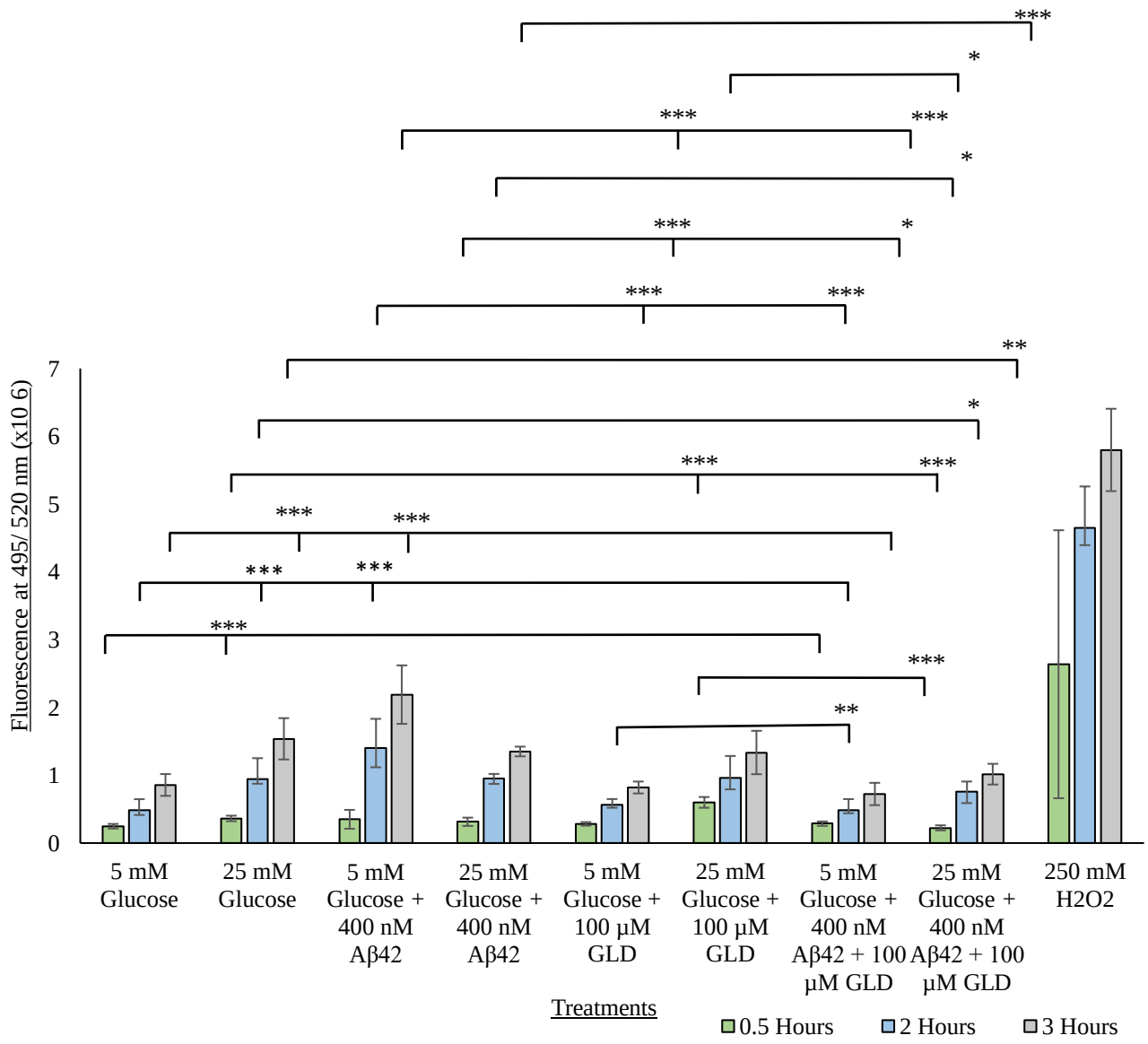
***
*
***
***
*
***
*
***
***
**
*
***
***
***
***
***
***
***
**
***
Fluorescence at 495/ 520 nm (x10 6)
0
1
2
3
4
5
6
7
5 mM Glucose
25 mM Glucose
5 mM Glucose + 400 nM Aβ42
25 mM Glucose + 400 nM Aβ42
5 mM Glucose + 100 µM GLD
25 mM Glucose + 100 µM GLD
5 mM Glucose + 400 nM Aβ42 + 100 µM GLD
25 mM Glucose + 400 nM Aβ42 + 100 µM GLD
250 mM H2O2
Treatments
0.5 Hours
2 Hours
3 Hours

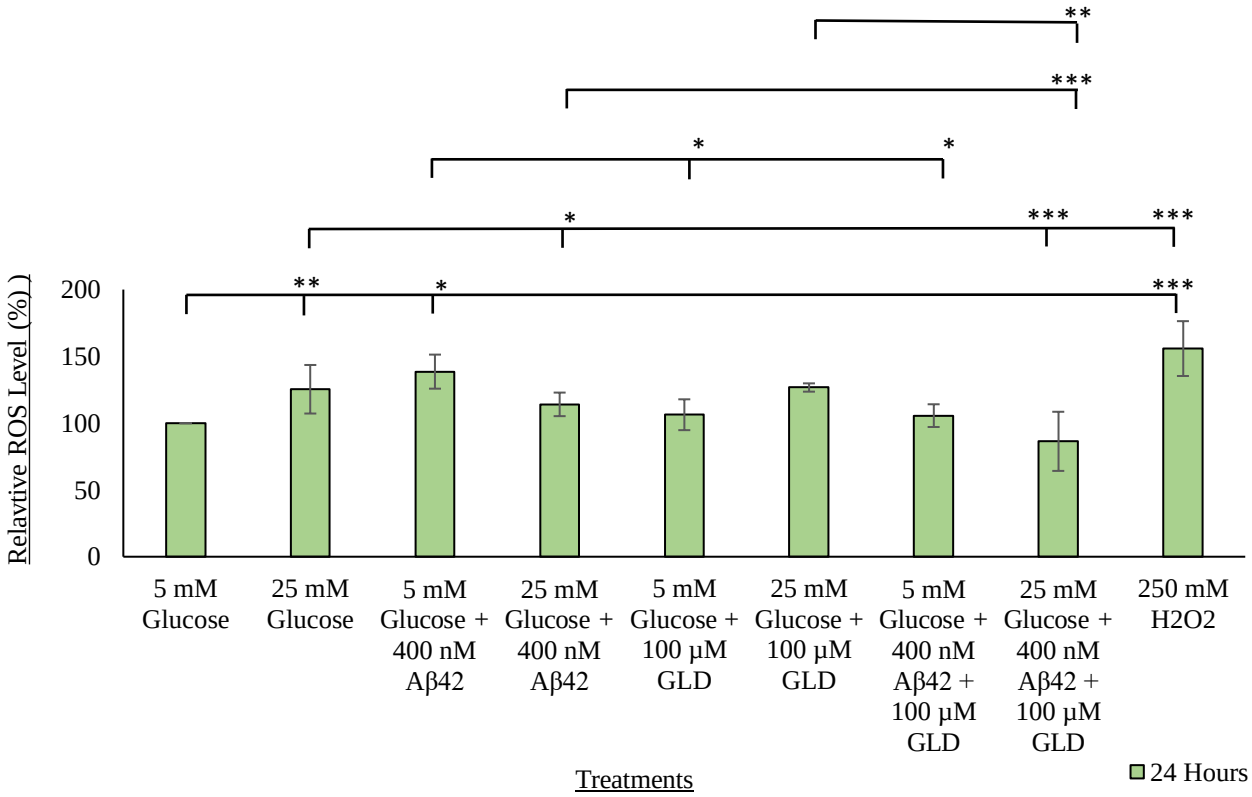

Figure 9: Hyperglycaemic and Alzheimer's induced conditions increases ROS whilst GLD decreases spikes in ROS in a T2DM-AD HEK293 cell model.

A ROS assay was conducted on the HEK293 cell line to measure ROS levels within the media post treatment. Here, 5 mM glucose and 250 mM H_2O_2 were respectively used as the untreated low glucose and positive ROS control groups, whilst the experimental treatment groups included singular and co-treatments with 25 mM glucose, 400 nM Aβ42 and 100 µM GLD for up to 24 hours. There was an increase in ROS levels after singular treatments with 25 mM glucose and 400 nM Aβ42 and 100 µM GLD, whilst the co-treatment groups with the drug (T2DM-AD-GLD) decreased ROS production. The data presented is a representative of the mean taken across three biological replicates. All treated samples where then compared to their respective untreated 5 mM glucose control groups, using the student's t test at a confidence interval of 95 % (where *$p<0.05$, **$p<0.01$, ***$p<0.001$ and $p>0.05$ was considered non -significant (NS)). Additionally, standard deviation (SD) is represented by the error bars.

Upon investigating ROS levels (Fig. 9), a spike is ROS was observed as early as 30 minutes after exposure to the various treatments. These ROS levels continued to gradually increase over time with a respective 25, 39, 14, 6, 27 and 6 % increase in ROS levels within the T2DM, AD, T2DM-AD, GLD, T2DM-GLD, AD-GLD groups in comparison to the untreated 5 mM glucose control group after 24 hours. Whilst the T2DM-AD-GLD group presented with a 14 % decrease in ROS production, suggesting that the drug decreased ROS levels in the double disease cell

model but not the single disease cell models. In comparison to the 25 mM glucose (T2DM group) treatment, the various T2DM-AD, T2DM-GLD and T2DM-AD-GLD groups displayed a respective 8 % decrease, 3 % increase and 32 % decrease in ROS after 24 hours. Thus, demonstrating that the T2DM and AD conditions elevated ROS production in comparison to the normal control group and that GLD decreases ROS in the double disease cell model in comparison to the normal and T2DM group. In literature it is illustrated that ROS promotes β- and γ-secretase expression and activity, exacerbating Aβ production (Macdonald *et al.,* 2018; Pagani and Eckert, 2011; Payne and Chinnery, 2015). These Aβ oligomers then translocate into the mitochondria and further impair mitochondrial function promoting additional ROS generation, which can activate kinases that hyperphosphorylate Tau, leading NFT formation, synaptic dysfunction, apoptosis and ultimately Alzheimer's disease (Agrawal and Jha, 2020). Hence, following obtaining these ROS data, Aβ42 levels were investigated.

4.5 GLD increases internalised Aβ42 and Aβ42 shedding under hyperglycaemic conditions compared to the T2DM cell model

To assess differences in the AD related protein concentrations of the treated cells, Aβ42 ELISA was used. Statistical analysis was completed as per method 3.12 and the data is represented as a bar graph below (Figure 10).

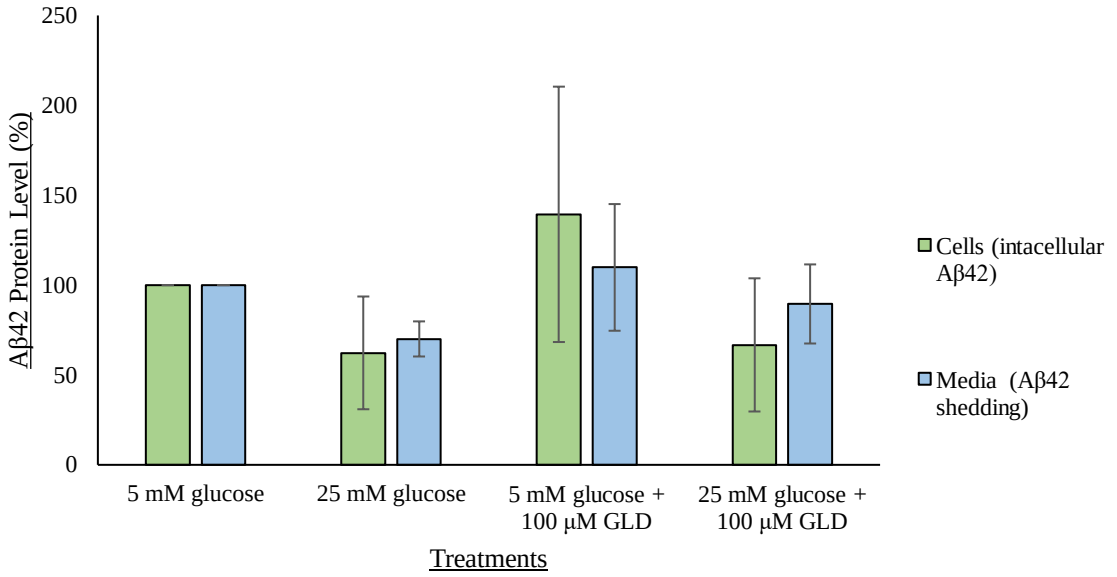

Figure 10: GLD alters internalised Aβ42 levels and Aβ42 shedding.

Aβ42 ELISA was conducted on the HEK293 cell line to measure Aβ42 levels within the cell and Aβ42 shedding present within the media after two days. Here 5 mM glucose was used as the untreated low glucose control group. Post treatment with 25 mM glucose, 100 μM GLD and 25 mM glucose with 100 μM GLD, there was a respective 38 % and 30 % decrease, a 39 % and 10 % increase as well as a 33 % and 10 % decrease in Aβ42 levels within the cells and media. The data presented is a representative of the mean taken across three biological replicates. All treated samples where then compared to the 5 mM glucose untreated control group, using the student's t test at a confidence interval of 95 % (where *$p<0.05$, **$p<0.01$, ***$p<0.001$ and $p>0.05$ was considered non-significant (NS)). Additionally, standard deviation (SD) is represented by the error bars.

Upon investigating Aβ42 levels (Fig. 10), it was observed that both the T2DM group and the T2DM-GLD group exhibited reduced intracellular Aβ42 and Aβ42 shedding compared to the 5 mM glucose untreated group. Post treatment with 25 mM glucose (T2DM group), 5 mM glucose with 100 μM GLD (GLD group) and 25 mM glucose with 100 μM GLD (T2DM-GLD group) presented with a respective 38 and 30 % decrease, 39 and 10 % increase as well as a 33 and 10 % decrease in intracellular Aβ42 and Aβ42 shedding after 48 hours compared to the untreated (5 mM glucose) control group. This suggests that the drug diminishes Aβ42 levels in the disease cell model (T2DM-GLD group) but not in the normal cell model (GLD group). Interestingly, the glucose lowering drug elevated these Aβ42 levels compared to the 25 mM glucose untreated group. Here, the T2DM-GLD cell model presented with a respective 7 and

28 % increase in intracellular Aβ42 and Aβ42 shedding after 48 hours compared to the T2DM (25 mM glucose) group. Notably, high glucose was found to decrease both intracellular Aβ42 and Aβ42 shedding. In literature these Aβ oligomers have been implicated in binding to the telomere-TERC structure, blocking and preventing telomerase from extending the telomeric DNA (Ohyagi *et al*., 2005). Since the high glucose treatment was found to alter Aβ42 levels, telomerase activity and telomere length were investigated as telomere shortening has been strongly linked to the risk of developing AD (Honig *et al*., 2012).

4.6 Hyperglycaemic-AD conditions affect telomerase activity and telomere length: Hyperglycaemic-AD conditions increases telomerase activity and telomere length

Previous studies have found that increased risk of AD has been associated with both, overly elongated telomeres which accumulate DNA damage, and significantly shortened telomeres which have been linked to cell death (Fani *et al*., 2020). Herein, the regulation of telomere length is by telomerase, which adds telomeric repeats to shortened telomeres (Glasspool *et al*., 2005). Hence, the activity of telomerase and subsequent changes in telomere length was assessed.

To assess the changes in telomerase activity potentially linking T2DM and AD the qPCR TRAP method using the thermal cycler was used. Briefly, post treatment samples were harvested, and non-denaturing protein extraction was performed followed by qPCR. Thereafter, statistical analysis was completed as per method 3.12 and resulting data is presented as a bar graph below in Figure 11A. Changes in telomere length was measured using qPCR to assess the potential increase in risk of developing AD. Post treatment, samples were harvested, and total cellular DNA was extracted, followed by qPCR with the telomere and genomic DNA primers described in Table 6. Statistical analysis was completed as per method 3.12 and resulting data is presented as a bar graph below in Figure 11B.

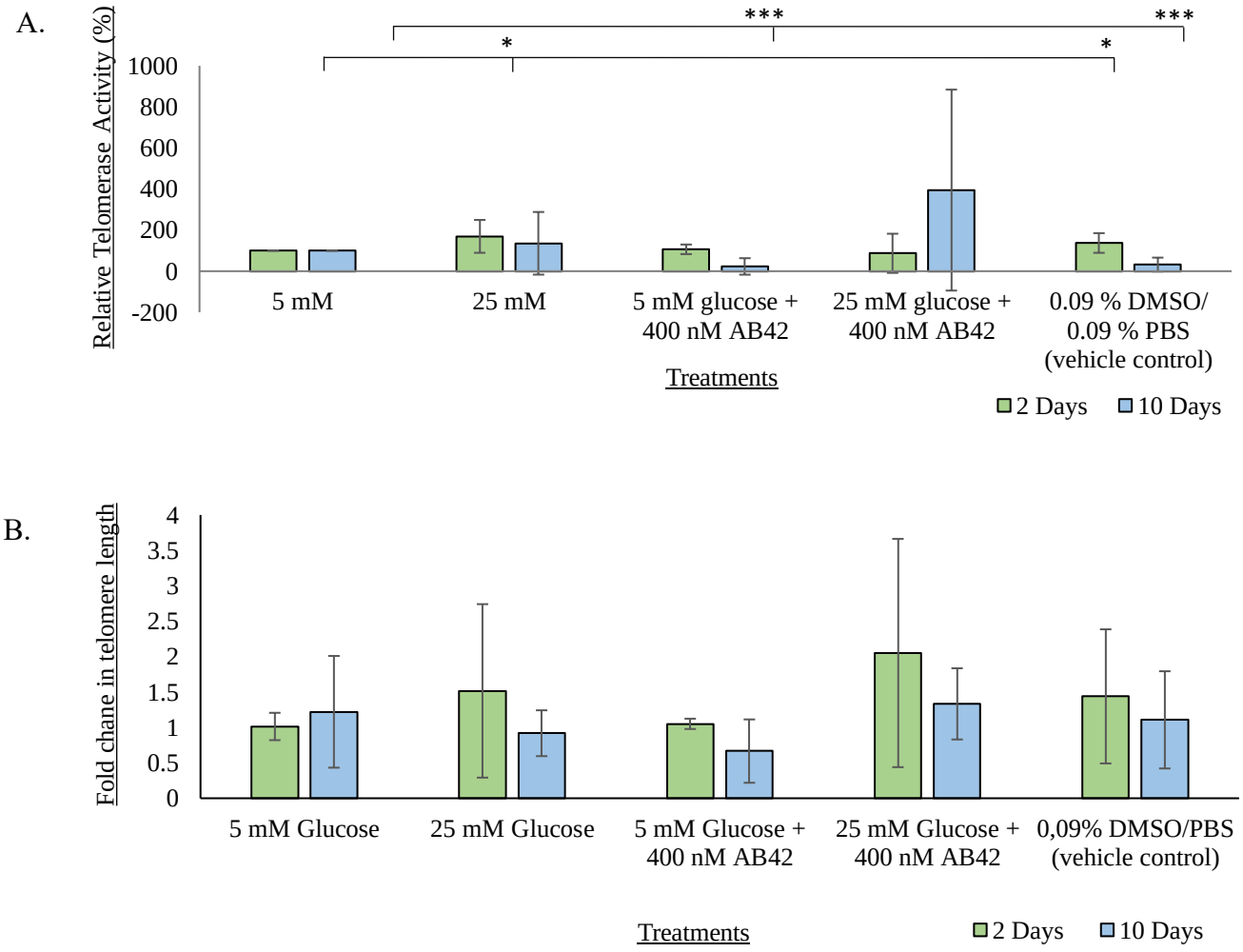

Figure 11: The effects of hyperglycaemic Alzheimer's disease conditions on telomerase activity and telomere length in HEK293 cells using qPCR.

(A): The TRAP assay was conducted on the HEK293 cell line. Here, 0.09 % PBS/ 0.09 % DMSO and 5 mM glucose were respectively used as the vehicle control and as the untreated low glucose control group. The cells were treated with 25 mM and 400 nM Aβ42 for two and ten days. Hyperglycaemic-AD conditions decreased telomerase activity by 13 % after two days and increased telomerase activity by 295 % after ten days. (B): Relative changes in HEK293 telomere length post treatment were measured using qPCR. Here, 0.09 % PBS/ 0.09 % DMSO and 5 mM glucose were respectively used as the vehicle control and as the untreated low glucose control group. The cells were treated with 25 mM and 400 nM Aβ42 for two and ten days. Hyperglycaemic-AD conditions increased telomere length by 102 % after two days and by 9 % after ten days. All treated samples where then compared to the untreated 5 mM control group, using the student's *t* test at a confidence interval of 95 % (where *$p<0.05$, **$p<0.01$, ***$p<0.001$ and $p>0.05$ was considered non-significant (NS)). Additionally, standard deviation (SD) is represented by the error bars.

Upon qPCR TRAP analysis the results indicated that after 2 days the elevated glucose levels contributed to a 70 % increase in telomerase activity (Fig. 11A) and a 50 % increase in telomere length (Fig. 11B) in the T2DM group. Similarly, the AD-associated protein Aβ42 contributed to a 6 % increase in telomerase activity (Fig. 11A) and a 4 % increase in telomere length (Fig. 11B) in the 2-day-AD group. Whilst prolonged exposure to the 400 nM Aβ42 treatment caused a 77 % decrease in telomerase activity and a 45 % decrease in telomere length in the 10-day-AD group. Additionally, 10 days with the 25 mM glucose and 400 nM Aβ42 treatment resulted in a 295 % increase in telomerase activity (Fig. 11A) and a 9 % increase in telomere length (Fig. 11B). Together these results indicate consistent alterations in telomerase activity and telomere length after 2 and 10 days of treatment. This implies that the observed changes in telomerase activity in these groups contributed to the differences in telomere length induced by the treatments. Conversely, the 2-day-AD-T2DM group presented with a 13 % decrease in telomerase activity (Fig. 11A) and a 102 % increase in telomere length (Fig. 11B). Additionally, the 10-day-T2DM group presented with a 36 % increase in telomerase activity (Fig. 11A) and 25 % decrease in telomere length (Fig. 11B). Thus implying that these changes in telomere length might not be directly related to the changes in telomerase activity.

5. Discussion

Due to the severity of AD, and absence of effective non-palliative therapeutic treatments, the research areas pertaining to dementia and more specifically AD have been a major target in neurodegeneration research. It has been established that Aβ is accumulated producing extracellular senile plaques eliciting synaptic and neuron loss. It is additionally known that Tau is hyperphosphorylated resulting in the development of NFTs, which can decrease connections between neurons and trigger neuronal degeneration. Collectively, these hallmarks lead to the crippling cognitive and behavioural symptoms seen in AD patients. Despite extensive efforts, finding a cure for the disease remains elusive. Therefore, it is necessary to approach the problem from new perspectives and identify the upstream molecular mechanisms leading up to the disease. It is well known that metabolic disorders are one of the risk factors associated with AD. Wherein the metabolic syndrome, T2DM is linked to neurodegeneration through the accumulation of neurotoxins, neuronal stress, synaptic communication, and brain atrophy. It has additionally been established that patients suffering from T2DM, possess a greater risk of obtaining dementia, whilst hyperglycaemia can exacerbate the effects of AD. The current study serves to investigate this link, to understand the upstream events that lead up to AD. This will aid in uncovering novel biomarkers and drug targets, in order to design efficacious therapeutic tools to diagnose, prevent, manage or treat the disease.

Together the results from this project suggest that hyperglycaemia decreased glucose uptake over ten days and led to signs of cellular stress. The dysregulation of glucose metabolism in turn increased ROS production over 24 hours leading to a series of detrimental effects on a cellular level. These included, increased cellular stress and mitochondrial dysfunction through decreased mtDNA content (Fig. 7) coupled with increased mitochondrial activity (Fig. 6). In addition to this, upstream of AD an increase telomerase activity (Fig. 11A) was observed, which was coupled with a coherent increase in telomere length. Whilst downstream of AD, hyperglycaemia and the hyperglycaemic-AD conditions increased telomerase activity (Fig. 11A). This was coupled with a decrease and increase in telomere length (Fig. 11B) respectively. Whilst the hyperglycaemic and hyperglycaemic-AD conditions decreased Aβ42 production and shedding. Lastly this study demonstrates for the first time that the novel glucose lowering drug caused an increase in Aβ42 production and shedding in the T2DM cell model and successfully lowered ROS production over 24 hours in comparison to the untreated cell model.

5.1 Hyperglycaemic-AD conditions caused cellular stress

Previous studies have indicated that high glucose concentrations can induce hyperglycaemic stress and in turn cell injury (Russell *et al*., 2002; Yu *et al*., 2008). Hence, post treatment an inverted light microscope was used to monitor the morphology of the treated cells. The control group (5 mM glucose) (Fig 5: 1A, 2A, 3A) displayed an epithelial like morphology throughout the 10 days and these cells were adherent to the bottom of the plates, which is consistent with the normal morphology associated with HEK293 cells. The T2DM group (25 mM glucose) (Fig 5: 1B, 2D, 3D) shared similar a morphology with the control group until day 5, where some of the cells began to appear slightly rounded indicative of cellular stress. Additionally, these control and T2DM groups displayed an increase in confluency as the study progressed. However, when the concentration of glucose was increased to 35 mM the confluency of the cells decreased greatly (Fig 5: 1C, F), as the cells may have lost their proliferative abilities or may have entered apoptotic pathways induced by the hyperglycaemic conditions. These cells showed signs of stress coherent with early stages of apoptotic morphology, as the cells appeared rounded with increased cell shrinking as opposed to the typical epithelial like morphology of HEK293 cells (Elmore, 2007). There was an increase in cell debris and floating cells, indicating that some of the cells may have lost their adherent nature and/ or have died. Hence, the 35 mM treatment group was excluded for five- and ten-day incubation periods.

These morphology changes can be linked to hyperglycaemia which can stimulate programmed cell death by increasing the expression of the proapoptotic protein called BCL2 homology domain 3-only protein (Bim), which promotes mitochondrial dependent apoptosis in epithelial cells through the BAX/BAK pathway (Zhang *et al*., 2017). Additionally, this upregulation of Bim is said to be facilitated by the activation of transcription factors FOXO1 and FOXO3a (Zhang *et al*., 2017). Specifically, FOXO1 is involved in in the regulation of glucose production and gluconeogenesis, whilst FOXO3a promotes cell death through regulating the expression of genes involved in cell cycle arrest and apoptosis (Nho and Hergert, 2014; Ponugoti *et al*., 2012). Hence, it is likely that through this pathway the hyperglycaemic conditions in the present study could be promoting apoptosis resulting in the decreased confluency and apoptotic morphology observed. Thus suggesting the necessity for further investigation.

On the other hand the AD groups in the absence of the hyperglycaemic conditions (5 mM glucose with 200 nM Aβ42 and 5 mM glucose with 400 nM Aβ42) showed similar signs of

stress, including a rounded morphology and a slight decrease in confluency. Aβ42 peptides in plaque deposits have a great copper and iron reduction potential, these peptides generate ROS and trigger oxidative stress through the reduction of these metal irons (Huang *et al*., 1999). Which in turn triggers the stress activated c-Jun NH2-terminal kinase (JNK) death signalling pathway leading to apoptosis, explaining the slight decrease in confluency and increase in rounded cells (Mehan *et al*., 2011). Interestingly, the T2DM-AD groups (25 mM glucose with 200 nM Aβ42 and 25 mM glucose with 400 nM Aβ42) displayed more signs of cellular stress, similar to the 35 mM glucose group, except with a less drastic decrease in confluency. According to previous studies a 48-hour treatment with 200 nM Aβ42 was found to elicit a mild decrease in cell viability, wherein the Aβ42 treated group displayed 77.4 % live cells in comparison to the untreated control had 89.6 % live cells (Da Costa Dias *et al*., 2014). This would imply that hyperglycaemic conditions enhanced the Aβ induced cellular stresses. Hence, highlighting that T2DM can exacerbate the effects of AD on a cellular level, motivating for the development of therapeutic strategies targeting the effects caused by both diseases.

5.2 Hyperglycaemic-AD conditions may lead to mitochondrial dysfunction over time

Hyperglycaemia resulting from the metabolic disorder leads to ROS production, exacerbating Aβ production which translocates to mitochondria and impairs mitochondrial function further promoting ROS generation (Macdonald *et al*., 2018; Pagani and Eckert, 2011; Payne and Chinnery, 2015). This cascade activates kinases causing Tau hyperphosphorylation ultimately leading to AD (Agrawal and Jha, 2020). Hence making mitochondrial dysfunction a key upstream factor linking T2DM to AD.

5.2.1 Hyperglycaemic-AD conditions increased mitochondrial activity over 10 days

Mitochondrial activity (Fig. 6) can be measured through investigating the reductive capacity of mitochondria by reducing resazurin into resorufin using mitochondrial reductases which are partly encoded for in mtDNA. Mitochondrial activity was found to progressively increase over time in the 25 mM glucose or hyperglycaemic group in comparison the 5 mM glucose control group, with a 16, 21 and 141 % increase after 2, 5 and 10 days respectively (Fig. 6). Whereas, in the co-treated or hyperglycaemic-AD group a higher 36 % increase in mitochondrial activity was observed just after 2 days. Whilst the 5- and 10-day groups had similar trends to the

hyperglycaemic group, with a 21 and 137 % increase respectively in comparison to the untreated (5 mM glucose) control group. However, in comparison to the current literature available involving diabetic studies, a 48-hour treatment with 25 mM glucose caused a slight decrease in mitochondrial activity in periodontal ligament fibroblast (PDLFs) cells (Aldoss *et al*., 2023). Whilst studies on human PDL cells with prolonged incubation periods, for up to 17 days, in 25 mM glucose report an increase in proliferation (Li *et al*., 2016; Seubbuk *et al*., 2017). Hence suggesting that the increase in mitochondrial activity might instead be proportional to the number of cells present for each group rather than an actual increase in mitochondrial activity. This is in line with the results presented in Fig. 5, which confirmed an increase in confluency post treatment with 25 mM glucose. Additionally, it was found that the treatment with 35 mM glucose for 48 hours resulted in a 6 % decrease in mitochondrial activity and a drastic reduction in confluency (Fig. 5: 1C). As a result, the treatment group was excluded from further experimentation.

Furthermore, Aβ42 peptides reduce mitochondrial functions, increase ROS production, and induce both cytotoxicity and apoptosis, which would result in decreased mitochondrial activity (Chen and Petranovic, 2015). Accordingly, treatment with 200 nM Aβ42 decreased mitochondrial activity by 15 % after 5 days in comparison to the untreated control group (5 mM glucose), whilst 400 nM Aβ42 decreased mitochondrial activity by 12 % after 5 days of incubation (Fig. 6: B). Additionally, treatment with 200 nM Aβ42 (in the T2DM group) decreased mitochondrial activity by 8 % after days in comparison to the T2DM group (25 mM glucose), whilst 400 nM Aβ42 (in the T2DM group) decreased mitochondrial activity by 1 % after 5 and 10 days of incubation. Similarly, all Aβ42 – treated groups presented with decreased mitochondrial activity in comparison to the T2DM group after 5 and 10 days. After the 2 and 10-day (Fig. 6: A, C) incubation, treatment with 400 nM Aβ42 caused an unexpected increase in mitochondrial activity. However, as this is a study investigating upstream AD the Aβ42 concentration was not further increased. Since, when Aβ42 clearance is interrupted in the brain the estimated concentration of synaptotoxic Aβ42 peptides that accumulate within the first few days or weeks lies with the approximate range of 50 to 500 nM, with 400 nM being close to the upper limit (Raskatov, 2019). Whereas synaptotoxic Aβ42 peptides within the range of 10 to 100 μM fall into the neurotoxic category (Raskatov, 2019). Hence, this could explain why little to no decrease in mitochondrial activity was observed after incubation with 400 nM Aβ42 for 2 and 10 days in comparison to the 5 mM glucose control group. These findings highlight

an unpredicted increase in mitochondrial activity downstream of T2DM and upstream of AD which could be another form of mitochondrial dysfunction which was further investigated through mtDNA content analysis. Alternatively, this could be a protective function of the cell in an attempt to counteract the hyperglycaemic effects of T2DM.

A study conducted on rat brains demonstrated that Aβ42, at concentrations ranging from 2–20 μM, has the ability to prevent protein and lipid oxidation. Additionally, it reduces the formation of ROS generated from the exposure of mitochondria to FeSO4 through its metal chelation properties (Sinha *et al*., 2013). However, the study also found that while Aβ42 may play a protective antioxidant role, Aβ42 also exhibits toxic effects leading to mitochondrial functional impairment, such as membrane depolarization and a decrease in phosphorylation capacity, independently of ROS (Sinha *et al*., 2013). Furthermore, the study proposes that Aβ may function as an endogenous antioxidant, which could explain the observation that in normal aging, where oxidative stress is heightened, there is an increase in Aβ production. In AD, this could result in a redox imbalance state, where the excessive production of Aβ eventually can no longer compensate for the increase in ROS can becomes toxic to the cell (Smith *et al*., 2002). This rationale could explain the 36 % increase in mitochondrial activity following Aβ42 treatment after 2 days (Fig. 6A), which then declines to a 21 % increase after 5 days (Fig. 6B) in comparison to the 5 mM glucose control group. Similarly, this could also explain the 12 % increase in mitochondrial activity following Aβ42 treatment after 2 days (Fig. 6A), which then declines to a 0 % increase after 5 days (Fig. 6B) and remains somewhat consistent until day 10 (Fig. 6B – C) in comparison to the 25 mM glucose group. This suggests that Aβ42 initially works to prevent the rise in hyperglycaemia-induced ROS through its metal chelating antioxidant properties by scavenging ROS. However, over time, the antioxidant effects of Aβ42 are overwhelmed, leading to a decline in mitochondrial activity (Smith *et al*., 2002).

5.2.2 Hyperglycaemic-AD conditions decreased mitochondrial DNA content

The pathogenesis of T2DM has been associated with a reduction in mtDNA copy number. As mentioned previously, the hyperglycaemic condition of T2DM contributes to increased oxidative stress through elevated ROS (Rolo and Palmeira, 2006). Consequently, the close proximity of mtDNA to sites that generate ROS makes mtDNA susceptible to oxidative damage. This can result in insufficient mitochondrial biogenesis, impaired mtDNA repair,

mtDNA base and strand damage (Aran, 2023; Rolo and Palmeira, 2006). ROS can oxidize guanine nucleotides in mtDNA, resulting in the production of 8-hydroxy-2'-deoxyguanosine (8-OHdG). This oxidation leads to single-strand breaks, which contributes to a loss of genetic information. The presence of these oxidized nucleotides creates physical obstructions that hinder base pairing during mtDNA transcription (Aran, 2023). Additionally, these 8-OHdG structures obstruct mtDNA replication, leading to mutations. Collectively, these factors contribute to an increase in damaged mtDNA, resulting in decreased mitochondrial biogenesis (Aran, 2023). This leads to the activation of autophagy-mediated removal of dysfunctional mitochondrial contributing to decreased mtDNA copy number (Wang *et al*., 2021). Which would explain the respective 0.07 and 1.81 decrease in fold change after two and ten days of treatment with 25 mM glucose (T2DM group) (Fig. 7). This is a significant area of research linking the diseases, as there is evidence indicating that mtDNA copy number plays an important role in the pathogenesis of AD. Wherein, the cognitive impairment of AD patients has been associated with decreased mtDNA copy number in the hippocampus region of the brain (Dezfouli *et al*., 2019).

This theory supports the results in the present study, wherein mtDNA content was analysed and found to have a respective 0.03 and 1.88 decrease in fold change after two and ten days of treatment with 400 nM Aβ42 (AD group) (Fig. 7). According to the proposed mechanism, Aβ has the ability to translocate to the mitochondria and interact with various components, such as the inner mitochondrial membrane, respiratory chain complexes, and enzymes such as ETC complex IV (Pagani and Eckert, 2011; Pinho *et al*., 2015). Normally, ETC complex IV oxidises cytochrome c by transferring a hydrogen group from cytochrome c to a superoxide group creating a water molecule (Zhao *et al*., 2019). However, due to interference by Aβ, the mitochondrial membrane potential (MMP) is disrupted by decreasing the transport of hydrogen molecules to the intermembrane space from the matrix leading to ETC dysfunction. In turn decreasing ETC complex IV activity and increasing superoxide content by preventing the conversion of the ROS species into water molecules (Pagani and Eckert, 2011). As a result, the presence of Aβ42 can stimulate the generation of ROS, leading to increased vulnerability of mtDNA to peroxidative damage. This, in turn, compromises mitochondrial function and triggers the elimination of damaged mitochondria through autophagy. Consequently, there is a reduction in the overall number of mitochondria and a subsequent decrease in mtDNA copy number (Pagani and Eckert, 2011).

Notably, the co-treatment groups consisting of both high glucose and Aβ42 displayed the greatest decrease in mtDNA content, as seen by the 0.15 and 1.90 decrease in fold change after two and ten days of treatment. Thus indicating that the molecular mechanisms by which each disease contributes to lowering mtDNA content work synergistically to enhance one another. Taken together these data demonstrate that the metabolic disorder causes a hyperglycaemic state impairing glucose uptake (Fig. 8). This promotes the generation of ROS (Fig. 9) leading to mitochondrial damage, triggering its autophagy and subsequently a decrease in mtDNA copy number contributing to the neurodegenerative pathology of AD. This is then further facilitated by the AD protein Aβ42, which can generate ROS independently, in turn expediting the reduction in mtDNA copy number advancing neurodegeneration. Additionally, the 10 day groups displayed a greater decrease in fold change in comparison with the 2 day groups. This demonstrates a time dependent relationship between hyperglycaemic induced oxidative damage and the reduction in mtDNA copy number. This notion has been previously described in literature, where it has been implicated that over time mitochondrial function is affected through mtDNA damage as a consequence of prolonged hyperglycaemic exposure (Czajka and Malik, 2016). It was reported that after 8 days of hyperglycaemic exposure mesangial cells displayed lowered respiration which was further exacerbated after 12 days of exposure (Czajka and Malik, 2016).

Furthermore, there is relationship between mtDNA copy number and mitochondrial activity. Neurons have a high energy demand and can increase their energy production by increasing their mitochondria number through mitochondrial fission (Dong *et al*., 2023). This is particularly important for processes that require high metabolic activity in neurons, such as the formation, function, and maintenance of synapses (Edwards *et al*., 2010). Mitochondrial fission occurs when a single mitochondrion fragments into smaller mitochondria (Rocca *et al*., 2023). Previous research has shown that chronic stress, as in the case of T2DM, can promote increased mitochondrial fission (Edwards *et al*., 2010). Interestingly, studies have also found that mitochondrial biogenesis, which regulates the production of new mitochondrial material from existing mitochondria, acts as a protective mechanism against glucotoxicity (Edwards *et al*., 2010). This capacity is reduced over time and in T2DM patients resulting in mitochondrial fission without mtDNA replication (Edwards *et al*., 2010; Karamanlidis *et al*., 2010). Therefore, it is proposed that the increase in mitochondrial activity in the present study can be explained through increased mitochondrial fission, while the decrease in mtDNA content can

be attributed to a reduction in mitochondrial biogenesis capacity, which declines over time decreasing mtDNA further with time.

Notably, in the current study, a decrease of approximately 0.64-fold and 1.95-fold was observed after 2 and 10 days of treatment with 0.09 % DMSO (Fig. 7). Whilst the research on the specific effects of DMSO on HEK293 mtDNA is limited, DMSO is a commonly used polar organic solvent in neuroscience research, typically at concentrations of 0.5–1.5 % (Yuan *et al.,* 2014). Accordingly, 0.09 % DMSO was used for reconstituting amyloid beta in the present study. However, DMSO itself exhibits cytotoxic effects. In line with this, previous research indicated that exposure to 1% DMSO for 24 hours did not significantly impact the growth and survival of astrocytes but did lead to a reduction in mitochondrial membrane potential in cultured astrocytes. This consequently reduced aerobic metabolism and increased the generation of mitochondrial ROS (Yuan *et al.,* 2014). It is hypothesized that the DMSO-induced ROS production contributes to mtDNA damage through the oxidative damage/ROS pathway, resulting in the observed decrease in mtDNA content in this study. However, further investigation is required to elucidate the precise mechanisms and outcomes in this specific context, potentially necessitating the exploration of alternative solvents for reconstituting amyloid beta.

5.3 Constant hyperglycaemia resulted in decreased glucose uptake

The dysregulated metabolism of glucose in T2DM has previously been linked to AD (Moreira *et al*., 2003). Wherein hyperglycaemia can lead to the damage or disabling of biological systems by various mechanisms, in turn promoting neurodegeneration, thus posing as a risk factor for cognitive decline and dementia (Barbagallo and Dominguez, 2014; Goyal and Jialal, 2020). The graphs in Fig. 8 show that with time the hyperglycaemic and hyperglycaemic-AD groups (25 mM glucose and 25 mM glucose with 400 nM Aβ42) displayed a gradual increase in cellular glucose uptake until day five, after which decreased glucose uptake is observed and indicated by the downwards slope until day seven. Thereafter an increase in glucose uptake is re-commences. This implies that when in a constant hyperglycaemic or a hyperglycaemic-AD state, HEK293 cells displayed decreased glucose uptake. Evidence suggests, persistent hyperglycaemia, as in the case of diabetes, has been found to decrease the transport of glucose within cells (Brown, 2000; Leão *et al*., 2020). This reduction in glucose transport is believed

to be associated with a decrease in the expression of key transporter proteins involved in glucose delivery and metabolism in the brain, specifically GLUT1 and GLUT3 (Maher *et al*., 1994; Pardridge *et al*., 1990). GLUT1 is primarily found in the endothelial cells of the blood-brain barrier (BBB) and facilitates the transport of glucose from the bloodstream into the brain tissue (Dick *et al*., 1984). Subsequently, GLUT3, which is situated on the neuronal cell membrane, is responsible for transporting glucose from the extracellular space into neuronal cells (Maher *et al*., 1994). In an *in vivo* diabetic rat study, it was observed that persistent hyperglycaemia led to a downregulated expression of genes encoding these glucose transporter proteins in the brain (Hou *et al*., 2007). It was further eluded that this downregulation may be an adaptive response aimed at preventing excessive glucose entry into the cells, which could potentially cause cellular damage (Hou *et al*., 2007). Therefore, proposing a rationale for the observed decline in glucose uptake over time observed in the current study after prolonged exposure to the hyperglycaemic conditions. However, the rise in glucose uptake post day 7 indicates an eventual failure in the protective cellular mechanism in preventing entry of glucose into the cell.

On the other hand the AD group in the absence of hyperglycaemia (5 mM glucose with 400 nM Aβ42) displayed comparable trends in glucose uptake to the T2DM and T2DM-AD groups. The AD group demonstrated a slight rise in glucose uptake until day two, followed by a gradual decline until day seven, and then a slight increase in glucose uptake until day 10. These changes were relatively minor, indicated by the flattened slopes. This aligns with existing literature, as studies on early-stage AD brains have shown decreased glucose uptake (De la Monte *et al*., 2008). A study aimed at investigating differences in GLUT1 levels associated with Aβ, it was observed that cortical areas exhibiting high Aβ levels and prominent senile plaques displayed decreased GLUT1 levels in comparison to regions with low Aβ levels and smaller immature plaques (Kuznetsova and Schliebs, 2013). In another study focusing on GLUTs, a decrease in the expression of GLUT1 and GLUT3 was observed in two amyloidogenic mouse models linked to early-onset AD (Tg2576 and APP/PS1). Similarly, reductions in GLUT1 and GLUT3 were also noted in an aging mouse study involving C57/6/SJL mice, suggesting a direct association between decreased levels of GLUT1 and Aβ (Gu *et al*., 2018, Kyrtata *et al*., 2021). Thus implying that the decrease in glucose uptake post treatment with Aβ42 could be linked to a reduction in GLUT1 and 3. It has been previously demonstrated in a study utilizing hyperglycaemic glucose concentrations (25 mM glucose) that Aβ decreases glucose uptake despite coinciding with a 30 minute increase in GLUT3 translocation to the neuronal cell

membrane (Prapong *et al*., 2002). As previously mentioned, GLUT3 is responsible for glucose uptake into neuronal cells through the cell membrane. It has been hypothesized that, Aβ might be inhibiting fusion of GLUT3 vesicles at the membrane through a reduction in the K^+-mediated immunolabeling of extracellular GLUT3 (Prapong *et al*., 2002). As high extracellular K^+ increases neuronal glucose uptake, by increasing GLUT3 fusion with the cell membrane (Prapong *et al*., 2002). Hence the development of a drug improving glucose uptake into cells might be beneficial in the prevention or treatment of AD (Domínguez-Prieto *et al*., 2018; Prapong *et al*., 2002). Evidence suggests that Aβ42 aggregates, which form part of neurotic plaques, are additionally expected to trigger oxidative modifications (Butterfield and Halliwell, 2019). These modifications hinder glucose metabolism by reducing the activity of enzymes responsible for this process (Butterfield and Halliwell, 2019. This impairment in glucose metabolism can result in synaptic dysfunction and, ultimately, neuronal death, contributing to the development of AD (Butterfield and Halliwell, 2019).

5.4 Individual hyperglycaemic and Alzheimer's induced conditions increased ROS production over 24 hours whilst GLD prevented ROS spikes in the T2DM-AD cell model

A common mechanism of glucose toxicity in T2DM involves oxidative stress through the generation of ROS (Ha *et al*., 2000). Hyperglycaemia triggers a specific metabolic pathway involving the activation of phospholipase C or D. These enzymes act on phosphatidylcholine and phosphatidylinositol bisphosphate (PIP2), leading to the upregulation of diacylglycerol (DAG). DAG then activates protein kinase C (PKC), which in turn activates the superoxide-generating phagocyte NADPH-oxidase complex (Volpe *et al*., 2018). Activation of this complex relies on the translocation of its various cytosolic components to the plasma membrane and their interaction with the integral membrane protein p22phox and its catalytic core, the membrane-associated protein NOX2 (Volpe *et al*., 2018). Wherein NOX mediates the transfer of electrons from cytosolic NADPH to oxygen leading to superoxide (ROS) generation in the cytoplasm (Tang *et al*., 2014). This is a possible explanation for the 24 % increase in ROS production within the T2DM group observed in Figure 9 compared to the untreated (5 mM glucose) control group. Notably, a spike is ROS was observed as early as 30 minutes after exposure to the hyperglycaemic conditions and continued to increase up to 24 hours later. This would imply that increased ROS production is mechanism of early pathogenesis in T2DM.

This notion has been previously confirmed, wherein hyperglycaemia induced cytosolic ROS within 15 minutes (Ha *et al*., 2000).

Other studies have also linked metabolic impairment and ROS formation to mitochondrial dysfunction, as an early mechanism contributing to disease progression preceding AD (Sharma *et al.,* 2021). AD is an age related disease, accordingly, with age mitochondria accumulate oxidative damage and subsequently cause the formation of free radicals such as ROS, as a result of electrons leaking during ATP production (Pagani and Eckert, 2011). Whilst the hyperglycaemic conditions of T2DM activates the ETC and glycation in the mitochondria producing ROS as a by-product, causing a cascade. Here ROS promotes the expression of both β- and γ-secretases as well as their activity, in turn exacerbating Aβ production (Pagani and Eckert, 2011; Payne and Chinnery, 2015; Macdonald *et al.,* 2018). These Aβ oligomers then translocate into mitochondria and impair mitochondrial function further promoting ROS (Agrawal and Jha, 2020). This proposition was confirmed by a 14 % increase in ROS production within 24 hours in the T2DM-AD group (Fig. 9) compared to the untreated (5 mM glucose) control group, which corroborates that the hyperglycaemic and Aβ42 treatments promote the production of ROS in early pathogenesis. Furthermore, these spikes in ROS could trigger a cascade effect eventually leading to AD. As is has been seen that increased ROS can activate the kinase GSK-3β which hyperphosphorylates Tau, leading to NFT formation, synaptic dysfunction, apoptosis and ultimately AD (Agrawal and Jha, 2020). Once again corroborating the premise that a mechanism linking T2DM to AD is increased ROS production.

However, when compared to the 25 mM glucose (T2DM group) treatment, the T2DM-AD group displayed a 8 % decrease in ROS after 24 hours. At nanomolar concentrations, some *in vitro* cell studies have validated the protective antioxidative properties of Aβ (Carrillo-Mora *et al*., 2014). The Aβ42 peptide contains two crucial sites within its internal structure for its redox function. The first site is situated in the N-terminal hydrophilic region and possesses the unique ability to efficiently bind transition metals, thereby reducing the likelihood of these metals participating in other redox reactions that could elevate oxidative damage (Carrillo-Mora *et al*., 2014). The second site is located in the peptide's C-terminal lipophilic segment, which can capture free radicals at one end and, at the other end, can reduce metals and convert them into more reactive forms with a lower valence, thus exhibiting both anti- and pro-oxidative effects. Through these mechanisms, cells that overexpress Aβ appear to exhibit reduced ROS production and decreased susceptibility to damage from metals (Carrillo-Mora *et al*., 2014).

This could elucidate the observed reduction in hyperglycaemia-induced ROS following treatment with 400 nM Aβ42 in the present study.

Additionally, the Aβ42 peptides forming part of the amyloid plaques affiliated with AD can lead to production of ROS in the absence of hyperglycaemia, as seen by the 39 % increase in ROS (Fig. 9) within the AD group (5 mM glucose with 400 nM Aβ) compared to the untreated (5 mM glucose) control group. These Aβ42 peptides in plaque deposits have a great copper and iron reduction potential. These peptides generate ROS and trigger oxidative stress through the reduction of these metal ions, which in turn triggers the JNK death signalling pathway leading to programmed cell death (Huang *et al*., 1999, Mehan *et al*., 2011). Normally, JNKs are involved in memory formation, brain repair and development as well as inflammatory responses. However, the aberrant activation of JNKs have been implicated with neuroinflammation and subsequently neuronal death contributing to the neurodegenerative pathology of AD (Mehan *et al*., 2011). JNKs are activated by stress stimuli which implies that hyperglycaemic effect of T2DM, and the Aβ42 peptides of AD may act synergistically through the production of ROS, leading to overactivation of JNKs and further strengthening the link between the metabolic and neurodegenerative disease.

This has previously been regarded as an apoptotic signal resulting in the inactivation of the anti-apoptotic protein BCL2. Thus prompting the release of cytochrome c from the mitochondria which triggers programmed cell death through apoptosis, leading to neuronal death (Bjorkblom *et al*., 2008; Mehan *et al*., 2011). Furthermore, the overactivation of JNKs in the brain can trigger the inflammatory processes (Mehan *et al*., 2011). Wherein JNKs have been considered to have pro-inflammatory functions in microglia, which are the resident immune cells of the central nervous system (Waetzig *et al*., 2005). JNKs promote the release of the pro-inflammatory and neurodegenerative cytokine, TNFα, whilst dopaminergic neurons express the complementary TNFα cell surface receptors, TNFR1 and TNFR2 (Amin *et al*., 2022; Hidding *et al*., 2002; Waetzig *et al*., 2005). This allows for the convenient binding of TNFα and TNFR1, activating caspases 8 and 3, culminating in the programmed cell death of dopaminergic neurons by apoptosis and promoting neurodegeneration contributing to the progression of AD (Amin *et al*., 2022). These data strongly implicate ROS as a key factor contributing to the enhancement of T2DM pathology and its progression toward AD. Hence, implying that the employment of therapeutic strategies aimed at lowering or preventing rises

in ROS as a consequence of the metabolic disorder could be greatly beneficial in lowering the incidence of AD.

The T2DM drug GLD is said to reduce oxidative stress through the reduction of hepatic glucose production, as well as by causing increased glucose uptake in muscles (Fouqueray *et al*., 2014). Surprisingly, in the absence of hyperglycaemia, treatment with GLD coincides with a slight increase in ROS production, as seen by a 6 % increase in the GLD and AD-GLD group compared to the untreated (5 mM glucose) control group. Additionally, in the absence of treatment with the AD related protein, Aβ42, GLD produced an unanticipated 27 and 3 % increase in ROS production as seen by the T2DM-GLD treated group compared to the untreated (5 mM glucose) control group and the T2DM (25 mM glucose) group. Hence implying that GLD does not lower ROS production in cells that do not fit the T2DM-AD double disease phenotype. This could be attributed to mechanism of action of the drug. Thus suggesting that the mechanism by which the drug works to lower ROS, namely by improving glucose uptake, might have an adverse effect and in turn increase ROS through a negative feedback loop. As mentioned previously, the downregulation of glucose transporter proteins may be an adaptive response aimed at preventing excessive glucose entry into the cells, which could potentially cause cellular damage through intracellular hyperglycaemia (Hou *et al*., 2007). More specifically, intracellular hyperglycaemia can cause increased mitochondrial ROS and lead to cellular damage through the elevation of AGEs, enhancing the expression AGE product receptors and activating its complementary ligands, prompting the activation of PKC as well as through the hexosamine pathway (Brownlee, 2005; Giacco and Brownlee, 2010). Therefore, by GLD improving glucose uptake into cells, this could be causing cellular damage through the increased production of ROS.

However, the existing literature contradicts the increase in ROS observed in the present study post GLD treatment. A study done on the immortalized HMEC-1 cell line revealed that 24 hours with 100 μM GLD decreases the production of ROS. This difference in results could be attributed to the variation in cell lines. The proposed mechanism is that in HMEC-1 cells GLD promotes reverse electron flux through the proton pump and thus reduces ROS production (Detaille *et al*., 2016). Notably, mitochondria produce the most ROS in a cell as the proton pump complex I in the respiratory chain can produce superoxide during forward and reverse electron flux. This superoxide can then be converted into H_2O_2 later by the enzyme superoxide dismutase. When this complex is inhibited by complex I inhibitors, ROS production is driven

through forward flux and decreased through reverse flux (Detaille *et al*., 2016). The production of ROS through reverse electron flux is sensitive to mitochondrial membrane potential (MMP). The production of ROS is decreased when MMP is lowered, and mitochondrial respiration is increased through the synthesis of ATP. Accordingly, the combination of low concentrations of Aβ42 and high concentrations of GLD may be synergistically producing a favourable 14 and 32 % reduction in ROS production post treatment with the drug in the T2DM-AD-GLD group (Fig. 9) compared to the untreated (5 mM glucose) control group and the T2DM (25 mM glucose) group. Therefore, the drug could potentially be used to address the increase in ROS associated with the hyperglycaemic conditions of T2DM leading to decreased precursor-AD pathologies and in turn potentially be used as a therapeutic for AD, by lowering ROS formed as a symptom of these diseases and ultimately halting their cascading neurodegenerative effects.

5.5 GLD increases internalised Aβ42 and Aβ42 shedding under hyperglycaemic conditions compared to the T2DM cell model

Collectively, the results discussed thus far, demonstrate that treatment with the AD hallmark protein, Aβ42, can induce cellular stress (Fig. 5), increase mitochondrial activity (Fig. 6) and decrease mtDNA content (Fig. 7) over 10 days and increase ROS production over 24 hours (Fig. 9). Furthermore, these effects were exaggerated when coupled with the hyperglycaemic treatment (25 mM glucose) mimicking T2DM. Hence, to assess differences in the AD related protein concentrations caused by hyperglycaemia and to investigate how the novel T2DM drug influences this, Aβ42 levels were measured using ELISA (Fig. 10). Here, the T2DM, GLD and T2DM-GLD cell models presented with a respective 38 and 30 % decrease, 39 and 10 % increase as well as a 33 and 10 % decrease in intracellular Aβ42 and Aβ42 shedding after 48 hours compared to the untreated (5 mM glucose) control group. In contrast to this, the increased ROS production (Fig. 9) caused by the hyperglycaemic conditions of T2DM have been shown to enhance the expression β- and γ-secretases which in turn leads to an upregulation in Aβ42 through the amyloidogenic processing of APP (Macdonald *et al.,* 2018; Pagani and Eckert, 2011; Payne and Chinnery, 2015). As a result of the same mechanism, the 6 % increase in ROS production after treatment with GLD (Fig. 9) could explain the 39 and 10 % increase in intracellular Aβ42 and Aβ42 shedding in the 5 mM glucose with 100 μM GLD (GLD group) compared to the untreated (5 mM glucose) control group. Similarly, the 2 % increase in ROS

production after treatment with GLD (Fig. 9) may have contributed to the 7 and 28 % increase in intracellular Aβ42 and Aβ42 shedding in the 25 mM glucose with 100 μM GLD (T2DM-GLD group) compared to the T2DM (25 mM glucose) group. As mentioned previously, the induction of low levels of Aβ42 may in fact be beneficial to cell under the condition of oxidative stress. Moreover, the rise in Aβ42 levels caused by the drug does not exceed the levels of Aβ42 in the untreated (5 mM glucose) control group, suggesting that the elevated Aβ42 levels induced by the drug may not be detrimental. This suggests that the rise in Aβ42 levels caused by GLD could potentially be working to prevent the rise in hyperglycaemia-induced ROS through its metal chelating antioxidant properties by scavenging ROS, in the presence of oxidative stress associated with T2DM (Smith *et al*., 2002).

Additionally, the 33 and 10 % decrease in intracellular Aβ42 and Aβ42 shedding (T2DM-GLD treated group) may have been due to a GLD-prevented hyperglycaemic induced spike in ROS. Herein, by GLD preventing the hyperglycaemic induced spike in ROS, the drug in turn also prevents the ROS mediated enhanced expression of the APP processing enzymes, ultimately reducing the production of Aβ42. Briefly, GLD decreases ROS caused by the generation of superoxide by complex I which would otherwise get converted into hydrogen peroxide (Detaille *et al*., 2016). Thereby making the T2DM drug an attractive therapeutic option for the treatment and/ or prevention of AD. However, it is worth noting that in comparison to the untreated (5 mM glucose) control group, the hyperglycaemic treatment group alone exhibited a decrease of 38 % and 30 % in intracellular Aβ42 levels and Aβ42 shedding, respectively, after 48 hours. This finding is not consistent with the existing literature. A study conducted on human umbilical vein endothelial cells (HUVECs) suggests that hyperglycaemia (30 mM glucose) can enhance Aβ42 shedding by up to 2-fold through the time-dependent increase in APP synthesis (Chao *et al*., 2016). Whilst the underlying mechanisms remain to be fully delineated, the transcription of the APP processing enzyme β-secretase was not related to this increase in Aβ42 production in HUVECs. Thus, elucidating to λ-secretase playing a role wherein the inhibition of enzyme decreased the hyperglycaemic induced increase in Aβ42 production (Chao *et al*., 2016). Conversely, another study using Human lens epithelial (HLE) cells found that an increase in Aβ42 production post incubation with 20 mM glucose for 24 hours to be associated with elevated mRNA levels of APP along with both β and λ -secretases. Suggesting that the hyperglycaemic conditions of T2DM increases Aβ42 production by increasing the expression of the genes responsible for the Aβ42 precursor protein APP, as well as upregulating the

expression of the enzymes involved in the amyloidogenic processing of APP into the cytotoxic version of Aβ involved in AD (Nagai *et al*., 2016). Herein, as APP processing enzymes within various cell lines respond differently to hyperglycaemia, the decrease in Aβ42 production found in the present study on HEK293 cells could be attributed to differences in β and λ -secretases on an mRNA or protein level favouring an alternated version of the Aβ protein.

In contrast to the previous notion, another research article utilizing the Human neuroblastoma (SH-SY5Y) and HEK293 cell lines reported findings inconsistent with this idea. The study revealed that the elevated generation of Aβ42 associated with high glucose levels was linked to increased levels of APP. However, this increase was not attributed to enhanced transcription of the APP gene, but rather to the through the inhibition of APP degradation and a reduction in APP turnover rate (Yang *et al*., 2013). The APP protein has a high turnover rate where about 70 % of newly synthesized protein is degraded through the proteasome and lysosome pathways which are additionally affected by hyperglycaemia (Knops *et al*., 1992; Queisser *et al*., 2010). It has been further revealed that the half-life of APP is increased to 1 hour from 25 minutes post treatment with high glucose (10 mM glucose). Therefore a decrease in the degradation of APP could result a punitive increase in APP protein levels (Yang *et al*., 2013). As a result the hyperglycaemic conditions in the present study should be enhancing the generation of Aβ through a decrease in APP degradation and turnover rate which would explain the similar glucose uptake trends observed in the T2DM and T2DM-AD groups. Hence control of glycaemic levels in patients suffering from the metabolic disease might be beneficial in decreasing the incidence and progression of the neurodegenerative diseases (Yang *et al*., 2013).

Prior to secretase activity, APP can follow one of two pathways. After being produced in the endoplasmic reticulum and Golgi apparatus, APP can either be transported to the cell surface where it can be processed into Aβ or alternatively the protein may submit to the pathway of proteolytic degradation by lysosome metabolism or the ubiquitin-proteasome pathway (Kaneko *et al*., 2010; Nixon, 2017). Furthermore, hyperglycaemia has been reported to affect both the proteasome and lysosome degradation pathways (Knops *et al*., 1992; Queisser *et al*., 2010). Thus, these findings suggest that the increased levels of Aβ42 associated with T2DM may also be attributed to a decrease in the degradation of APP caused by the hyperglycaemic conditions associated with the disease. This impairment in degradation pathways may favour the translocation of APP to the cell surface, where it can be processed into Aβ (Nixon, 2017).

Similarly, the unexpected decrease in Aβ42 production observed in this study could be due to an increase of APP degradation, decreasing the amount of precursor protein being translocated to the cell membrane. Although the mechanisms by which T2DM increases Aβ42 production remains elusive, the overall premise is that the hyperglycaemic conditions upregulate the AD hallmark protein by affecting APP.

5.6 Hyperglycaemic-AD conditions affect telomerase activity and telomere length

Additionally, the increased risk of AD has been associated with both, overly elongated telomeres which accumulate DNA damage, and significantly shortened telomeres which have been linked to cell death and senescence (Fani *et al*., 2020). The regulation of telomere length involves a combination of telomerase-dependent elongation, which adds telomeric repeats to shortened telomeres, and telomere trimming events (Fani *et al*., 2020; Glasspool *et al*., 2005). Imbalanced telomere length has been associated with an increased risk of amnestic mild cognitive impairment (Fani *et al*., 2020). While most neurons do not have telomerase activity, it is primarily observed in neural stem cells found in specific regions like the hippocampal dentate gyrus (Lee *et al*., 2012). This region of the brain plays a crucial role in spatial cognition and is implicated in neurodegenerative disorders like AD (Miwa *et al*., 2016). Therefore, investigating the relationship between hyperglycaemia and telomerase activity can provide insights into the changes in telomere length that occur during the progression from T2DM to AD.

5.6.1 Hyperglycaemic-AD conditions increased telomerase activity

Changes in telomerase activity potentially linking T2DM and AD were measured using the qPCR TRAP assay (Fig. 11A). Herein, an initial 70 and 6 % increase in telomerase activity was observed after 48 hours post treatment with high glucose (T2DM group) and Aβ42 (AD group) Whilst an initial 13 % decrease in telomerase activity was observed after 48 hours post treatment with high glucose and Aβ42 (T2DM-AD group). After 10 days, a 36 and 295 % (Fig. 11A) increase was seen in the T2DM and T2DM-AD groups. Whilst AD group presented a 77 % (Fig. 11A) decrease in telomerase activity after 10 days. Contradictory to the initial 70 % (Fig. 11A) increase seen in the hyperglycaemic group, previous studies show a decrease in telomerase activity after 72 hours with 22 mM glucose (Maeda *et al*., 2015). Notably, after

persistent exposure to the hyperglycaemic conditions, this increase in telomerase activity decreases from 70 % (Fig. 11A: T2DM group – 2 day sample) after 2 days to 36 % (Fig. 11A: T2DM group – 10 day sample) after 10 days. Notably, in the current study, the T2DM-AD groups presented an initial decrease telomerase activity after 2 days and then an increased activity after 10 days. However, how the metabolic disorder influences telomerase activity as a function of the neurodegenerative disease is still unclear, as the development of AD has been associated with both, elongated, and shortened telomeres (Fani *et al*., 2020).

The reduction in activity was attributed to the increase in ROS resulting from the hyperglycaemic conditions. Patients suffering with T2DM display increased levels of cellular glucose, which induces ROS through glucose toxicity, further promoting oxidative stress (Zhao *et al*., 2013). ROS can lead to DNA damage which is owed to the fact that the 3' overhangs of telomeres are Guanine-rich, and form G-quadruplex motifs, thereby making telomeres prone to ROS damage. Here, ROS promotes guanine lesions, by oxidizing guanine into 8-oxoguanine. The accumulation of oxidized guanine structures physically obstruct telomerase from binding the shortened telomeres, and in turn reduces telomerase activity (Lu *et al*., 2013; Singh *et al*., 2019; Zhao *et al*., 2013). Hence, the hyperglycaemic ROS induced damage could be contributing to the 13 % decrease (Fig. 11A) in telomerase activity observed after 48 hours post treatment with high glucose and Aβ42 (T2DM-AD group). Decreased telomerase activity through ROS is not solely linked to hyperglycaemia but also to Aβ42. Subsequently, treatment with Aβ42 decreases telomerase activity and a similar trend was observed after 10 days with 400 nM Aβ42 (77 % reduction). Oxidative stress has been shown to promote the intracellular localisation of Aβ in the nuclei and at telomeres (Misonou *et al*., 2002; Wang *et al*., 2015). Wherein the β-sheet structures that form part of the Aβ42 aggregates are involved in inhibiting telomerase. These Aβ oligomers can directly bind to the telomere-TERC structure, blocking and preventing telomerase from extending the telomeric DNA. Although the exact interaction is not fully understood, it has been shown that the Aβ-telomere-TERC interaction is linked to the G-rich nature of telomeric DNA, as the Aβ protein has been found to bind to the specific "GGATTGGGGT" sequence (Ohyagi *et al*., 2005; Wang *et al*., 2015).

Furthermore Literature describes an increase in telomerase activity under hyperglycaemic conditions of T2DM as a consequence of mitochondrial ROS. Diabetic studies done on islets from non-human primates, islets from human pancreas and podocytes demonstrate that hyperglycaemia leads to increased mitochondrial oxygen consumption as more energetic fuel

is available for ATP production, in turn causing hypoxia, which is a reduction in the normal level of oxygen tension (Stieger *et al*., 2012; Wang *et al*., 2005). Alternatively, hyperglycaemia resulting from T2DM elevates mitochondrial ROS, triggering the suppression of aquaporin-1 (AQP1) expression which induces cellular hypoxia in Bovine aortic endothelial cells (BAECs) (Sada *et al*., 2016). Hence, it is possible that the hyperglycaemic treatments in the present study activates one of these pathways, as an increase in ROS and mitochondrial activity was observed. T2DM causes hypoxia in multiple tissues and adaptive responses to hypoxia are impaired. This is due to insufficient activation of the transcription factor Hypoxia-Inducible Factor (HIF), which results from inhibition of the oxygen-regulated α-subunit HIF-1α stability and function due to hyperglycaemia (Catrina and Zheng *et al*., 2021). ROS inhibits HIF-prolyl hydroxylase (PHD) activity by oxidation of its Fe^{2+} active site.

The amount of ROS is proportional to HIF-1α stability, as it is responsible for HIF-1α activation and impairs its proteasomal degradation. Herein, ROS blocks PHD-HIF-1α hydroxylation, which promotes HIF-1α stability and the transactivation of HIF-1 (Köhl *et al*., 2006). Interestingly, mitochondrial generated ROS specifically has been implicated in this pathway. Wherein hypoxia increases mitochondrial ROS formation at mitochondrial complex III. ROS generated here is released into the intermembrane space and enters the cytosol to decrease PHD activity, thus preventing hydroxylation of the HIF-1α protein (Bell *et al*., 2007). Whereas, in the absence of ROS, HIF-1α is hydroxylated by PHD and recognised by the von-Hippel Lindau tumor suppressor (pVHL) of the E3 ubiquitin ligase. This leads to HIF-1α ubiquitylation and its subsequent degradation by the proteasome. Therefore, increased ROS leads to the accumulation of HIF-1α in HEK293 cells (Köhl *et al*., 2006). HIF-1 containing HIF-1α transactivates hTERT promoter activity thereby upregulating hTERT expression, increasing telomerase activity and preserving telomere length (Nishi *et al*., 2004). This could explain the 70 and 36 % increase in telomerase activity observed in the T2DM groups after 2 and 10 days which additionally presented with elevated ROS and enhanced mitochondrial activity.

This increase in hTERT expression could also be counteracting the telomerase activity reducing effects of the Aβ42 treatment in the T2DM-AD treatment groups, resulting in the 295 % increase in telomerase activity after 10 days. Literature demonstrates extra-telomeric cytoplasmic functions in which upregulated hTERT aids in decreasing ROS and improving mitochondrial activity after exposure to Aβ (Haendeler *et al*., 2009; Zhu *et al*., 2000). This is achieved by the physical binding of hTERT to mtDNA under oxidative stress conditions, in

turn protecting the integrity of mtDNA, and improving mitochondrial function (Haendeler *et al*., 2009). Thereby, enabling the mitochondria to function under the condition of oxidative stress, as well as bypass ROS and Aβ- induced cell death (Haendeler *et al*., 2009; Saretzki, 2009). Wherein the upregulation of nuclear hTERT activates the Wnt/β-catenin pro-proliferative pathway. Here hTERT acts as cofactor mediating the activation of transcription of β-catenin-dependent genes which may promote cell survival in AD (Zhou *et al*., 2014). It is additionally suggested that the Aβ- induced apoptosis cascade is suppressed by hTERT prior to mitochondrial dysfunction through the extension of telomeric DNA by telomerase (Zhu *et al*., 2000). However, this neuroprotective upregulation of hTERT and thus the increase in telomerase activity resulting in elongated telomeres might in fact be aiding cellular dysfunction in T2DM leading to the progression of AD. As overly elongated telomeres may become brittle and are prone to DNA damage (Fani *et al.,* 2020).

Notably, in the present study, a 37 % increase and a 68 % decrease in telomerase activity were observed after 2 and 10 days of treatment with 0.09 % DMSO (Fig. 11A). Unfortunately, previous research has shown that DMSO can influence telomerase activity, suggesting the exploration of alternative solvents for reconstituting amyloid beta in future investigations. Herein, a study demonstrated that exposure to 1.5 % DMSO for 96 hours reduced telomerase activity in lymphoblast-like Raji cells (Sharma *et al.,* 1998). Similarly, the current study revealed a decrease in telomerase activity after 10 days of treatment with 0.09 % DMSO in HEK293 cells. This decrease may be attributed to the repression of telomerase during the G0 or early G1 phase of the cell cycle (Sharma *et al.,* 1998). Furthermore, resumption of telomerase activity upon release from DMSO treatment, reaching near-control levels after 24 hours, further supports this mechanism in the Raji cell line (Sharma et al., 1998). In another investigation, treatment with 1.4 % DMSO resulted in a progressive decrease in telomerase activity in the promyelocytic leukaemia HL-60 cell line, reaching a 30 % decrease after 1 day to a 90 % decrease after 4 days of treatment (Chang *et al.,* 2002). This downregulation of telomerase activity was linked to the suppression of the catalytic subunit hTERT expression by DMSO (Chang *et al.,* 2002). Whilst these studies support the decrease in telomerase activity after 10 days of treatment, the absence of a decrease in telomerase activity after 2 days of treatment with DMSO may be attributed to the relatively low concentration of DMSO utilized. Together these data suggest that DMSO represses telomerase activity during the G0 or early G1 phase of the cell cycle by affecting the expression of telomerase components (Chang *et al.,* 2002 and Sharma *et al.,* 1998).

Another study found that varying concentrations of DMSO (0.07 %, 0.1 %, and 1.0 %) could transiently stimulate telomerase activity in telomerase-positive SW626 cancer cells after 8 hours (Alfonso-De Matte *et al.,* 2001). These cells constitutively expressed both hTERC and hTERT mRNA. Hence rise in telomerase activity induced by DMSO was not linked to an upsurge in hTERC or hTERT transcription. Instead, the proposed mechanism is that DMSO may enhance phosphatidylinositol 3-kinase (PI3K) activity levels, which can be activated by external cellular stress. This potentially leads to the activation of protein kinase B (Akt), a downstream target of PI3K known to activate telomerase through direct phosphorylation of hTERT. In turn, this pathway demonstrates an increase telomerase activity independent of changes in hTERT and hTERC transcription levels (Alfonso-De Matte *et al.,* 2001). This mechanism could potentially explain the observed 37 % increase in telomerase activity after 2 days of treatment with 0.09 % DMSO in the current study (Fig. 11A). Therefore these modulations by DMSO may contribute to the variations in telomerase activity seen in the amyloid beta treatment groups, suggesting the exploration of alternative solvents for reconstituting amyloid beta in future investigations (Sharma *et al.,* 1998 and Chang *et al.,* 2002).

5.6.2 Hyperglycaemia-AD conditions increase telomere length

Telomere length was investigated using qPCR in order to evaluate potential T2DM related alterations that may contribute to an increased risk of developing AD. Herein, an initial increase in telomere length (Fig. 11B) was recorded for all treatment groups after 48 hours, namely, a respective 50, 4 and 102 % increase post treatment with high glucose (T2DM group), Aβ42 (AD group) and high glucose with Aβ42 (T2DM-AD group). After 10 days, a respective 25, 45 % decrease was seen in the high glucose and Aβ42 groups. Whilst the co-treatment, high glucose with Aβ42 group presented a 9 % increase in telomere length after 10 days (Fig. 11B). Additionally, these alterations in telomere length complement the increases and decreases in telomerase activity for their respective treatment groups, apart from the 2-day-T2DM-AD and 10-day-T2DM groups. This, suggests that the differences in telomere length are related to changes in telomerase activity induced by the treatments. Whilst the uncomplimentary differences in telomere length might not be directly related to changes in telomerase activity. Nevertheless, hyperglycaemia and Aβ42 can lead to decreased telomerase activity through

ROS and as a result also decreases telomere length. Wherein, the G-rich 3' overhangs of telomeres are prone to ROS damage through guanine lesions, by oxidizing guanine into 8-oxoguanine, causing the telomeres to unfold and further destabilizes the G-quadruplex motifs (Singh *et al*., 2019). In doing so, the telomeric 3' overhangs become exposed and susceptible to nucleolytic cleavage, single and double stranded breaks, leading to telomere shortening and subsequently the erosion of coding DNA. Additionally, the accumulation of oxidized guanine structures physically obstruct telomerase from binding the shortened telomeres and reducing telomerase activity and as a result leads to shortened telomeres (Lu *et al*., 2013; Singh *et al*., 2019; Zhao *et al*., 2013). Accordingly, an aging study conducted on leukocytes, with more than 1000 participants over the age of 65, reported a strong association between telomere shortening and the risk of developing AD. The study suggests that a reduction of a single kilobase pair in telomere length can increase the probability of developing AD by 21% (Honig *et al.,* 2012). This together with the decrease in telomere length observed after 10 days seen in the T2DM model in the present study, demonstrates that T2DM increases the risk of developing AD by decreasing telomere length through elevated ROS.

As mentioned previously, the metabolic disorder can increase the generation of mitochondrial ROS triggering a cascade leading to the upregulation of hTERT and subsequently telomerase activity, leading to telomere elongation. Albeit there is less known about the mechanisms connecting longer telomeres and AD. Where increased risk of the neurodegenerative disease has also been linked with overly elongated telomeres which become fragile and are prone to DNA damage (Fani *et al.,* 2020). Herein, telomeres within the hippocampal cells of Alzheimer's disease brains were found to be significantly longer (Thomas *et al*., 2008). Conversely to somatic cells, adult hippocampal cells maintain telomerase activity. An alternative explanation for the increased telomere length in these cells is by increased telomerase accessibility to telomeres caused by ROS. As previously mentioned hyperglycaemia and Aβ42 can promote the generation of ROS leading to the formation of 8-oxoguanine structures in the G-strand overhang of telomeres. These oxidized structures destabilize the formation the G-quadruplex structure by disrupting the Hoogsteen hydrogen bond responsible for holding the G-quadruplex together (Fouquerel *et al*., 2016). Hence resulting in a more relaxed chromatin structure in telomeres, enabling increased accessibility for telomerase to efficiently elongate telomeres. This heightened elongation of telomeres is associated with increased telomeric DNA damage and susceptibility to accumulating stalled replication forks, presenting a hurdle to DNA replication (Fouquerel *et al*., 2016) This leads to

telomere replication stress, ultimately promoting genome instability (Rivera *et al*., 2017). Often genomic instability leads to cell cycle stress as well as alterations in gene expression and regulation contributing to cellular degeneration and degenerative disease pathology (Vijg and Montagna, 2017). Therefore from these data, it is apparent that hyperglycaemia contributes to an initial increase in telomere length, followed by a decrease in telomere length after persistent hyperglycaemic conditions contributing to the incidence of AD.

An alternative hypothesis put forward to explain the presence of longer telomeres in the hippocampal cells of AD patients, despite the absence of telomerase activity, is the occurrence of decreased DNA methylation in brain regions typically affected in AD (Milicic *et al*., 2023; Thomas *et al*., 2008). These reductions in methylation in sub-telomeric regions lead to a more open chromatin structure in telomeres, facilitating greater access for proteins involved in the alternative lengthening of telomeres mechanism (Thomas *et al*., 2008). As mentioned previously, ROS generated from hyperglycaemic and Aβ42 treatments can also contribute to this more open chromatin structure (Fouquerel *et al*., 2016). Collectively, these mechanisms may be responsible for telomeric elongation through increased telomeric recombination events (Thomas *et al*., 2008). Thus accounting for the 102 % rise in telomere length observed in the 2-day-T2DM-AD group, despite the reduction in telomerase activity (Fig. 11B).

Notably, in the present study, a 42 % increase and a 9 % decrease in telomere length were observed after 2 and 10 days of treatment with 0.09 % DMSO (Fig. 11B). As previously described in section 5.6.1, DMSO can influence telomerase activity. Herein, DMSO could be repressing telomerase activity during the G0 or early G1 phase of the cell cycle by affecting the expression of hTERT, which is responsible for adding telomeric repeats to the ends of chromosomes. By potentially downregulating hTERT expression, DMSO can supress telomerase activity, leading to decreased telomere length. This may explain the 9 % decrease in telomere length observed after 10 days of treatment with 0.09 % DMSO (Chang *et al.,* 2002 and Sharma *et al.,* 1998). In contrast, DMSO may enhance PI3K activity levels, which can be activated by external cellular stress. This activation could subsequently lead to the activation of Akt, which in turn can stimulate telomerase activity by directly phosphorylating hTERT, resulting in longer telomeres (Alfonso-De Matte *et al.,* 2001). This alternate mechanism could potentially explain the observed 42 % increase in telomere length after 2 days of treatment with 0.09 % DMSO in the current study (Fig. 11B). Together, these modulations induced by the DMSO treatment may contribute to the variations in telomerase activity and complementary

alterations in telomere length seen in the amyloid beta treatment groups. These data advocate for the exploration of alternative solvents for reconstituting amyloid beta in future projects (Chang *et al.,* 2002 and Sharma *et al.,* 1998).

6. Conclusion

Despite extensive research efforts, discovering a definitive cure for the AD remains a challenge. Therefore, it is imperative to explore new perspectives and identify the upstream molecular mechanisms that contribute to the onset of the AD. This study provided an analysis into the impact of hyperglycaemia associated with T2DM and its contributions to AD. The analysis was demonstrated *in vitro* from an upstream perspective of AD. This research also explored the potential of utilizing a novel glucose lowering drug, GLD as a therapeutic intervention for modulating the hyperglycaemic induced pathology in AD. In the present study, the hyperglycaemic group exhibited a progressive increase in mitochondrial activity over time, which was correlated with a proportional increase in cell number. Conversely, reductions in mitochondrial activity observed after treatment with Aβ42 were potentially associated with Aβ42-induced ROS production, triggering cytotoxicity and apoptosis (Chen and Petranovic, 2015). Whilst the initial surge in mitochondrial activity following Aβ42 treatment in the T2DM-AD group, as compared to the T2DM group, was followed by a subsequent decline that persisted until day 10. This pattern suggests that Aβ42 initially counteracts the elevation of hyperglycaemia-induced ROS through its metal-chelating antioxidant properties by scavenging ROS. However, with time, the antioxidant effects of Aβ42 become overwhelmed, resulting in a decrease in mitochondrial activity (Smith *et al*., 2002).

Furthermore, the T2DM-AD groups exhibited the most reduction in mtDNA content. This suggests that the molecular mechanisms through which each disease contributes to the decrease in mtDNA content may work together synergistically to amplify their effects. These findings may indicate that the metabolic disorder induces a hyperglycaemic state that impairs glucose uptake, leading to the generation of ROS and subsequent mitochondrial damage. This, in turn, likely triggers autophagy and results in a decrease in mtDNA copy number, contributing to the neurodegenerative pathology of AD. Additionally, the presence of the AD protein Aβ42 couble be exacerbating this process by independently generating ROS, accelerating the reduction in mtDNA copy number and advancing neurodegeneration. Moreover, the groups studied over a period of 10 days exhibited a more pronounced decrease in fold change compared to those

studied over 2 days, indicating a time-dependent relationship between hyperglycaemia-induced oxidative damage and the reduction in mtDNA copy number. The observed increase in mitochondrial activity in the current study can also be attributed to heightened mitochondrial fission, serving as a protective mechanism against glucotoxicity. While the decline in mtDNA content over time may be linked to a decrease in mitochondrial biogenesis capacity, once again diminishing over time, resulting in a progressive reduction in mtDNA levels (Edwards *et al*., 2010; Karamanlidis *et al*., 2010).

In the present study prolonged exposure to hyperglycaemic conditions led to a decline in glucose uptake. This could be attributed to a reduction of glucose transporter proteins in the brain, serving as an adaptive mechanism to prevent excessive glucose influx into cells, potentially averting cellular damage (Hou *et al*., 2007). Whilst the diminished glucose uptake post-treatment with Aβ42 could be correlated with a decrease in GLUT1 and 3 levels, as previously noted in studies involving early-onset AD mice and aging mice (Gu *et al*., 2018; Kyrtata *et al*., 2021). Notably, after day 7 an increase in glucose uptake was once again observed. Potentially allowing for glucose toxicity through ROS to commence. This was confirmed by the decrease in mtDNA, as well as a increase in telomerase activity and telomere length in the T2DM-AD group compared to the untreated (5 mM glucose) control group after 10 days. Herein, ROS generated from hyperglycaemic and Aβ42 treatments likely contribute to a more open chromatin structure allowing for increased telomerase accessibility, contributing to longer fragile telomeres prone to single and double stranded breaks. Furthermore, alterations in telomere length correlating with modifications in telomerase activity influenced by the treatment groups imply that hyperglycaemia and Aβ42 may diminish telomerase activity through ROS, ultimately resulting in a gradual reduction in telomere length. Additionally, this study demonstrates for the first time that the novel glucose lowering drug led to an elevation in Aβ42 production within the T2DM cell model. Moreover, the drug effectively reduced ROS production over a 24-hour period when compared to the untreated cell model. The increase in Aβ42 levels induced by GLD may potentially function to counteract the escalation of hyperglycaemia-induced ROS by leveraging its metal chelating antioxidant properties to scavenge ROS in the presence of oxidative stress associated with T2DM (Smith *et al*., 2002). Thereby making GLD an attractive therapeutic option for the treatment and/ or prevention of AD.

7. Future studies and limitation

Since the pathway leading to AD is a complex and dynamic process, future studies focusing on these pathways should aim to explore how these processes mutually influence each other in greater detail. This could be achieved through an early-stage mouse model study combined with proteomic and transcriptomic analysis to comprehensively understand the gene expression patterns and signalling pathways altered by hyperglycaemia, which contribute to AD. Moreover, it is crucial to explore the effects of GLD on metabolic, mitochondrial, and telomeric functions. Should GLD demonstrate the ability to improve metabolic, mitochondrial and telomeric function, it may present itself as a viable therapeutic avenue for AD.

Several potential improvements could have been implemented in the current study. Firstly, utilizing a neuronal cell line such as the SH-SY5Y cell line, commonly used in neurodegenerative disease research. The non-differentiated form of the SH-SY5Y cell line resembles immature catecholaminergic neurons, containing neurotransmitters, and exhibits neurite structure along with expressing immature neuronal markers. These cells can be further differentiated using retinoic acid to attain a more mature neuron-like phenotype characterized by neuronal markers, in turn provide a more reliable cell model. Another area for enhancement would be the inclusion of the GLD treatment group in the assays investigating mitochondria, given that the drug functions to reduce mitochondrial ROS levels.

8. References

Agrawal, I. and Jha, S., 2020. Mitochondrial dysfunction and Alzheimer's disease: Role of microglia. *Frontiers in Aging Neuroscience*, p.252.

Aldoss, A., Lambarte, R. and Alsalleeh, F., 2023. High-Glucose Media Reduced the Viability and Induced Differential Pro-Inflammatory Cytokines in Human Periodontal Ligament Fibroblasts. *Biomolecules*, *13*(4), p.690.

Alfonso-De Matte, M.Y., Cheng, J.Q. and Kruk, P.A., 2001. Ultraviolet irradiation-and dimethyl sulfoxide-induced telomerase activity in ovarian epithelial cell lines. *Experimental Cell Research*, *267*(1), p.13-27.

Alhajj, M. and Farhana, A., 2021. Enzyme linked immunosorbent assay. *StatPearls [Internet]*.

Amin, R., Quispe, C., Docea, A.O., Ydyrys, A., Kulbayeva, M., Daştan, S.D., Calina, D. and Sharifi-Rad, J., 2022. The role of tumour necrosis factor in neuroinflammation associated with Parkinson's disease and targeted therapies. *Neurochemistry International*, *158*, p.105376.

Andreasen, N., Hesse, C., Davidsson, P., Minthon, L., Wallin, A., Winblad, B., Vanderstichele, H., Vanmechelen, E. and Blennow, K., 1999. Cerebrospinal fluid β-amyloid (1-42) in Alzheimer disease: differences between early-and late-ons*et al*zheimer disease and stability during the course of disease. *Archives of neurology*, *56*(6), p.673-680.

Andrés Juan, C., Pérez de Lastra, J.M., Plou Gasca, F.J. and Pérez-Lebeña, E., 2021. The chemistry of Reactive oxygen Species (ROS) revisited: Outlining their role in biological macromolecules (DNA, lipids and proteins) and induced pathologies.

Aran, K.R., 2023. Mitochondrial dysfunction and oxidative stress in Alzheimer's disease-A step towards mitochondria based therapeutic strategies. *Aging and Health Research*, p.100169.

Arvanitakis, Z., Wilson, R.S., Bienias, J.L., Evans, D.A. and Bennett, D.A., 2004. Diabetes mellitus and risk of Alzheimer disease and decline in cognitive function. *Archives of neurology*, *61*(5), p.661-666.

Ashby, F.J., Dodd, W.S., Helm, E.W., Stribling, D., Spiryda, L.B., Heldermon, C.D. and Xia, Y., 2023. A Pilot Study on Burnout in Medical Students (BuMS) over an Academic Year. *International Medical Education*, *2*(3), p.161-174.

Avila, J., 2006. Tau phosphorylation and aggregation in Alzheimer's disease pathology. *FEBS letters*, *580*(12), p.2922-2927.

Bachstetter, A.D., Xing, B., de Almeida, L., Dimayuga, E.R., Watterson, D.M. and Van Eldik, L.J., 2011. Microglial p38α MAPK is a key regulator of proinflammatory cytokine up-regulation induced by toll-like receptor (TLR) ligands or beta-amyloid (Aβ). *Journal of neuroinflammation*, *8*, pp.1-12.

Barbagallo, M. and Dominguez, L.J., 2014. Type 2 diabetes mellitus and Alzheimer's disease. *World journal of diabetes*, *5*(6), p.889.

Bell, E.L., Klimova, T.A., Eisenbart, J., Moraes, C.T., Murphy, M.P., Budinger, G.S. and Chandel, N.S., 2007. The Qo site of the mitochondrial complex III is required for the transduction of hypoxic signaling via reactive oxygen species production. *The Journal of cell biology*, *177*(6), p.1029-1036.

Bergman, O. and Ben-Shachar, D., 2016. Mitochondrial oxidative phosphorylation system (OXPHOS) deficits in schizophrenia: possible interactions with cellular processes. *The Canadian Journal of Psychiatry*, *61*(8), pp.457-469.

Bjorkblom, B., Vainio, J.C., Hongisto, V., Herdegen, T., Courtney, M.J. and Coffey, E.T., 2008. All JNKs can kill, but nuclear localization is critical for neuronal death. *Journal of Biological Chemistry*, *283*(28), p.19704-19713.

Blázquez, E., Velázquez, E., Hurtado-Carneiro, V. and Ruiz-Albusac, J.M., 2014. Insulin in the brain: its pathophysiological implications for States related with central insulin resistance, type 2 diabetes and Alzheimer's disease. *Frontiers in endocrinology*, *5*, p.161.

Boodhun, N., 2018. Protein analysis: key to the future. *BioTechniques*, *64*(5), p.197-201.

Braak, H. and Braak, E., 1991. Neuropathological stageing of Alzheimer-related changes. *Acta neuropathologica*, *82*(4), pp.239-259.

Brown, G.K., 2000. Glucose transporters: structure, function and consequences of deficiency. *Journal of inherited metabolic disease*, *23*(3), p.237-246.

Brownlee, M., 2005. The pathobiology of diabetic complications: a unifying mechanism. *diabetes*, *54*(6), p.1615-1625.

Burnette, W.N., 1981. "Western blotting": electrophoretic transfer of proteins from sodium dodecyl sulfate-polyacrylamide gels to unmodified nitrocellulose and radiographic detection with antibody and radioiodinated protein A. *Analytical biochemistry*, *112*(2), p.195-203.p.e79993.

Butler, J.M., 2011. *Advanced Topics in Forensic DNA Typing: Methodology*. Academic press. P.49-67.

Butterfield, D.A., Di Domenico, F. and Barone, E., 2014. Elevated risk of type 2 diabetes for development of Alzheimer disease: a key role for oxidative stress in brain. *Biochimica et Biophysica Acta (BBA)-Molecular Basis of Disease*, *1842*(9), p.1693-1706.

Butterfield, D.A. and Halliwell, B., 2019. Oxidative stress, dysfunctional glucose metabolism and Alzheimer disease. *Nature Reviews Neuroscience*, *20*(3), p.148-160.

Caetano, F.A., Beraldo, F.H., Hajj, G.N., Guimaraes, A.L., Jürgensen, S., Wasilewska-Sampaio, A.P., Hirata, P.H., Souza, I., Machado, C.F., Wong, D.Y.L. and De Felice, F.G., 2011. Amyloid-beta oligomers increase the localization of prion protein at the cell surface. Journal of neurochemistry, 117(3), p.538-553.

Carrillo-Mora, P., Luna, R. and Colín-Barenque, L., 2014. Amyloid beta: multiple mechanisms of toxicity and only some protective effects?. *Oxidative medicine and cellular longevity*, *2014*.

Castellani, C.A., Longchamps, R.J., Sun, J., Guallar, E. and Arking, D.E., 2020. Thinking outside the nucleus: Mitochondrial DNA copy number in health and disease. *Mitochondrion*, *53*, p.214-223.

Catrina, S.B. and Zheng, X., 2021. Hypoxia and hypoxia-inducible factors in diabetes and its complications. *Diabetologia*, *64*, p.709-716.

Cawthon, R.M., 2002. Telomere measurement by quantitative PCR. *Nucleic acids research*, *30*(10), p.e47-e47.

Centers for Disease Control and Prevention (CDC), 2014. Estimates of diabetes and its burden in the United States: National diabetes statistics report. *Atlanta: Centers for Disease Control and Prevention*.

Chakrabarti, S., Khemka, V.K., Banerjee, A., Chatterjee, G., Ganguly, A. and Biswas, A., 2015. Metabolic risk factors of sporadic Alzheimer's disease: implications in the pathology, pathogenesis and treatment. *Aging and disease*, *6*(4), p.282.

Chang, J.T.C., Chen, Y.L., Yang, H.T., Chen, C.Y. and Cheng, A.J., 2002. Differential regulation of telomerase activity by six telomerase subunits. *European journal of biochemistry*, *269*(14), p.3442-3450.

Chang, R., Yee, K.L. and Sumbria, R.K., 2017. Tumor necrosis factor α inhibition for Alzheimer's disease. *Journal of central nervous system disease*, *9*, p.1179573517709278.

Chao, A.C., Lee, T.C., Juo, S.H.H. and Yang, D.I., 2016. Hyperglycemia increases the production of amyloid beta-peptide leading to decreased endothelial tight junction. *CNS neuroscience & therapeutics*, *22*(4), p.291-297.

Chatterjee, S. and Mudher, A., 2018. Alzheimer's disease and type 2 diabetes: A critical assessment of the shared pathological traits. *Frontiers in neuroscience*, *12*, p.383.

Cho, D.H., Nakamura, T., Fang, J., Cieplak, P., Godzik, A., Gu, Z. and Lipton, S.A., 2009. S-nitrosylation of Drp1 mediates β-amyloid-related mitochondrial fission and neuronal injury. *Science*, *324*(5923), p.102-105.

Choi, B.R., Cho, W.H., Kim, J., Lee, H.J., Chung, C., Jeon, W.K. and Han, J.S., 2014. Increased expression of the receptor for advanced glycation end products in neurons and astrocytes in a triple transgenic mouse model of Alzheimer's disease. *Experimental & molecular medicine*, *46*(2), p.e75-e75.

Correia, S.C., Santos, R.X., Carvalho, C., Cardoso, S., Candeias, E., Santos, M.S., Oliveira, C.R. and Moreira, P.I., 2012. Insulin signaling, glucose metabolism and mitochondria: major players in Alzheimer's disease and diabetes interrelation. *Brain research*, *1441*, p.64-78.

Cotman, C.W., Poon, W.W., Rissman, R.A. and Blurton-Jones, M., 2005. The role of caspase cleavage of tau in Alzheimer disease neuropathology. *Journal of neuropathology & experimental neurology*, *64*(2), p.104-112.

Czajka, A. and Malik, A.N., 2016. Hyperglycemia induced damage to mitochondrial respiration in renal mesangial and tubular cells: Implications for diabetic nephropathy. *Redox biology*, *10*, p.100-107.

Danysz, W. and Parsons, C.G., 2012. Alzheimer's disease, β-amyloid, glutamate, NMDA receptors and memantine–searching for the connections. *British journal of pharmacology*, *167*(2), p.324-352.

de Jager, C.A., Msemburi, W., Pepper, K. and Combrinck, M.I., 2017. Dementia prevalence in a rural region of South Africa: a cross-sectional community study. *Journal of Alzheimer's Disease*, *60*(3), p.1087-1096.

De la Monte, S.M. and Wands, J.R., 2008. Alzheimer's disease is type 3 diabetes—evidence reviewed. *Journal of diabetes science and technology*, *2*(6), p.1101-1113.

Detaille, D., Vial, G., Borel, A.L., Cottet-Rouselle, C., Hallakou-Bozec, S., Bolze, S., Fouqueray, P. and Fontaine, E., 2016. Imeglimin prevents human endothelial cell death by

inhibiting mitochondrial permeability transition without inhibiting mitochondrial respiration. *Cell death discovery*, *2*(1), p.1-8.

Dezfouli, M.A., Zahmatkesh, M., Farahmandfar, M. and Khodagholi, F., 2019. Melatonin protective effect against amyloid β-induced neurotoxicity mediated by mitochondrial biogenesis; involvement of hippocampal Sirtuin-1 signaling pathway. *Physiology & behavior*, *204*, p.65-75.

Dick, A.P., Harik, S.I., Klip, A. and Walker, D.M., 1984. Identification and characterization of the glucose transporter of the blood-brain barrier by cytochalasin B binding and immunological reactivity. *Proceedings of the National Academy of Sciences*, *81*(22), p.7233-7237.

Domínguez-Prieto, M., Velasco, A., Tabernero, A. and Medina, J.M., 2018. Endocytosis and transcytosis of amyloid-β peptides by astrocytes: a possible mechanism for amyloid-β clearance in Alzheimer's disease. *Journal of Alzheimer's Disease*, *65*(4), p.1109-1124.

Dong, W.T., Long, L.H., Deng, Q., Liu, D., Wang, J.L., Wang, F. and Chen, J.G., 2023. Mitochondrial fission drives neuronal metabolic burden to promote stress susceptibility in male mice. *Nature Metabolism*, *5*(12), p.2220-2236.

Edwards, J.L., Quattrini, A., Lentz, S.I., Figueroa-Romero, C., Cerri, F., Backus, C., Hong, Y. and Feldman, E.L., 2010. Diabetes regulates mitochondrial biogenesis and fission in mouse neurons. *Diabetologia*, *53*, p.160-169.

Elmore, S., 2007. Apoptosis: a review of programmed cell death. *Toxicologic pathology*, *35*(4), p.495-516.

Enns, G.M., 2003. Oxidative Metabolism. In Michael J. Aminoff, Robert B. Daroff (Eds.), Encyclopedia of the Neurological Sciences (p. 708-713). Retrieved from https://doi.org/10.1016/B0-12-226870-9/00012-5.

Fani, L., Hilal, S., Sedaghat, S., Broer, L., Licher, S., Arp, P.P., Van Meurs, J.B., Ikram, M.K. and Ikram, M.A., 2020. Telomere length and the risk of Alzheimer's disease: The Rotterdam Study. *Journal of Alzheimer's Disease*, *73*(2), p.707-714.

Freeman, A. M., Acevedo, L. A., & Pennings, N. (2023). Insulin Resistance. In *StatPearls*. StatPearls Publishing.

Fouqueray, P., Leverve, X., Fontaine, E., Baquié, M., Wollheim, C., Lebovitz, H. and Bozec, S., 2011. Imeglimin-a new oral anti-diabetic that targets the three key defects of type 2 diabetes. *J Diabetes Metab*, *2*(4), p.126.

Fouquerel, E., Lormand, J., Bose, A., Lee, H.T., Kim, G.S., Li, J., Sobol, R.W., Freudenthal, B.D., Myong, S. and Opresko, P.L., 2016. Oxidative guanine base damage regulates human telomerase activity. *Nature structural & molecular biology*, *23*(12), p.1092-1100.

Gamblin, T.C., Chen, F., Zambrano, A., Abraha, A., Lagalwar, S., Guillozet, A.L., Lu, M., Fu, Y., Garcia-Sierra, F., LaPointe, N. and Miller, R., 2003. Caspase cleavage of tau: linking amyloid and neurofibrillary tangles in Alzheimer's disease. *Proceedings of the national academy of sciences*, *100*(17), p.10032-10037.

Garcia-Martin, I., Penketh, R.J., Janssen, A.B., Jones, R.E., Grimstead, J., Baird, D.M. and John, R.M., 2018. Metformin and insulin treatment prevent placental telomere attrition in boys exposed to maternal diabetes. *PloS one*, *13*(12), p.e0208533.

Gendron, T.F. and Petrucelli, L., 2009. The role of tau in neurodegeneration. *Molecular neurodegeneration*, *4*(1), p.1-19.

Giacco, F. and Brownlee, M., 2010. Oxidative stress and diabetic complications. *Circulation research*, *107*(9), p.1058-1070.

Gilson, V., Mbebi-Liegeois, C., Sellal, F. and de Barry, J., 2015. Effects of low amyloid-β (aβ) concentration on aβ 1–42 oligomers binding and GluN2b membrane expression. *Journal of Alzheimer's Disease*, *47*(2), p.453-466.

Goyal, R. and Jialal, I., 2020. Diabetes Mellitus Type 2. [Updated 2019 Dec 20]. *StatPearls [Internet]. Treasure Island (FL): StatPearls Publishing*.

Graves, P.R. and Haystead, T.A., 2002. Molecular biologist's guide to proteomics. *Microbiology and molecular biology reviews*, *66*(1), p.39-63.

Gu, J., Jin, N., Ma, D., Chu, D., Iqbal, K., Gong, C.X. and Liu, F., 2018. Calpain I activation causes GLUT3 proteolysis and downregulation of O-GlcNAcylation in Alzheimer's disease brain. *Journal of Alzheimer's Disease*, *62*(4), pp.1737-1746.

Guo, C., Sun, L., Chen, X. and Zhang, D., 2013. Oxidative stress, mitochondrial damage and neurodegenerative diseases. *Neural regeneration research*, *8*(21), p.2003.

Ha, H. and Lee, H.B., 2000. Reactive oxygen species as glucose signaling molecules in mesangial cells cultured under high glucose. *Kidney international*, *58*, p.S19-S25.

Hansson, O., Lehmann, S., Otto, M., Zetterberg, H. and Lewczuk, P., 2019. Advantages and disadvantages of the use of the CSF Amyloid β (Aβ) 42/40 ratio in the diagnosis of Alzheimer's Disease. *Alzheimer's research & therapy*, *11*, p.1-15.

Hardy, J. and Selkoe, D.J., 2002. The amyloid hypothesis of Alzheimer's disease: progress and problems on the road to therapeutics. *science*, *297*(5580), pp.353-356.

Harland, M., Torres, S., Liu, J. and Wang, X., 2020. Neuronal mitochondria modulation of LPS-induced neuroinflammation. *Journal of Neuroscience*, *40*(8), pp.1756-1765.

Hayflick, L. and Moorhead, P.S., 1961. The serial cultivation of human diploid cell strains. *Experimental Cell Research*, *25*(3), pp.585-621.

Heppner, F.L., Ransohoff, R.M. and Becher, B., 2015. Immune attack: the role of inflammation in Alzheimer disease. *Nature Reviews Neuroscience*, *16*(6), pp.358-372.

Hettich, M.M., Matthes, F., Ryan, D.P., Griesche, N., Schröder, S., Dorn, S., Krauß, S. and Ehninger, D., 2014. The anti-diabetic drug metformin reduces BACE1 protein level by interfering with the MID1 complex. *PloS one*, *9*(7), p.e102420.

Hibbs, A.R., 2004. Fluorescence immunolabelling. In *Confocal Microscopy for Biologists* (p. 259-277). Boston, MA: Springer US.

Hickman, S.E., Allison, E.K. and El Khoury, J., 2008. Microglial dysfunction and defective β-amyloid clearance pathways in aging Alzheimer's disease mice. *Journal of Neuroscience*, *28*(33), p.8354-8360.

Hidding, U., Mielke, K., Waetzig, V., Brecht, S., Hanisch, U., Behrens, A., Wagner, E. and Herdegen, T., 2002. The c-Jun N-terminal kinases in cerebral microglia: immunological functions in the brain. *Biochemical pharmacology*, *64*(5-6), p.781-788.

Holmes, C., 2013. Systemic inflammation and A lzheimer's disease. *Neuropathology and applied neurobiology*, *39*(1), pp.51-68.

Honig, L.S., Kang, M.S., Schupf, N., Lee, J.H. and Mayeux, R., 2012. Association of shorter leukocyte telomere repeat length with dementia and mortality. *Archives of neurology*, *69*(10), p.1332-1339.

Hou, W.K., Xian, Y.X., Zhang, L., Hong, L.A.I., Hou, X.G., Xu, Y.X., Ting, Y.U., Xu, F.Y., Jun, S.O.N.G., Fu, C.L. and Zhang, W.W., 2007. Influence of blood glucose on the expression of glucose transporter proteins 1 and 3 in the brain of diabetic rats. *Chinese medical journal*, *120*(19), p.1704-1709.

Huang, X., Atwood, C.S., Hartshorn, M.A., Multhaup, G., Goldstein, L.E., Scarpa, R.C., Cuajungco, M.P., Gray, D.N., Lim, J., Moir, R.D. and Tanzi, R.E., 1999. The Aβ peptide of Alzheimer's disease directly produces hydrogen peroxide through metal ion reduction. *Biochemistry*, *38*(24), p.7609-7616.

Hurtado, M.D. and Vella, A., 2019. What is type 2 diabetes?. *Medicine*, *47*(1), p.10-15.

Jiang, S., Nandy, P., Wang, W., Ma, X., Hsia, J., Wang, C., Wang, Z., Niu, M., Siedlak, S.L., Torres, S. and Fujioka, H., 2018. Mfn2 ablation causes an oxidative stress response and eventual neuronal death in the hippocampus and cortex. *Molecular neurodegeneration*, *13*(1), pp.1-15.

Kaneko, M., Koike, H., Saito, R., Kitamura, Y., Okuma, Y. and Nomura, Y., 2010. Loss of HRD1-mediated protein degradation causes amyloid precursor protein accumulation and amyloid-β generation. *Journal of Neuroscience*, *30*(11), p.3924-3932.

Kaneto, H., Katakami, N., Matsuhisa, M. and Matsuoka, T.A., 2010. Role of reactive oxygen species in the progression of type 2 diabetes and atherosclerosis. *Mediators of Inflammation*, *2010*.

Karamanlidis, G., Nascimben, L., Couper, G.S., Shekar, P.S., del Monte, F. and Tian, R., 2010. Defective DNA replication impairs mitochondrial biogenesis in human failing hearts. *Circulation research*, *106*(9), p.1541-1548.

Kim, B., Backus, C., Oh, S. and Feldman, E.L., 2013. Hyperglycemia-induced tau cleavage in vitro and in vivo: a possible link between diabetes and Alzheimer's disease. *Journal of Alzheimer's Disease*, *34*(3), p.727-739.

Kirpichnikov, D., McFarlane, S.I. and Sowers, J.R., 2002. Metformin: an update. *Annals of internal medicine*, *137*(1), p.25-33.

Klein, H.U., Trumpff, C., Yang, H.S., Lee, A.J., Picard, M., Bennett, D.A. and De Jager, P.L., 2021. Characterization of mitochondrial DNA quantity and quality in the human aged and Alzheimer's disease brain. *Molecular neurodegeneration*, *16*(1), p.1-17.

Knops, J., Lieberburg, I. and Sinha, S., 1992. Evidence for a nonsecretory, acidic degradation pathway for amyloid precursor protein in 293 cells. Identification of a novel, 22-kDa, beta-peptide-containing intermediate. *Journal of Biological Chemistry*, *267*(23), p.16022-16024.

Köhl, R., Zhou, J. and Brüne, B., 2006. Reactive oxygen species attenuate nitric-oxide-mediated hypoxia-inducible factor-1α stabilization. *Free Radical Biology and Medicine*, *40*(8), p.1430-1442.

Korczyn, A.D., 2012. Why have we failed to cure Alzheimer's disease?. *Journal of Alzheimer's Disease*, *29*(2), p.275-282.

Kukull, W.A., Higdon, R., Bowen, J.D., McCormick, W.C., Teri, L., Schellenberg, G.D., van Belle, G., Jolley, L. and Larson, E.B., 2002. Dementia and Alzheimer disease incidence: a prospective cohort study. *Archives of neurology*, *59*(11), p.1737-1746.

Kumar, A., Sidhu, J., Goyal, A. and Tsao, J.W., 2018. Alzheimer disease.

Kumar, P.S., Pavithra, K.G. and Naushad, M., 2019. Characterization techniques for nanomaterials. In *Nanomaterials for solar cell applications* (p. 97-124). Elsevier.

Kuznetsova, E. and Schliebs, R., 2013. β-Amyloid, cholinergic transmission, and cerebrovascular system-a developmental study in a mouse model of Alzheimer's disease. *Current pharmaceutical design*, *19*(38), pp.6749-6765.

Kyrtata, N., Emsley, H.C., Sparasci, O., Parkes, L.M. and Dickie, B.R., 2021. A systematic review of glucose transport alterations in Alzheimer's disease. *Frontiers in neuroscience*, *15*, p.626636.

Leão, L.L., Tangen, G., Barca, M.L., Engedal, K., Santos, S.H.S., Machado, F.S.M., de Paula, A.M.B. and Monteiro-Junior, R.S., 2020. Does hyperglycemia downregulate glucose transporters in the brain?. *Medical Hypotheses*, *139*, p.109614.

Lee, J. and Pellegrini, M.V., 2022. Biochemistry, Telomere and Telomerase. In *StatPearls [Internet]*. StatPearls Publishing.

Lee, J.C., Kim, S.J., Hong, S. and Kim, Y., 2019. Diagnosis of Alzheimer's disease utilizing amyloid and tau as fluid biomarkers. *Experimental & molecular medicine*, *51*(5), p.1-10.

Letsolo, B.T., Bernert, M. and Weiss, S.F.T., University of the Witwatersrand, 2020. *A nanoparticle-based telomerase assay*. U.S. Patent Application 16/772,699.

Li, A.D. and Liu, W.C., 2010. Optical properties of ferroelectric nanocrystal/polymer composites. In *Physical Properties and Applications of Polymer Nanocomposites* (p. 108-158). Woodhead Publishing.

Li, M. and Li, C.Z., 2016. High glucose improves healing of periodontal wound by inhibiting proliferation and osteogenetic differentiation of human PDL cells. *International Wound Journal*, *13*(1), p.39-43.

Li, X.H., Du, L.L., Cheng, X.S., Jiang, X., Zhang, Y., Lv, B.L., Liu, R., Wang, J.Z. and Zhou, X.W., 2013. Glycation exacerbates the neuronal toxicity of β-amyloid. *Cell death & disease*, *4*(6), p.e673-e673.

Liao, Y.F., Wang, B.J., Cheng, H.T., Kuo, L.H. and Wolfe, M.S., 2004. Tumor necrosis factor-α, interleukin-1β, and interferon-γ stimulate γ-secretase-mediated cleavage of amyloid precursor protein through a JNK-dependent MAPK pathway. *Journal of Biological Chemistry*, *279*(47), p.49523-49532.

Liste-Calleja, L., Lecina, M., Lopez-Repullo, J., Albiol, J., Solà, C. and Cairó, J.J., 2015. Lactate and glucose concomitant consumption as a self-regulated pH detoxification mechanism in HEK293 cell cultures. *Applied Microbiology and Biotechnology*, *99*(23), p.9951-9960.

Lu, W., Zhang, Y., Liu, D., Songyang, Z. and Wan, M., 2013. Telomeres—structure, function, and regulation. *Experimental Cell Research*, *319*(2), p.133-141.

Lynch, J., Chung, J., Huang, Z., Pierce, V., Saunders, N.S. and Niu, L., 2021. Enhancing transient protein expression in HEK-293 cells by briefly exposing the culture to DMSO. *Journal of neuroscience methods*, *350*, p.109058.

Macdonald, R., Barnes, K., Hastings, C. and Mortiboys, H., 2018. Mitochondrial abnormalities in Parkinson's disease and Alzheimer's disease: can mitochondria be targeted therapeutically?. *Biochemical Society Transactions*, *46*(4), p.891-909.

Madhusudhanan, J., Suresh, G. and Devanathan, V., 2020. Neurodegeneration in type 2 diabetes: Alzheimer's as a case study. *Brain and behavior*, *10*(5), p.e01577.

Maher, F., Vannucci, S.J. and Simpson, I.A., 1994. Glucose transporter proteins in brain. *The FASEB Journal*, *8*(13), p.1003-1011.

Mahmood, T. and Yang, P.C., 2012. Western blot: technique, theory, and trouble shooting. *North American Journal of Medical Sciences*, *4*(9), p.429.

Malek-Ahmadi, M., Perez, S.E., Chen, K. and Mufson, E.J., 2020. Braak stage, cerebral amyloid angiopathy, and cognitive decline in early Alzheimer's disease. *Journal of Alzheimer's Disease*, *74*(1), pp.189-197.

Mehan, S., Meena, H., Sharma, D. and Sankhla, R., 2011. JNK: a stress-activated protein kinase therapeutic strategies and involvement in Alzheimer's and various neurodegenerative abnormalities. *Journal of Molecular Neuroscience*, *43*(3), p.376-390.

Mender, I. and Shay, J.W., 2015. Telomerase repeated amplification protocol (TRAP). *Bio-protocol*, *5*(22), p.e1657-e1657.

Milicic, L., Porter, T., Vacher, M. and Laws, S.M., 2023. Utility of DNA Methylation as a Biomarker in Aging and Alzheimer's Disease. *Journal of Alzheimer's Disease Reports*, (Preprint), pp.1-29.

Misonou, H., Morishima-Kawashima, M. and Ihara, Y., 2000. Oxidative stress induces intracellular accumulation of amyloid β-protein (Aβ) in human neuroblastoma cells. *Biochemistry*, *39*(23), p.6951-6959.

Mo, D., Li, X., Raabe, C.A., Rozhdestvensky, T.S., Skryabin, B.V. and Brosius, J., 2020. Circular RNA encoded amyloid beta peptides—a novel putative player in Alzheimer's disease. *Cells*, *9*(10), p.2196.

Moreira, P.I., Santos, M.S., Moreno, A.M., Seiça, R. and Oliveira, C.R., 2003. Increased vulnerability of brain mitochondria in diabetic (Goto-Kakizaki) rats with aging and amyloid-β exposure. *Diabetes*, *52*(6), p.1449-1456.

Nagai, N., Ito, Y. and Sasaki, H., 2016. Hyperglycemia enhances the production of amyloid β1–42 in the lenses of otsuka long-evans tokushima fatty rats, a model of human type 2 diabetes. *Investigative ophthalmology & visual science*, *57*(3), p.1408-1417.

Negritto, M.C. and Manthey, G.M., 2016. Overview of blotting. *Current Protocols Essential Laboratory Techniques*, *13*(1), p.8-1.

Nguyen, T.T., Ta, Q.T.H., Nguyen, T.K.O., Nguyen, T.T.D. and Van Giau, V., 2020. Type 3 diabetes and its role implications in Alzheimer's disease. *International journal of molecular sciences*, *21*(9), p.3165.

Nho, R.S. and Hergert, P., 2014. FoxO3a and disease progression. *World journal of biological chemistry*, *5*(3), p.346.

Nishi, H., Nakada, T., Kyo, S., Inoue, M., Shay, J.W. and Isaka, K., 2004. Hypoxia-inducible factor 1 mediates upregulation of telomerase (hTERT). *Molecular and cellular biology*, *24*(13), p.6076-6083.

Nita, M. and Grzybowski, A., 2016. The role of the reactive oxygen species and oxidative stress in the pathomechanism of the age-related ocular diseases and other pathologies of the anterior and posterior eye segments in adults. *Oxidative medicine and cellular longevity*, *2016*.

Nixon, R.A., 2017. Amyloid precursor protein and endosomal–lysosomal dysfunction in Alzheimer's disease: inseparable partners in a multifactorial disease. *The FASEB Journal*, *31*(7), p.2729.

O'brien, R.J. and Wong, P.C., 2011. Amyloid precursor protein processing and Alzheimer's disease. *Annual review of neuroscience*, *34*, p.185-204.

Pagani, L. and Eckert, A., 2011. Amyloid-Beta interaction with mitochondria. *International Journal of Alzheimer's Disease*, *2011*.

Pardridge, W.M., Boado, R.J. and Farrell, C.R., 1990. Brain-type glucose transporter (GLUT-1) is selectively localized to the blood-brain barrier. Studies with quantitative western blotting and in situ hybridization. *Journal of Biological Chemistry*, *265*(29), p.18035-18040.

Payne, B.A. and Chinnery, P.F., 2015. Mitochondrial dysfunction in aging: much progress but many unresolved questions. *Biochimica et Biophysica Acta (BBA)-Bioenergetics*, *1847*(11), p.1347-1353.

Piaceri, I., Nacmias, B. and Sorbi, S., 2013. Genetics of familial and sporadic Alzheimer's disease. *Frontiers in Bioscience-Elite*, *5*(1), p.167-177.

Pinho, C.M., Teixeira, P.F. and Glaser, E., 2014. Mitochondrial import and degradation of amyloid-β peptide. *Biochimica et Biophysica Acta (BBA)-Bioenergetics*, *1837*(7), p.1069-1074.

Ponugoti, B., Dong, G. and Graves, D.T., 2012. Role of forkhead transcription factors in diabetes-induced oxidative stress. *Experimental diabetes research*, *2012*.

Prapong, T., Buss, J., Hsu, W.H., Heine, P., Greenlee, H.W. and Uemura, E., 2002. Amyloid β-peptide decreases neuronal glucose uptake despite causing increase in GLUT3 mRNA transcription and GLUT3 translocation to the plasma membrane. *Experimental neurology*, *174*(2), p.253-258.

Ohyagi, Y., Asahara, H., Chui, D.H., Tsuruta, Y., Sakae, N., Miyoshi, K., Yamada, T., Kikuchi, H., Taniwaki, T., Murai, H. and Ikezoe, K., 2005. Intracellular Aβ42 activates p53 promoter: a pathway to neurodegeneration in Alzheimer's disease. *The FASEB Journal*, *19*(2), p.1-29.

Queisser, M.A., Yao, D., Geisler, S., Hammes, H.P., Lochnit, G., Schleicher, E.D., Brownlee, M. and Preissner, K.T., 2010. Hyperglycemia impairs proteasome function by methylglyoxal. *Diabetes*, *59*(3), p.670-678.

Rabinovici, G.D., 2021. Controversy and progress in Alzheimer's disease—FDA approval of aducanumab. *New England Journal of Medicine*, *385*(9), pp.771-774.

Readnower, R.D., Sauerbeck, A.D. and Sullivan, P.G., 2011. Mitochondria, amyloid β, and Alzheimer's disease. *International Journal of Alzheimer's Disease*, *2011*.

Reckzeh, E.S., Karageorgis, G., Schwalfenberg, M., Ceballos, J., Nowacki, J., Stroet, M.C., Binici, A., Knauer, L., Brand, S., Choidas, A. and Strohmann, C., 2019. Inhibition of glucose transporters and glutaminase synergistically impairs tumor cell growth. *Cell chemical biology*, *26*(9), p.1214-1228.

Refinetti, P., Warren, D., Morgenthaler, S. and Ekstrøm, P.O., 2017. Quantifying mitochondrial DNA copy number using robust regression to interpret real time PCR results. *BMC research notes*, *10*(1), pp.1-7.

Ren, S., Breuillaud, L., Yao, W., Yin, T., Norris, K.A., Zehntner, S.P. and D'Adamio, L., 2021. TNF-α–mediated reduction in inhibitory neurotransmission precedes sporadic Alzheimer's disease pathology in young Trem2R47H rats. *Journal of Biological Chemistry*, *296*.

Rivera, T., Haggblom, C., Cosconati, S. and Karlseder, J., 2017. A balance between elongation and trimming regulates telomere stability in stem cells. *Nature structural & molecular biology*, *24*(1), p.30-39.

Rocca, C., Soda, T., De Francesco, E.M., Fiorillo, M., Moccia, F., Viglietto, G., Angelone, T. and Amodio, N., 2023. Mitochondrial dysfunction at the crossroad of cardiovascular diseases and cancer. *Journal of Translational Medicine*, *21*(1), p.635.

Rolo, A.P. and Palmeira, C.M., 2006. Diabetes and mitochondrial function: role of hyperglycemia and oxidative stress. *Toxicology and applied pharmacology*, *212*(2), p.167-178.

Ross, W.N., 2012. Understanding calcium waves and sparks in central neurons. *Nature Reviews Neuroscience*, *13*(3), pp.157-168.

Ruparel, N.B., Teixeira, F.B., Ferraz, C.C. and Diogenes, A., 2012. Direct effect of intracanal medicaments on survival of stem cells of the apical papilla. *Journal of Endodontics*, *38*(10), p.1372-1375.

Russell, J.W., Golovoy, D., Vincent, A.M., Mahendru, P.I.A., Olzmann, J.A., Mentzer, A. and Feldman, E.L., 2002. High glucose-induced oxidative stress and mitochondrial dysfunction in neurons. *The FASEB Journal*, *16*(13), p.1738-1748.

Sada, K., Nishikawa, T., Kukidome, D., Yoshinaga, T., Kajihara, N., Sonoda, K., Senokuchi, T., Motoshima, H., Matsumura, T. and Araki, E., 2016. Hyperglycemia induces cellular hypoxia through production of mitochondrial ROS followed by suppression of aquaporin-1. *PloS one*, *11*(7), p.e0158619.

Schwabenland, M., Brück, W., Priller, J., Stadelmann, C., Lassmann, H. and Prinz, M., 2021. Analyzing microglial phenotypes across neuropathologies: a practical guide. *Acta neuropathologica*, pp.1-14.

Scott, I. and Youle, R.J., 2010. Mitochondrial fission and fusion. *Essays in biochemistry*, *47*, pp.85-98.

Selivanov, V.A., Votyakova, T.V., Pivtoraiko, V.N., Zeak, J., Sukhomlin, T., Trucco, M., Roca, J. and Cascante, M., 2011. Reactive oxygen species production by forward and reverse electron fluxes in the mitochondrial respiratory chain. *PLoS computational biology*, *7*(3), p.e1001115.

Serrano-Pozo, A., Frosch, M.P., Masliah, E. and Hyman, B.T., 2011. Neuropathological alterations in Alzheimer disease. *Cold Spring Harbor perspectives in medicine*, *1*(1), p.a006189.

Seubbuk, S., Sritanaudomchai, H., Kasetsuwan, J. and Surarit, R., 2017. High glucose promotes the osteogenic differentiation capability of human periodontal ligament fibroblasts. *Molecular Medicine Reports*, *15*(5), p.2788-2794.

Shafiei, S.S., Guerrero-Muñoz, M.J. and Castillo-Carranza, D.L., 2017. Tau oligomers: cytotoxicity, propagation, and mitochondrial damage. *Frontiers in aging neuroscience*, *9*, p.83.

Sharma, C., Kim, S., Nam, Y., Jung, U.J. and Kim, S.R., 2021. Mitochondrial dysfunction as a driver of cognitive impairment in Alzheimer's disease. *International Journal of Molecular Sciences*, *22*(9), p.4850.

Sharma, S., Raymond, E., Soda, H., Izbicka, E., Davidson, K., Lawrence, R. and Von Hoff, D.D., 1998. Dimethyl sulfoxide (DMSO) causes a reversible inhibition of telomerase activity in a Burkitt lymphoma cell line. *Leukemia research*, *22*(8), p.663-670.

Singh, A., Kukreti, R., Saso, L. and Kukreti, S., 2019. Oxidative stress: Role and response of short guanine tracts at genomic locations. *International Journal of Molecular Sciences*, *20*(17), p.4258.

Singh, T.J., Haque, N., Grundke-Iqbal, I. and Iqbal, K., 1995. Rapid Alzheimer-like phosphorylation of tau by the synergistic actions of non-proline-dependent protein kinases and GSK-3. *FEBS letters*, *358*(3), p.267-272.

Sinha, M., Bhowmick, P., Banerjee, A. and Chakrabarti, S., 2013. Antioxidant role of amyloid β protein in cell-free and biological systems: implication for the pathogenesis of Alzheimerdisease. *Free Radical Biology and Medicine*, *56*, pp.184-192.

Smith, B.J., 1984. SDS polyacrylamide gel electrophoresis of proteins. In *Proteins* (p. 41-55). Humana Press.

Smith, M.A., Casadesus, G., Joseph, J.A. and Perry, G., 2002. Amyloid-β and τ serve antioxidant functions in the aging and Alzheimer brain. *Free Radical Biology and Medicine*, *33*(9), pp.1414-1419

Stieger, N., Worthmann, K., Teng, B., Engeli, S., Das, A.M., Haller, H. and Schiffer, M., 2012. Impact of high glucose and transforming growth factor–β on bioenergetic profiles in podocytes. *Metabolism*, *61*(8), p.1073-1086.

Sun, H., Saeedi, P., Karuranga, S., Pinkepank, M., Ogurtsova, K., Duncan, B.B., Stein, C., Basit, A., Chan, J.C., Mbanya, J.C. and Pavkov, M.E., 2022. IDF Diabetes Atlas: Global, regional and country-level diabetes prevalence estimates for 2021 and projections for 2045. *Diabetes research and clinical practice*, *183*, p.109141.

Szablewski, L., 2017. Glucose transporters in brain: in health and in Alzheimer's disease. *Journal of Alzheimer's disease*, *55*(4), p.1307-1320.

Szablewski, L., 2021. Brain Glucose Transporters: Role in Pathogenesis and Potential Targets for the Treatment of Alzheimer's Disease. *International Journal of Molecular Sciences*, *22*(15), p.8142.

Tang, Y., Long, J. and Liu, J., 2014. Hyperglycemia-associated oxidative stress induces autophagy: involvement of the ROS-ERK/JNK-p53 pathway. In *Autophagy: Cancer, Other Pathologies, Inflammation, Immunity, Infection, and Aging* (p. 105-115). Academic Press.

Teich, A.F. and Arancio, O., 2012. Is the amyloid hypothesis of Alzheimer's disease therapeutically relevant?. *Biochemical Journal*, *446*(2), p.165-177.

Thomas, P., O'Callaghan, N.J. and Fenech, M., 2008. Telomere length in white blood cells, buccal cells and brain tissue and its variation with ageing and Alzheimer's disease. *Mechanisms of ageing and development*, *129*(4), p.183-190.

Vial, G., Chauvin, M.A., Bendridi, N., Durand, A., Meugnier, E., Madec, A.M., Bernoud-Hubac, N., Pais de Barros, J.P., Fontaine, É., Acquaviva, C. and Hallakou-Bozec, S., 2015. Imeglimin normalizes glucose tolerance and insulin sensitivity and improves mitochondrial function in liver of a high-fat, high-sucrose diet mice model. *Diabetes*, *64*(6), p.2254-2264.

Vijg, J. and Montagna, C., 2017. Genome instability and aging: Cause or effect?. *Translational Medicine of Aging*, *1*, p.5-11.

Volpe, C.M.O., Villar-Delfino, P.H., Dos Anjos, P.M.F. and Nogueira-Machado, J.A., 2018. Cellular death, reactive oxygen species (ROS) and diabetic complications. *Cell death & disease*, *9*(2), p.141.

Waetzig, V., Czeloth, K., Hidding, U., Mielke, K., Kanzow, M., Brecht, S., Goetz, M., Lucius, R., Herdegen, T. and Hanisch, U.K., 2005. c-Jun N-terminal kinases (JNKs) mediate pro-inflammatory actions of microglia. *Glia*, *50*(3), p.235-246.

Wang, H., Chen, H., Han, S., Fu, Y., Tian, Y., Liu, Y., Wang, A., Hou, H. and Hu, Q., 2021. Decreased mitochondrial DNA copy number in nerve cells and the hippocampus during

nicotine exposure is mediated by autophagy. *Ecotoxicology and Environmental Safety*, *226*, p.112831.

Wang, W., Upshaw, L., Strong, D.M., Robertson, R.P. and Reems, J., 2005. Increased oxygen consumption rates in response to high glucose detected by a novel oxygen biosensor system in non-human primate and human islets. *Journal of Endocrinology*, *185*(3), p.445-455.

Waugh, D.G., Hussain, I., Lawrence, J., Smith, G.C., Cosgrove, D. and Toccaceli, C., 2016. In vitro mesenchymal stem cell response to a CO2 laser modified polymeric material. *Materials Science and Engineering: C*, *67*, p.727-736.

Wei, Y.H., Lu, C.Y., Wei, C.Y., Ma, Y.S. and Lee, H.C., 2001. Oxidative stress in human aging and mitochondrial disease-consequences of defective mitochondrial respiration and impaired antioxidant enzyme system. *Chinese journal of physiology*, *44*(1), pp.1-12.

Winkler, E.A., Nishida, Y., Sagare, A.P., Rege, S.V., Bell, R.D., Perlmutter, D., Sengillo, J.D., Hillman, S., Kong, P., Nelson, A.R. and Sullivan, J.S., 2015. GLUT1 reductions exacerbate Alzheimer's disease vasculo-neuronal dysfunction and degeneration. *Nature neuroscience*, *18*(4), p.521-530.

World Health Organization, 2021. Global status report on the public health response to dementia.

Worsfold, P., Townshend, A., Poole, C.F. and Miró, M., 2019. *Encyclopedia of Analytical Science*. Elsevier.

Xie, J., Gorlé, N., Vandendriessche, C., Van Imschoot, G., Van Wonterghem, E., Van Cauwenberghe, C., Parthoens, E., Van Hamme, E., Lippens, S., Van Hoecke, L. and Vandenbroucke, R.E., 2021. Low-grade peripheral inflammation affects brain pathology in the App NL-GF mouse model of Alzheimer's disease. *Acta Neuropathologica Communications*, *9*, pp.1-23.

Xie, J., Van Hoecke, L. and Vandenbroucke, R.E., 2022. The impact of systemic inflammation on Alzheimer's disease pathology. *Frontiers in immunology*, *12*, p.796867.

Yamamoto, M., Kiyota, T., Horiba, M., Buescher, J.L., Walsh, S.M., Gendelman, H.E. and Ikezu, T., 2007. Interferon-γ and tumor necrosis factor-α regulate amyloid-β plaque deposition and β-secretase expression in Swedish mutant APP transgenic mice. *The American journal of pathology*, *170*(2), p.680-692.

Yang, Y., Wu, Y., Zhang, S. and Song, W., 2013. High glucose promotes Aβ production by inhibiting APP degradation. *PloS one*, *8*(7), p.e69824.

Yuan, C., Gao, J., Guo, J., Bai, L., Marshall, C., Cai, Z., Wang, L. and Xiao, M., 2014. Dimethyl sulfoxide damages mitochondrial integrity and membrane potential in cultured astrocytes. *PloS one*, *9*(9), p.e107447.

Zhang, H., Wei, W., Zhao, M., Ma, L., Jiang, X., Pei, H., Cao, Y. and Li, H., 2021. Interaction between Aβ and tau in the pathogenesis of Alzheimer's disease. *International journal of biological sciences*, *17*(9), p.2181.

Zhang, X.Q., Dong, J.J., Cai, T., Shen, X., Zhou, X.J. and Liao, L., 2017. High glucose induces apoptosis via upregulation of Bim expression in proximal tubule epithelial cells. *Oncotarget*, *8*(15), p.24141.

Zhao, J., Miao, K., Wang, H., Ding, H. and Wang, D.W., 2013. Association between telomere length and type 2 diabetes mellitus: a meta-analysis. *PloS one*, *8*(11), p.e79993.

Zhao, R.Z., Jiang, S., Zhang, L. and Yu, Z.B., 2019. Mitochondrial electron transport chain, ROS generation and uncoupling. *International journal of molecular medicine*, *44*(1), p.3-15.

Zheng, W.H., Bastianetto, S., Mennicken, F., Ma, W. and Kar, S., 2002. Amyloid β peptide induces tau phosphorylation and loss of cholinergic neurons in rat primary septal cultures. *Neuroscience*, *115*(1), p.201-211.

Zhou, J., Ding, D., Wang, M. and Cong, Y.S., 2014. Telomerase reverse transcriptase in the regulation of gene expression. *BMB reports*, *47*(1), p.8.

Zhu, H., Fu, W. and Mattson, M.P., 2000. The catalytic subunit of telomerase protects neurons against amyloid β-peptide-induced apoptosis. *Journal of neurochemistry*, *75*(1), p.117-124.

Zilberstein, G., Korol, L., Antonioli, P., Righetti, P.G. and Bukshpan, S., 2007. SDS-PAGE under focusing conditions: an electrokinetic transport phenomenon based on charge neutralization. *Analytical Chemistry*, *79*(3), p.821-827.

9. Appendix

Table 6: List of Primer Sequences

Nucleic Acid	**5´- 3´ sequence**	**Reference**
Mitochondrial Forward Primer	ACACCCTCCTAGCCTTACTAC	(Refinetti *et al*, 2017)
Mitochondrial Reverse Primer	GATATAGGGTCGAAGCCGC	(Refinetti *et al*, 2017)
Nuclear Forward Primer	AGGGTATCTGGGCTCTGG	(Refinetti *et al*, 2017)
Nuclear Reverse Primer	GGCTGAAAAGCTCCCGATTAT	(Refinetti *et al*, 2017)
Forward Primer (TS)	AATCCGTCGAGCAGAGTT	(Kim and Wu, 1997)
Reverse Primer (ACX)	GCGCGGCTTACCCTTACCCTTACCCTA	(Kim and Wu, 1997)
Forward Primer (36B4)	CAGCAAGTGGGAAGGTGTAATCC	(Cawthon, 2002)
Reverse Primer (36B4)	CCCATTCTATCATCAACGGGTACAA	(Cawthon, 2002)
Forward Primer (Tel 1)	TCCCGACTATCCCTATCCCTATCCCTATCCCTATCCCTA	(Cawthon, 2002)
Reverse Primer (Tel 2)	GGTTTTTTGAGGGTGAGGGTGAGGGGTGAGGGTGAGGGT	(Cawthon, 2002)

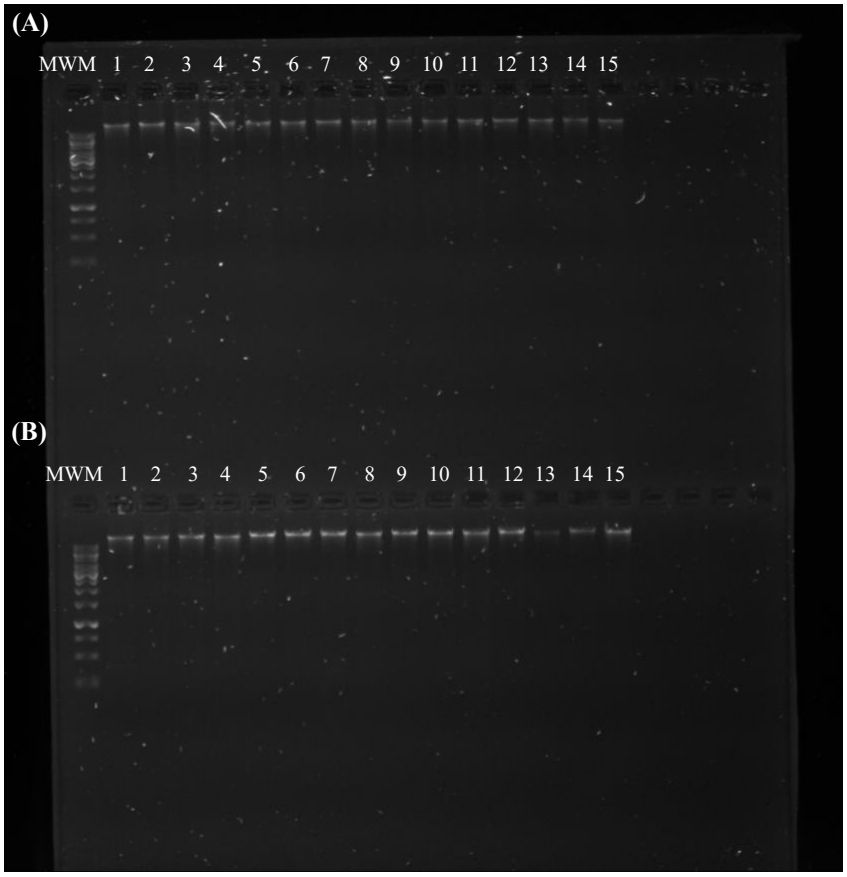

Key:
MWM: Molecular weight marker
(A): 2-day DNA samples
(B): 10-day DNA samples
Lane 1-5: Biological repeat 1
Lane 6-11: Biological repeat 2
Lane 11-15: Biological repeat 3

Figure 12: Agarose gel electrophoresis displaying DNA extracted samples from HEK293 cells post treatment.

A 1% agarose gel was used to evaluate DNA integrity post DNA isolation. Each lane showed a distinct band at the top, indicating intact DNA present. Approximately 200 ng of DNA was loaded per sample. Lanes A1-A15 represent the 2-day DNA samples, with A1-A5 showing different conditions (5 mM glucose, 25 mM glucose, 5 mM glucose with 400 nM Aβ42, 5 mM glucose with 400 nM Aβ42, 0.09% DMSO or non-treated, T2DM group, AD group, AD-T2DM group, vehicle control), and A6-A10, A11-A15 representing biological repeats 1-3. Similarly, Lanes B1-B15 represent the 10-day DNA samples.

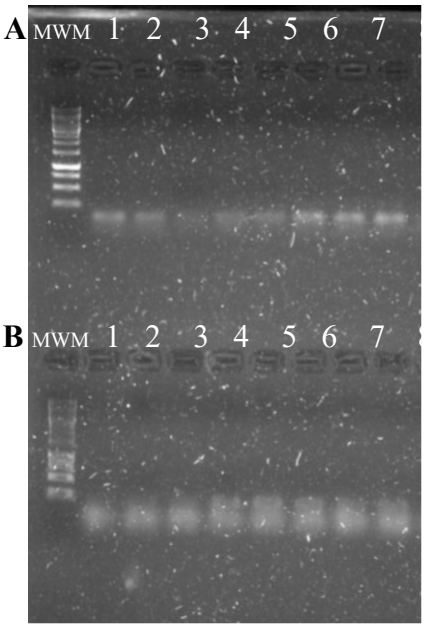

Key:
MWM: Molecular weight marker
(A): Amplified mtDNA
(B): Amplified gDNA
Lane 1-8: annealing temperatures (55.0, 55.5, 56.4, 57.7, 59.3, 60.6, 61.5, 62.0 °C)

Figure 13: Agarose gel electrophoresis showing temperature gradient PCR products after treatment in HEK293 cells.

A 1% agarose gel was used to evaluate DNA integrity post DNA isolation. Approximately 200 ng of DNA was loaded per sample. Lanes A1-A8 represent the amplified mtDNA, with A2-A9 representing different annealing temperatures (55.0, 55.5, 56.4, 57.7, 59.3, 60.6, 61.5, 62.0 °C). Similarly, Lanes B1-B8 represent the amplified gDNA at various annealing temperature. Each lane displayed a band at the bottom, with Lanes 6 to 8 (60.6 to 62.0 °C) showing the most distinct bands for both mitochondrial and genomic DNA.

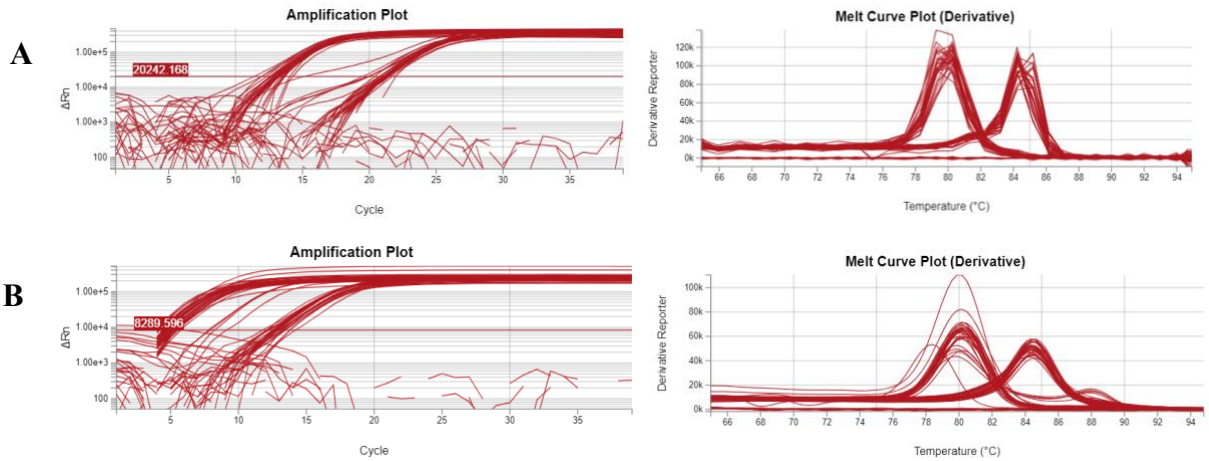

Figure 14: Amplification curve and Melt peak analysis of the mtDNA and nuclear specific DNA sequence.

Amplification curves following qPCR amplification of mtDNA as well as a nuclear specific sequence in HEK293 cell treatment groups, namely: 5 mM glucose, 25 mM glucose, 5 mM glucose with 400 nM Aβ42, 5 mM glucose with 400 nM Aβ42, 0.09% DMSO or non-treated, T2DM group, AD group, AD-T2DM group, vehicle control. The curves show that two distinct genomic products were amplified; one for the mtDNA and the other for the nuclear specific sequence. This was done for three biological groups after 2 (A) and 10 days (B) of treatment. Representative qPCR melt peak analysis of the various treatment groups confirmed that only a single gene product was amplified per primer set evidenced by the two separate peaks. Minimal amplification was observed in the NTC's.

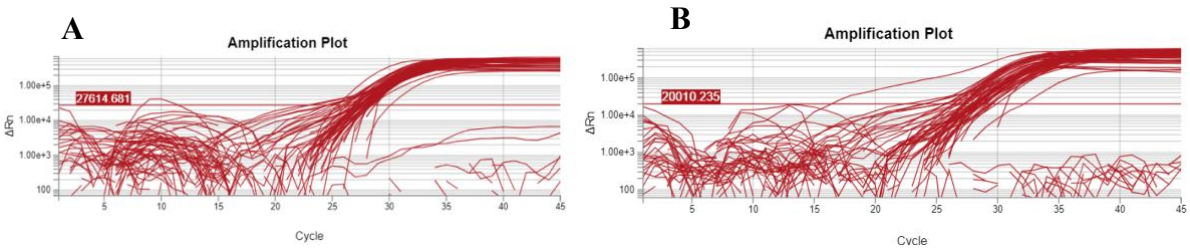

Figure 15: Amplification curves for telomerase activity in HEK293 cells post treatment.

Amplification curves following telomerase extension and subsequent qPCR amplification of a telomeric substrate to quantify telomerase in HEK293 cell treatment groups, namely: 5 mM glucose, 25 mM glucose, 5 mM glucose with 400 nM Aβ42, 5 mM glucose with 400 nM Aβ42, 0.09% DMSO or non-treated, T2DM group, AD group, AD-T2DM group, vehicle control. This was done for three biological groups after 2 (A) and 10 days (B) of treatment. Minimal amplification was observed in the NTC's and Heat treated (HT) controls.

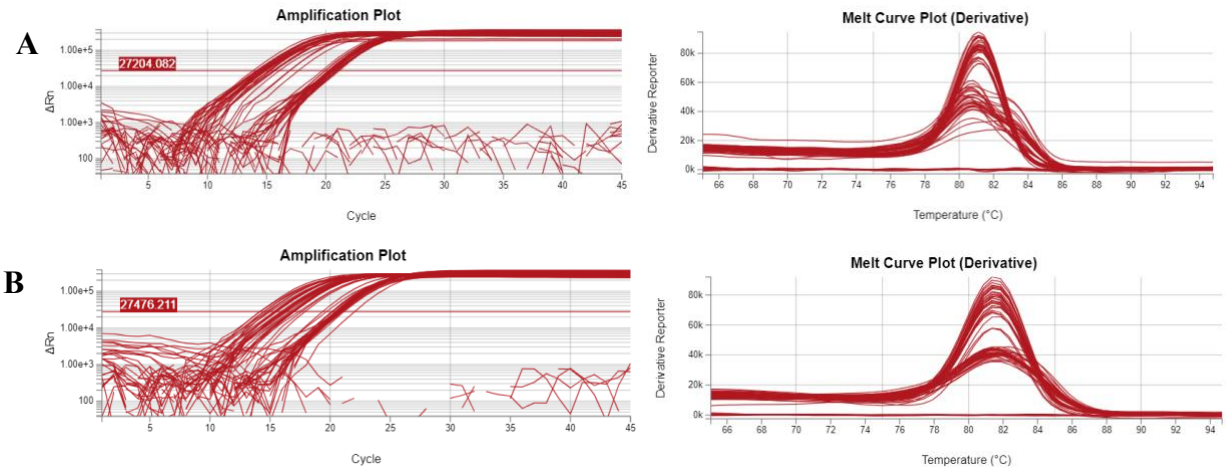

Figure 16: Amplification curve and Melt peak analysis for telomere length as well as the reference gene 36B4.

Amplification curves following qPCR amplification of the 36B4 reference gene as well as the telomeres in HEK293 cell treatment groups, namely: 5 mM glucose, 25 mM glucose, 5 mM glucose with 400 nM Aβ42, 5 mM glucose with 400 nM Aβ42, 0.09% DMSO or non-treated, T2DM group, AD group, AD-T2DM group, vehicle control. The curves show that two distinct genomic products were amplified; one for the amplified telomeres and the other for the reference gene 36B4. This was done for three biological groups after 2 (A) and 10 days (B) of treatment. Representative qPCR melt peak analysis of the various treatment groups confirmed that only a single gene product was amplified per primer set evidenced by the two separate peaks. Minimal amplification was observed in the NTC's.